ROLE OF CD34 IN LPS INDUCED ACUTE LUNG INFLAMMATION

A Thesis Submitted to the
College of Graduate and Postdoctoral Studies
In Partial Fulfillment of the Requirements
For the Degree of Master of Science
In the Department of Veterinary Biomedical Sciences
University of Saskatchewan
Saskatoon

By

SUSHMITA MALTARE

PERMISSION TO USE

In presenting this thesis/dissertation in partial fulfillment of the requirements for a Postgraduate degree from the University of Saskatchewan, I agree that the Libraries of this University may make it freely available for inspection. I further agree that permission for copying of this thesis/dissertation in any manner, in whole or in part, for scholarly purposes may be granted by the professor or professors who supervised my thesis/dissertation work or, in their absence, by the Head of the Department or the Dean of the College in which my thesis work was done. It is understood that any copying or publication or use of this thesis/dissertation or parts thereof for financial gain shall not be allowed without my written permission. It is also understood that due recognition shall be given to me and to the University of Saskatchewan in any scholarly use which may be made of any material in my thesis/dissertation.

DISCLAIMER

Reference in this thesis/dissertation to any specific commercial products, process, or service by trade name, trademark, manufacturer, or otherwise, does not constitute or imply its endorsement, recommendation, or favoring by the University of Saskatchewan. The views and opinions of the author expressed herein do not state or reflect those of the University of Saskatchewan and shall not be used for advertising or product endorsement purposes.

Requests for permission to copy or to make other uses of materials in this thesis/dissertation in whole or part should be addressed to:

1. Dean

   College of Graduate and Postdoctoral Studies

   University of Saskatchewan

   116 Thorvaldson Building, 110 Science Place

   Saskatoon, Saskatchewan S7N 5C9

   Canada

2. Head of the Department of Veterinary Biomedical Sciences

   Western College of Veterinary Medicine

   University of Saskatchewan

   Saskatoon, Saskatchewan, Canada

ABSTRACT

CD34, a pan-selectin binding protein when glycosylated, has been shown to be involved in leukocyte migration to the site of inflammation. However, only one report is available on the expression and role of CD34 in neutrophil recruitment during acute lung inflammation. Hence, we proceeded to study the expression of CD34 in lung tissue and its role in migration of neutrophils into the lungs using a mouse model of endotoxin induced acute lung inflammation.

Acute lung inflammation was induced via intranasal *E. coli* O55:B5 LPS (50 μg) instillation in CD34 KO and WT C57BL/6 mice. Mice (male and female) from each phenotype (i.e. WT and CD34 KO) were divided into five sub-groups comprising of 0, 3, 9, 15 and 24-hour LPS treatment time-points. Each time-point had five-seven WT mice and five-seven CD34 KO mice. Experiments were carried out to look at several factors associated with an inflammatory response in the lungs of mice, including peripheral blood cell counts, total and differential leukocyte cell counts in BALF, adherent neutrophils left in the lung after lavage (MPO levels, Gr-1 IF staining), lung vascular permeability (BAL total protein), lung inflammation scoring (H&E staining), and cytokine and chemokine levels in BALF.

Our results demonstrate that intranasal LPS challenge induces time-dependent inflammatory responses in WT mice (N = 5-7/time-point) and CD34 KO mice (N = 5-7/time-point). While there was no difference in the total or differential leukocyte counts, lung MPO content in CD34 KO was lower than WT group at 3 h time-point (p=0.0308). The MPO levels in CD34 KO mice begin to rise at 9 h (p=0.0021), as opposed to an early 3 h rise in WT mice (p=0.0001), indicating that CD34 KO mice display delays in lung neutrophil recruitment kinetics. CD34 KO mice do not display loss of lung vascular barrier properties as suggested by lower total protein in BAL supernatant in CD34 KO mice at 3 h (p=0.0452) and 24 h (p=0.0113) time-points. In addition, immunofluorescence lung staining shows distinct alveolar staining with Gr-1, a marker for polymorphonuclear leukocytes and a subset of inflammatory monocytes/macrophages. Lung immunofluorescent staining in WT mice at baseline (0 h No LPS) reveals CD34 expression in the bronchiolar epithelium, in addition to alveolar septa.

Several pro-inflammatory cytokines and chemokines (TNF-α, IL-1β, KC, MIP-1α, IL-6, IL-10 and IL-12 p40 sub-unit; $p<0.05$) had higher levels in WT compared to CD34 KO group, at 3 h. These results indicate that CD34 KO mice potentially lack in neutrophil activation responses like TLR4 mediated IL-1β inflammasome activation when compared to WT mice since LPS induces innate immune (TLR4) mediated NF-κB activation, IL-1β inflammasome activation as well as cell-death induced cytokine/chemokine responses.

Thus, given that CD34 has pan-selectin affinity, the high CD34 expression in the bronchiolar epithelium as well as alveolar septa, point towards a possible role of CD34 in lung neutrophil adherence and activation but not vascular permeability kinetics, as indicated by higher lung MPO, histological lung inflammatory changes as well as lung innate cytokine and chemokine secretion, and higher BAL total protein content in LPS exposed WT mice when compared to CD34 KO.

ACKNOWLEDGEMENTS

I would first like to thank my supervisor, Dr. Baljit Singh, for giving me the opportunity to join his lab. He has been extremely supportive and has provided valuable guidance throughout my program. I would also like to thank Dr. Singh for encouraging me to participate in the NSERC-CREATE ITraP program, which was a great experience for me. I would not have been able to finish my studies without his guidance, support and patience, for which I am forever grateful.

I would like to acknowledge my co-supervisor, Dr. Gurpreet Aulakh, for her immense support and guidance during my program. She has been pivotal in my project for providing her expertise during my experiments, data analysis as well as during the thesis writing process. Dr. Aulakh has been most supportive and patient throughout. She always made time for meetings and discussions regarding my project. I am very thankful for all her help and support.

I would also like to acknowledge my committee members, Dr. John Gordon and Dr. Julia Montgomery for their guidance and patience, the committee chair, Dr. Daniel MacPhee, for his support in facilitating committee meetings. They all have provided their valuable perspective into my project.

I would like to thank several people for their technical assistance during my experiments. I would like to thank the animal facility staff of the Laboratory Animal Services Unit and Animal Care Unit. Especially, Brandee Pastoor, Kerri Walker, Amila Nawarathne, and Michele Moroz for providing immense support in animal care and guiding me through their facilities for my experiments. I would like to acknowledge Eiko Kawamura for her assistance with confocal microscopy, and Larhonda Sobchishin for her assistance in immunoelectron microscopy. I would also like to thank Karen Yuen for her tissue processing assistance. I would also like to thank Cindy Pollard for her administrative support, Paula Nordick for assistance with handling finances for our lab, and Cheryl Hack for her support with shipping and receiving. I would also like to thank Jim Gibbons and Dr. Jaswant Singh, for teaching and guiding me during my time as a teaching assistant for veterinary microscopic anatomy course. I would also like to thank Monica Salles, Rhonda

Shewfelt, Nicole Wood, Brent Bobick, for their guidance during my term as a teaching assistant for comparative anatomy of domestic animals.

I am forever grateful to my family for their unconditional love and support throughout. I am thankful to my lab mates for their support and motivation. They have been most helpful during difficult times and have been very kind to provide guidance and assistance during my experiments.

TABLE OF CONTENTS

TABLE OF FIGURES

LIST OF ABBREVIATIONS

ALI	Acute lung injury
ARDS	Acute respiratory distress syndrome
BAL	Broncho-alveolar lavage
BALF	Broncho-alveolar lavage fluid
CD34 KO	CD34 knock-out
IF	Immunofluorescence staining
IHC	Immunohistochemistry
LPS	Lipopolysaccharide
MPO	Myeloperoxidase
ROS	Reactive oxygen species
vWF	von Willebrand Factor
WBC	White blood cell
WT	Wild-type

CHAPTER 1: INTRODUCTION

Inflammation is essential for tissue homeostasis and protection against external infections and injury. Acute Lung Injury (ALI) in humans is characterized by an increase in permeability of the alveolar-capillary barrier, edema, and infiltration of neutrophils in the lung. ALI is marked by increased mortality (40%) due to activated neutrophil alveolar infiltrates comprising of chemotactic peptides, cytokines like IL-1, IL-6, IL-8, and damaging mediators like reactive oxygen species (ROS), and granule proteins, which are responsible for tissue damage in the lungs (Haslett et al., 1989; Haslett, 1999; Matute-Bello et al., 2003; Matute-Bello, 2008 ; Grommes et al., 2011). Therefore, it is important to find novel proteins that regulate neutrophil migration and activation.

Lipopolysaccharide, which is found on the outer surface of most of the gram-negative bacteria, triggers immunological response by binding to the molecular receptors present on the surface of immune cells. In humans, this initiates a cascade of intracellular signals, leading to activation of nuclear transcription factors (Inagawa et al., 2011). TLR4 recognizes LPS (Alexander. C., 2001). Tissue-resident macrophages and mast cells are the mediators of this recognition of damage. Macrophages, epithelial cells and endothelial cells release cytokines, chemokines, and inflammatory mediators (Maas et al., 2018). They release pro-inflammatory cytokines, like tumor necrosis factor-alpha (TNF-α), IL-6, IL-12, Interferon gamma (IFN-γ), interleukin-1-beta (IL-1β) (Alexander. C., 2001; Ashley, 2012). TNF-α, which is released predominantly by macrophages and monocytes, plays a vital role in responding to host injury by starting an immune/cytokine cascade. Levels of pro-inflammatory cytokines IL-6 and CXCL8 (IL-8) increase following the release of TNF-α. CXCL8 (IL-8) is an essential chemotactic factor and plays a role in the development of ALI. However, mice do not have a gene for CXCL8, but they have KC and MIP-2. KC and MIP-2 are considered functional homologs of human CXCL8 since they play an essential role in the neutrophil recruitment into the lungs. KC and MIP-2 share 89% amino acid sequence similarity and adaptor protein MyD88 regulates their TLR-dependent production, but MIP-2 has also been shown to be produced via an alternative pathway utilizing a different adaptor protein,

TRIF (De Filippo et al., 2008). Therefore, we included KC in the cytokine analysis for this project. IL-10, which is the critical anti-inflammatory cytokine, primarily acts on macrophages, neutrophils, mast cells, and eosinophils. IL-10 can inhibit transcription of genes encoding pro-inflammatory cytokines like TNFα, IL-6, IL-8, IL-12, and IL-1. NF-κB activates the gene transcription for cytokines mentioned above. IL-10 levels increase after LPS challenge (Hackett et al., 2008).

Neutrophils, at least in the peripheral circulation, migrate from venules in response to luminal chemotactic gradients initiated by an infection or injury. Neutrophil migration begins through the formation of (E/P-selectin) selectin-mediated nascent contacts with the endothelial PSGL-1, followed by firm adhesion induced by integrin-mediated contacts with VCAM-1/ICAM-1, intraluminal crawling, and finally, transmigration across specific sites termed as endothelial "domes" or transmigratory "cups" (Ley et al., 2007; Phillipson et al., 2008; Petri et al., 2011). Endothelial cell shape is maintained by cytoskeletal actin, vimentin, and cortical actin linkers like ERM (ezrin, radixin, and moesin) proteins (Niggli, 2003; Niggli et al., 2008).

CD34-family proteins are proposed to play various roles depending on the site of expression (Nielsen, 2008). The cell surface protein CD34 is reported in multiple human tissues and cells including hematopoietic stem cells (Andrews, 1989), vascular endothelial cells and inactivated platelets (Lewandowska et al., 2003). Although, CD34 is expressed in vascular endothelium, it is glycosylated only in high endothelial venules in secondary lymphoid organs, to allow binding of L-selectin expressed on lymphocytes (Nielsen, 2008). In the absence of HEV-specific glycosylation elsewhere, negatively charged and large extracellular domains of CD34 may create repulsion and steric hindrance, which prevent interaction of integrin on endothelium with their ligands on lymphocytes, thereby blocking cell adhesion (Nielsen, 2008). CD34 inhibited cell adhesion and cell rounding and induced microvillus formation in HEK293T cells. CD34 expression was forced in HEK293T cells, which led to microvilli formation, rounding of cells, and phosphorylation of ezrin/radixin/moesin (ERM) proteins, while inhibiting integrin-mediated cell re-attachment to HEK293T cells (Delia et al., 1993; Ohnishi et al., 2013). CD34 does not interact with the NHERF ligands (PDZ-family proteins ezrin-radixin-moesin-binding phosphoprotein 50), unlike podocalyxin (Haslett, 1999; Tan et al., 2006).

In a mast cell and eosinophil-dependent asthma (Th2-dependent) model, eosinophils from CD34 -/- mice show significantly less pulmonary migration compared with eosinophils from WT mice. CD34 KO and WT mice mount a comparable immune response. This suggests that CD34 plays an essential role in the cell trafficking by acting as an anti-adhesive or pro-adhesive molecule, depending on the cell and tissue type (Blanchet et al., 2007).

Mucosal dendritic cells have been shown to express CD34. CD34 KO DCs were unable to migrate to lymph nodes to present antigen to T cells while preserving the innate inflammatory response (Blanchet, 2011). In this murine hypersensitivity pneumonitis (Th1/Th17-dependent disease) model, CD34 KO mice protected against the development of hypersensitivity pneumonitis.

Given its expression on vascular endothelial cells and leukocytes, to my knowledge, not many reports are available on the role of CD34 in acute lung inflammation. One recent report in bleomycin-induced lung inflammation showed that absence of CD34 led to loss of structural integrity of the alveoli (Lo et al., 2017). Considering the role of CD34 in cell shape and attachment (Delia et al., 1993; Ohnishi et al., 2013), and its role in leukocyte recruitment in allergic (Blanchet et al., 2007) and hypersensitivity models (Blanchet, 2011), we hypothesized that CD34 KO mice will show lower vascular permeability, cytokine and chemokine release, and lower leukocyte transmigration in response to intranasal endotoxin (Lipopolysaccharide, LPS) compared with the WT mice.

CHAPTER 2: LITERATURE REVIEW

2.1 Acute Lung injury:

Acute lung injury (ALI) and acute respiratory distress syndrome (ARDS), which is a severe form of ALI, have a mortality rate of 30-65% with a very high incidence rate (Williams, 2014). Per the American-European consensus conference definition, ALI is marked by acute onset, partial pressure of arterial oxygen to fraction of inspired oxygen ratios (Pa_{O2}/FI_{O2}) of less than 300 mm Hg, bilateral alveolar infiltrates on chest radiograph and Pulmonary artery wedge pressure (PAWP) less than 18 mm Hg or no clinical evidence of left atrial hypertension. ALI can be caused by several factors including bacterial infections, sepsis, aspiration of gastric contents, toxic inhalation, near drowning, acute pancreatitis, hemorrhagic shock, traumatic brain injury, cardiopulmonary bypass surgery etc. (Grommes et al., 2011; Han et al., 2015). ALI is marked by increased permeability of alveolar-capillary barrier, hypoxemia, activated neutrophil alveolar infiltrates, lung edema, the release of chemotactic peptides like IL-8, cytokines (IL-1, IL-6, etc.) and damaging mediators like reactive oxygen species (ROS) (Grommes et al., 2011; Williams, 2014). Neutrophils undergo degranulation at the site of inflammation, thereby, releasing antimicrobial agents such as ROS, proteinases, and cationic peptides (Grommes et al., 2011; Williams, 2014). During migration, proteinases aid in degrading the extracellular matrix. Neutrophils are the primary line of defense against external injury in ALI. However, excessive neutrophil recruitment, and activation to the site of inflammation can lead to further tissue damage. Researchers have shown that the neutrophil concentration in the bronchoalveolar lavage fluid (BALF) is correlated with the severity of ARDS in ARDS patients (Grommes et al., 2011; Han et al., 2015).

2.2 Acute inflammation:

Inflammation is the immune response to tissue injury due to infection or physical damage. The damage is detected when the Toll-like receptors (TLRs) and nucleotide binding domain and leucine-rich-repeat-containing receptor (NOD-like receptors or NLRs) recognize pathogen-associated molecular patterns (PAMPs), such as, lipid A domain in bacterial lipopolysaccharides (LPS) and damage-associated molecular patterns (DAMPs) (Medzhitov, 2008; Ashley, 2012; Han et al., 2015). Lipopolysaccharide (LPS) is the essential constituent of the outer membrane of gram-negative bacteria, and LPS's primary structure contains three portions, lipid A, core sugar, and O antigen (O-polysaccharide). LPS is amphipathic due to its hydrophilic polysaccharide and hydrophobic lipid moieties. Lipid A comprises 4-7 fatty acid chains bound to two glucosamines, and core oligosaccharide contains eight carbon sugar, heptose and keto-deoxyoctulosonate (KDO), that is highly conserved among bacterial species.

Lipopolysaccharide (LPS) triggers immunological response by binding to the surface molecular receptors present on the immune cells, which initiates a cascade of intracellular signals, leading to activation of nuclear transcription factors (Inagawa et al., 2011). TLR4 recognizes LPS which is found on the outer surface of most of the gram-negative bacteria (Alexander. C., 2001; Han et al., 2015). Tissue-resident macrophages and mast cells are the mediators of this recognition of damage, and lead to the expression of pro-inflammatory cytokines, like tumor necrosis factor-alpha (TNF-α), IL-6, IL-12, Interferon gamma (IFN-γ), interleukin-1-beta (IL-1β) (Alexander. C., 2001; Ashley, 2012). Researchers conducted an *ex vivo* study to understand the cytokine kinetics in human lung tissues challenged with LPS (100 ng/mL) to induce an acute inflammatory response (Hackett et al., 2008). Lung tissues were obtained from subjects with COPD. Cytokine levels were determined by performing ELISA on the lung tissue culture supernatant following LPS challenge. Supernatant samples were collected at several time points post-LPS challenge. Time points included were in the range of 0-24 hours post-LPS challenge. A critical pro-inflammatory cytokine is TNF-α, which is released predominantly by macrophages and monocytes, increased starting from 1-hour post-LPS challenge and peaked at 6-hour time-point. TNF-α plays a vital role in responding to host injury by beginning an immune/cytokine cascade. Levels of pro-inflammatory cytokines IL-6 and CXCL8 (IL-8) peaked later than those of TNF-α, at 48 hours and 24-hour time-point post-LPS challenge. CXCL8 (IL-8) is an essential chemotactic factor and plays a role in the development

of ALI. However, mice do not have a gene for CXCL8, but they have KC and MIP-2. KC and MIP-2 are considered functional homologs of human CXCL-8 since they play an essential role in the neutrophils' recruitment into the lungs (Matute-Bello, 2008). No changes were observed in IL-1β levels for LPS-challenge group compared with the control group. IL-10, which is the crucial anti-inflammatory cytokine, primarily acts on macrophages, neutrophils, mast cells, and eosinophils. IL-10 can inhibit transcription of genes encoding pro-inflammatory cytokines like TNFα, IL-6, IL-8, IL-12, and IL-1. NF-κB activates the gene transcription for cytokines mentioned above. IL-10 levels increased throughout 48 hours window and peaked at 48 hours post-LPS challenge. IL-5 levels were not significantly different in the two groups.

Along with chemokines and costimulatory molecules, the proinflammatory cytokines facilitate the recruitment of effector cells (like neutrophils and monocytes) to the site of damage (Ashley, 2012; Maas et al., 2018). Neutrophil extravasation takes place via activated endothelia of blood vessels. Neutrophils undergo degranulation to release toxic chemicals like reactive oxygen species (ROS), reactive nitrogen species (RNS) and proteinases, thereby creating a cytotoxic environment (Ashley, 2012). These substances are damaging to pathogens as well as host tissue. These interactions manifest in the form of cardinal signs of local inflammation that is, heat, redness, swelling, pain, and loss of function. Inflammation must be resolved to achieve tissue homeostasis and limit tissue damage, and macrophages lead the process of resolution. These cells switch to producing lipoxins to stop further neutrophil recruitment and enhance healing by monocyte infiltration (Ashley, 2012).

2.3 Animal models of ALI/ARDS:

ALI is marked by increased permeability of alveolar-capillary barrier, hypoxemia, activated neutrophil alveolar infiltrates, lung edema, the release of cytokines and chemokines. Due to difficulty of controlling several clinical variables in critically ill patients, it has been hard to test hypotheses about mechanisms of initiation and propagation of lung injury. Animal models provide a way to study mechanisms in an intact living system. While there are no perfect animal models that can capture human ALI/ARDS in all its complexity, there are many animal models available which can provide information on a subset of crucial elements of the disease response in humans (Matute-Bello, 2008). While the American-European consensus conference defines acute lung

injury in humans as an acute onset, a partial pressure of arterial oxygen to fraction of inspired oxygen ratios (Pa_{O2}/FI_{O2}) of less than 300 mm Hg, presence of bilateral alveolar infiltrates on chest radiograph and a pulmonary artery wedge pressure (PAWP) less than 18 mm Hg or no clinical evidence of left atrial hypertension, these criteria are very difficult to translate in animal models. This is due to unavailability of equipment required for these measurements in small animals in most laboratories (Matute-Bello et al., 2011). Therefore, a committee organised by the American Thoracic Society concluded that in order to determine if ALI is present, at least three of the four key features, which include histological evidence of tissue injury, alteration of the alveolar capillary barrier, presence of an inflammatory response, and evidence of physiological dysfunction, should be present (Matute-Bello et al., 2011).

Some of the commonly used models are listed below (Matute-Bello, 2008):

LPS: A reproducible model which induces a neutrophilic inflammatory response similar to ARDS, with an increase in intrapulmonary cytokines. However, shows higher species-specific variability, whereby rodents require a higher dose (mg/kg range) to develop lung injury response as opposed to humans, pigs or cats (μg/kg range). This is due to a lack of pulmonary intravascular macrophage in mice. LPS challenge also does not cause severe endothelial or epithelial damage in mice that occurs in humans with ARDS.

Intratracheal bleomycin: This model is most commonly used for studying pulmonary fibrosis. However, it is also used as an ALI model since it induces an acute inflammatory response which is followed by reversible fibrosis.

Hyperoxia: The features it has in common with ARDS are the acute epithelial injury and neutrophil infiltration which is followed by proliferation of type II cells and scarring.

Mechanical ventilation: This model is highly clinically relevant due to the changes it has resulted in clinical practice. However, it is complex and small animals like mice can not be ventilated for longer periods of time.

Ozone: Ozone induces neutrophilic inflammation, pro-inflammatory cytokine production and airway hyper-responsiveness.

Pulmonary ischemia/reperfusion: This method requires complex animal surgery and it results in a higher lung vascular permeability with neutrophil infiltration into the lungs, which is a feature of ARDS.

Acid aspiration: Humans can develop ARDS following aspiration of gastric contents. HCl is instilled intratracheally while the animal like mouse is mechanically ventilated. ARDS characteristics like alveolar/capillary barrier disruption and neutrophil infiltration are reproduced in this model.

Intravenous bacteria: This model shows interstitial edema, congested vasculature as well as neutrophil sequestration, which are also observed in ARDS.

Intrapulmonary bacteria: Neutrophil alveolitis can be observed in this model which is minimal in intravenous bacteria challenge. Other characteristics of ARDS share by this model are increased vascular permeability and interstitial edema

Surfactant depletion by saline lavage: This model lacks ARDS features like impaired permeability and neutrophil recruitment into the lungs, however, it does cause surfactant depletion and gas exchange impairment.

In this study, we have used a mouse model and administered intranasal LPS (50 µL/mice) from *Escherichia coli* O55:B5 (diluted in sterile saline at 1 g/L). LPS model is highly reproducible and shows neutrophilic inflammation response as well as increase in intrapulmonary cytokines which are similar to ARDS. However, alveolar-capillary permeability does not show drastic change unlike that of in ARDS (Matute-Bello, 2008). Mice do not express IL-8 but they have KC chemokine, which is a mouse homologue of human IL-8. IL-8 is induced by pro-inflammatory cytokines TNF-α, IL-6, IFN-γ, TNF-α and IL-1β and acts as a neutrophil chemoattractant (Brat et al., 2005; Matute-Bello, 2008).

2.4 Cell migration during inflammation:

2.4.1 Leukocyte migration to the site of inflammation:

2.4.1.1 Leukocyte Recruitment Cascade:

Leukocyte migration is a multi-step process composed of steps such as capturing, rolling, adhesion, activation, and movement across the endothelium (Muller, 2013; Williams, 2014). The blood flow rate decreases in post-capillary venules at the site of inflammation thereby increasing the probability of leukocytes encountering the endothelium. Inflammatory cytokines activate the endothelial cells, and activated endothelial cells express several molecules on their surface to allow leukocyte migration. P-selectin expressed on the luminal surface of activated endothelial cells interacts with selectin ligands such as P-selectin glycoprotein 1 (PSGL-1) on the leukocytes (Muller, 2013). Inflammatory response results in the release of chemokines by endothelial cells, and resident inflammatory cells. These chemokines activate leukocyte integrin $\alpha_L\beta_2$ (also known as leukocyte function-associated antigen-1, LFA-1) via G protein-coupled receptors. LFA-1 binds to the intercellular adhesion molecule-1 (ICAM-1) and intercellular adhesion molecule-2 (ICAM-2) on endothelium (Ley et al., 2007; Muller, 2013). L-selectin was recently shown to play major role in regulation of circulating leukocyte activation *in vivo* (McEver, 2015; Liu et al., 2017). Liu et al. showed that circulating leukocytes were primed (slightly activated) in mice expressing an L-selectin mutant and primed peripheral blood neutrophils from these mice released high amounts of ROS *in-vitro.* However, the cytokine and chemokine levels in plasma remained normal in the L-selectin mutant mice. The L-selectin mutant mice did not develop hypothermia because of prompt removal of injected *E. coli* from the peritoneum (Liu et al., 2017). The adhered leukocytes continue moving along the endothelium in crawling motion to the site of extravasation. In response to MIP-2 and TNF-α, Mac-1 on leukocytes interact with ICAM-1 on endothelial cells, to achieve intraluminal crawling (Phillipson et al., 2006; Muller, 2013). All the above steps are reversible, and leukocyte can return to the circulation at any point. Followed by firm adhesion and crawling, the leukocytes move across the endothelium to reach the site of inflammation. This process is called transendothelial migration. In an IL-1β model of inflammation in mice, disruption of PECAM-1

(CD31), CD99 and CD99L2 caused the arrest of migrating leukocytes at the basement membrane level (Bixel et al., 2010; Sullivan et al., 2014). VE-cadherin negatively regulates transmigration. Various anatomical features of the transmigratory cup or dome have been reported (Phillipson et al., 2008; Petri et al., 2011). Membrane at the endothelial cell borders is internalized and recycled by a compartment known as lateral border recycling compartment (LBRC). LBRC lies beneath the plasma membrane of the endothelial cell borders. LBRC contains PECAM and CD99. However, VE-cadherin is absent from this compartment (Muller, 2013). During leukocyte transmigration, LBRC membrane has been observed to be targeted at the location of transmigrating leukocyte (Mamdouh et al., 2003; Mamdouh et al., 2008; Muller, 2013). This redirection has been shown in vitro to be achieved by kinesin molecular motors along microtubules (Mamdouh et al., 2008; Muller, 2013).

2.4.1.2 Cytoskeletal Dynamics during Cell Migration:

Migrating leukocytes fall under the amoeboid-moving category. It involves cortical actin networks which are composed of branched actin filament sheets running parallel with the plasma membrane (Boekhorst, 2016). Dynamic filamentous actin (F-actin) cytoskeleton drives the physical behavior of migrating cells. The F-actin cytoskeleton is coupled to the extracellular matrix (ECM) via focal adhesions (FAs). FAs are dynamic assemblies of signaling proteins which are crucial for regulating cellular structure (Gardel, 2010). Rho family GTPases are essential regulators of FAs. Chemoattractant provides directional signals which induce the development of random pseudopods on neutrophils. These pseudopods allow migration of activated neutrophils into inflamed organs (Insall, 2010; Insall, 2013). Migration of neutrophils is guided by the leading edge, which is an extension of the main pseudopod. Aggregation of filamentous actin takes place to support this extension. G-protein coupled receptors (GPCRs) bind to chemoattractant. GPCRs signal through $\beta\gamma$ subunits via GTP-bound small G-proteins like Rac, Rho, and cdc42. Activation of mitogen-activated protein kinases (MAPK) and phosphatases takes place downstream of the Rho family of GTP-binding small G proteins (Niggli, 2003). Besides, neutrophil activation takes place through the p38 MAPK pathway during endotoxemia (Khan et al., 2005). During these events, heat shock protein (HSP)-27 phosphorylation leads to destabilization of the microtubule complex to favor the

formation of a significant protrusion in vitro and a pseudopod *in vivo* (Hino et al., 2000; Hino et al., 2003; Jog et al., 2007). The trailing edge is called the uropod. The intracellular cytoskeletal elements are intricately linked to adhesive proteins such as integrin and selectins expressed on the surface of neutrophils (Barreiro et al., 2007; Ley et al., 2007; Barreiro et al., 2010). Endothelial cell shape is maintained by cytoskeletal actin, vimentin and cortical actin linkers like ERM (ezrin, radixin, and moesin) proteins (Niggli, 2003; Niggli et al., 2008).

2.4.2 Neutrophil recruitment into the lung:

The typical steps of neutrophil rolling, adhesion and transmigration are not well characterized in the lungs largely because of the challenges of application of intravital microscopy. There actually is scant evidence of neutrophils actually migrating out of the alveolar capillaries in the lung. The microenvironment in the lungs requires neutrophils to change shape for transiting through the capillary lumen which is about 5-7 micron wide and for migrating through capillary endothelium and alveolar epithelium. As indicated in the prior sections, neutrophil migration involves a plethora of molecules including cytokines, adhesion molecules, cell signaling molecules, structural proteins, etc. Neutrophil migration in the lungs is different from the generally accepted leukocyte recruitment paradigm for several reasons. First, the narrow diameter and twisting nature of the lung capillaries result in retention of a large number of neutrophils (Doerschuk, 1990; Hellewell, 1994). Second, the pulmonary vasculature is a lower blood pressure region compared to the peripheral vasculature. Finally, depending upon the microbial stimulus for the inflammation, the recruitment appears to be independent of selectins and β2-integrins due to equivocal reports (Doerschuk, 1990; Windsor AC, 1993; Hellewell, 1994). Currently, there is a need to identify additional molecules that regulate recruitment of neutrophils into the lung and their migration across the alveolar blood-air barrier.

2.5. CD34-family proteins:

2.5.1 Introduction:

The CD34 protein belongs to a family of single-pass transmembrane sialomucin proteins. Glycosylated CD34 has a molecular weight of 90-120 kDa. CD34-family incorporates hematopoietic progenitor cell antigen CD34, podocalyxin, and endoglycan (Sassetti et al., 2000). These CD34-family proteins have a serine-, threonine- and proline-rich extracellular domain that is expansively O-glycosylated and sialylated. The extracellular part of these proteins also includes a cysteine-bonded globular domain and a juxtamembrane stalk, also putative N-linked glycosylation site. Each of these proteins contains a single transmembrane helix along with a highly conserved cytoplasmic tail that contains phosphorylation sites and a C-terminal PSD-95—D1g-ZO-1 (PDZ)-domain-binding motif. CD34 is glycosylated only in high endothelial venules (HEV) in secondary lymphoid organs, to allow binding of L-selectin expressed on lymphocytes (Rosen, 2004; Nielsen, 2008). CRKL, a member of the Crk family of adapter proteins, is an intracellular ligand for CD34. They contain one Src-homology 2 (SH2) domain (phosphotyrosine-binding) and two Src-homology 3 (SH3) domains (proline-rich-sequence-binding). Crk protein links proteins that do not have intrinsic kinase activity to intracellular signaling cascades, thereby enabling them to transmit signals indirectly (Nielsen, 2008).

2.5.2 CD34 expression:

CD34-family proteins are proposed to play various roles depending on the site of expression (Nielsen, 2008). The cell surface protein CD34 has been reported in multiple human tissues and cells. Two-color FACS was used to isolate $CD33^{-}CD34^{+}$ cell population from hematopoietic stem cells (Andrews, 1989). Long-term marrow cultures of $CD33^{-}CD34^{+}$ cells generated colony forming cells for more than five weeks. Vascular endothelial cells (Fina et al., 1990; Pusztaszeri et al., 2006), mucosal dendritic cells (Blanchet, 2011), mast cells (Drew, 2002), eosinophils (Radinger et al., 2004; Blanchet et al., 2007), microglia (Ladeby et al., 2005), fibrocytes (Schmidt, 2003),

muscle satellite cells (Beauchamp et al., 2000) and inactivated platelets (Lewandowska et al., 2003) have been shown to express CD34. Fibroblast-like cells situated in the submucosa flanked by SMA+ smooth muscle cells of the muscularis mucosae and the muscularis propriae have stained positive for CD34. CD34 was also expressed in the lamina propria's endothelial cells in the caecum of C57Bl/6 mice (Grassl et al., 2010). In dogs, CD34 expression has been observed in the hematopoietic stem cell in bone marrow (Suter et al., 2004), peripheral blood (Tsumagari et al., 2007) and hair follicle (Kobayashi et al., 2009).

2.5.3 Functions of CD34-family proteins:

CD34 is glycosylated only in high endothelial venules (HEV) in secondary lymphoid organs (except for spleen which lacks HEVs), to allow binding of L-selectin expressed on lymphocytes (Rosen, 2004; Nielsen, 2008). CD34 has been reported to bind all three selectins namely L-selectin (CD62L), E-selectin (CD62E) and P-selectin (CD62P) (Felschow et al., 2001; Alfaro et al., 2011; Ohnishi et al., 2013; AbuSamra et al., 2017). Platelets have been shown to bind to anti-CD34-coated expanded polytetrafluoroethylene vascular grafts (Mrówczyński et al., 2014). The contribution of CD34 in lymphocyte tethering and rolling has been shown *in vitro* using laminar flow assays (Puri et al., 1995). CD34 forms close to 30% of the total protein in peripheral node addressin (PNAd) which is comprised of several glycoproteins and plays a role in lymphocyte homing by showing L-selectin ligand activity in the tonsillar stroma. The CD34 rich fraction of PNAd demonstrated about half the total binding activity. CD34 was also isolated from spleen and KG1a hematopoietic cell line. The CD34 fraction from spleen did not show lymphocyte tethering since lymphocyte homing in the spleen is L-selectin independent. CD34 from KG1a hematopoietic cell line was also functionally active as an L-selectin ligand. All forms of CD34 actively bound to E-selectin (Puri et al., 1995).

In the absence of HEV-specific glycosylation elsewhere, negatively charged and large extracellular domains of CD34 may create repulsion and steric hindrance. This repulsion and steric hindrance can prevent interaction of integrin on endothelium with their ligands on lymphocytes, thereby blocking cell adhesion. Delia, et al. observed CD34 expression in a diffused cell surface pattern in

freshly cultured vascular endothelial cells, with some concentration on microvilli. Interleukin-18 (IL-18), interferon-y (INF-y), and tumor necrosis factor-a (TNF-a) downregulated CD34 expression at mRNA as well as protein level. These molecules upregulate adhesion molecules like endothelial leukocyte adhesion molecule (ELAM-1) and intracellular adhesion molecule 1 (ICAM-1). CD34 has been implicated in the negative control of endothelial adhesion due to this reversed pattern of expression (Delia et al., 1993). Forced expression of CD34 induced cell rounding, microvillus formation, and phosphorylation of ezrin/radixin/moesin (ERM) proteins in HEK293T cells while inhibiting integrin-mediated cell re-attachment to HEK 293T cells (Delia et al., 1993; Ohnishi et al., 2013). ERM proteins act as a crosslink between actin filaments and plasma membrane. These proteins co-localize and associate with CD44 through N-terminal domain and with actin through C-terminal domain (Mori, 2008). CD34 does not interact with the NHERF ligands (PDZ-family proteins ezrin-radixin-moesin-binding phosphoprotein 50) unlike podocalyxin (Haslett, 1999; Tan et al., 2006).

CD34's role on vascular endothelial cells is supported by results in the study where B16 melanoma tumor development was shown to be affected by the expression of CD34 in mice (Maltby et al., 2011). Fourteen days after subcutaneous injection of B16F1-OVA cells in WT $CD34^{+/+}$ C57Bl/6 mice and CD34 KO mice, there was a significant tumor size difference between CD34 KO mice and WT $CD34^{+/+}$ mice (measured using manual calipers), with tumor size being more prominent in the WT $CD34^{+/+}$ mice compared to the CD34 KO mice (Maltby et al., 2011). This difference in early tumor development at day 14 via subcutaneous injection in CD34 KO mice and WT mice has been attributed to the CD34 expression difference in the two groups in non-hematopoietic cells (mostly mast cells and eosinophils) rather than CD34 expression in hematopoietic cells (Maltby et al., 2011). Bone marrow reconstituted chimeras were used to that end. When the mice from both groups were irradiated and with bone marrow reconstituted from WT Ly5.1 congenic mouse, the resultant chimera expresses WT CD34 on hematopoietic lineages; however, the state of CD34 expression on non-hematopoietic cells remains unchanged. 14 days after subcutaneous injection, tumor volume measurements showed that CD34 KO mice reconstituted with bone marrow from WT mice had a smaller sized tumor, in comparison to $CD34^{+/+}$ mice reconstituted with bone marrow from WT animals. Also, twelve days after injecting B16F2-OVA cells intravenously, there were less metastatic lung nodules in CD34 KO mice in comparison to WT mice (Maltby et al., 2011). CD34 also affected the tumor vascular integrity as studied by using fluorescent dye,

carbocyanine, assay. CD34 KO mice had significantly higher vascular leakage of the dye compared to the WT control (Maltby et al., 2011). Above phenotypes support role of CD34 role in functioning of vascular endothelial cells. These are in line with the results of other studies which shed light on CD34's role in sustaining vascular integrity in embryonic growth as well as inflammatory disease (Strilić et al., 2009; Blanchet et al., 2010) An increase in tumor growth as well as reduction in intra-tumoral infiltration of mast cell was observed in CD34 KO mice at a later time-point of 19 days. It has also been shown that eosinophils display anti-tumor activity (Simson et al., 2007) and that CD34 plays an essential part in the migration of eosinophils (Blanchet et al., 2007). Hence, the tumor growth at later stages in CD34 KO can be attributed to decreased migration of eosinophils which might result in lesser anti-tumor growth activity (Maltby et al., 2011)

CD34 has an important role in the ability of peripheral blood-derived endothelial colony-forming cells (ECFCs) to form capillary-like tubes, and their barrier integrity (Tasev et al., 2016). Magnetic sorting of sub-cultured ECFCs was performed to select CD34- and CD34+ ECFCs (FACS: - CD34+: 95% positive; CD34-: 99% negative). Proliferation rate was the same for both CD34- and CD34+ ECFCs as calculated from the pictures taken using phase contrast microscopy (visualizing cell nuclei in 2% paraformaldehyde/HBSS fixed cells using DAPI). 3D human fibrin matrices were used to seed the two cell populations, and these cell cultures were then stimulated with vascular endothelial factor-A and fibroblast growth factor-2 (FGF-2) to induce tube development. The tube-forming capacity of CD34+ ECFCs was significantly more than that of CD34- ECFCs. CD34 silencing with siRNA in ECFC monolayers led to stronger cell-cell contacts and improved barrier function as determined by electric cell-substrate impedance sensing measurements. ECFCs also showed less tube development when CD34 was silenced (Tasev et al., 2016).

An early study showed that forced expression of the full-length CD34 protein in M1 myeloid leukemia cells inhibited their terminal differentiation when treated with differentiation-inducing agent interleukin-6 (Fackler et al., 1995). This effect was not observed when truncated form of CD34 lacking part of the cytoplasmic tail domain was force expressed instead, suggesting that CD34 exerts a differentiation blocking impact in hematopoietic cells through the cytoplasmic tail region. CD34 gene in humans and mice is highly conserved in the intracellular region with greater than 90% amino acid identity which points towards a common and essential function of this region as a differentiation blocker across species (Fackler et al., 1995).

Marone et al. used flow cytometry to observe that CD34 was transcriptionally activated in hematopoietic cell lines such as CD34+ TF-1, CD34+ KG-1a by exogenous transforming growth factor β1 (TGF- β1). TGF- β1 also stopped cells in early progenitor stage (CD34+ TF-1 cells) from differentiating. The study presented data implicating CD34's involvement in the anti-differentiating role of TGF- β1 (Marone et al., 2002).

CD34 has also been shown to play an essential role in skeletal muscle regeneration mediated by satellite cells (Alfaro et al., 2011). Notexin was injected to induce acute damage in mice, to study the role of CD34 in skeletal muscle regeneration. At time points of 0, 5, 10, 14 and 21 days post-notexin injection, Tibialis anterior muscles were harvested from adult CD34 KO and WT mice. Upon H&E staining of the paraffin-embedded tissue, the areas of damage were measured by using images taken with a light microscope and calculating density slices using OpenLab software (version 4.0.4). The measurements revealed that at 5-day time-point, size of damaged areas was not much different in CD34 KO vs. WT mice. However, the necrotic myofibers were significantly higher in number in CD34 KO mice in comparison to WT mice. Also, a delay was seen in the appearance of centrally nucleated fibers (typical of regenerating myofibers). The centrally nucleated fibers in WT animals were significantly bigger than that of CD34 KO mice, whereas the undamaged fibers were not much different, as determined by cross-sectional area measurements. These data suggest that despite being able to initiate repair, the regenerating fibers in CD34 KO mice failed to undergo hypertrophy (a crucial part of myogenesis) (Alfaro et al., 2011). At day-3 post damage, CD34 was found to be down-regulated on the myogenic progenitor cells (MPCs) as determined using FACS analysis and lost by day-5. MPCs start to show CD34 re-expression on the surface at day-10, which is right after their proliferation stops. The total CD34 mRNA down-regulation shortly post-damage was established using quantitative real-time PCR. Thus, suggesting CD34s' role as a differentiation blocker in MPCs which is supported by other studies (Beauchamp et al., 2000; Ieronimakis et al., 2010; Alfaro et al., 2011).

CD34 plays a crucial role in advancing MPCs and satellite cells over the initial steps of myogenic progression, which would be the time from the start of injury to the start of satellite cell division (Alfaro et al., 2011). Some of the critical events that happen throughout this period have been shown to be affected by CD34. Firstly, satellite cells cross the basement membrane, thus exiting the niche. Apparently, cells need to be motile for exiting the niche. Live imaging of single fibers

from CD34 KO and WT animals showed that CD34 KO satellite cells moved slower and traveled smaller distance in comparison to the WT satellite cells. However, the difference between the percentage of CD34 KO and WT satellite cells located above and below basement membrane was negligible, as studied using confocal microscopy of the relative position of Pax7+ satellite cells on the laminin+ basement membrane and cultured fibers. Thereby, showing that the even though CD34 KO satellite cells demonstrate ineffective motility, it does not hamper them from exiting the niche. Lastly, the proliferation of myogenic cells starts, and CD34 has been shown to be critical for satellite cells' effective entrance into the proliferation stage. Pax7 and MyoD expression were measured in single fiber cultures to look at the satellite cells' movement through the myogenic process. Inactive satellite cells show high expression of Pax7. However, these cells begin to express MyoD upon entering the cycle and ultimately Pax7 is down-regulated while committing to differentiation. Differentiation-committed myoblasts (Pax7- MyoD+) were absent in CD34 KO fibers at 48-hour time-point in culture compared to their presence in WT fibers. After 72 hours of culture, the frequency of these myoblasts is observed to be significantly lesser in CD34 KO fibers compared to the WT fibers. Hence, satellite cells lacking CD34 experience postponement while progressing through the myogenic program (Alfaro et al., 2011).

CD34 has been shown to facilitate inflammation by affecting neutrophil recruitment in the intestines of mice infected with *S. Typhimurium* (Salmonella) (Grassl et al., 2010). Upon oral streptomycin pretreatment and challenge with *S. Typhimurium*, CD34 KO mice had milder caecal inflammation compared to C57/Bl6 WT mice, as evident from the caecal contents of WT mice which were full of infected exudate at day-5 post-infection compared to brown-colored feces of CD34 KO mice at day-5. Caecal weights, which is inversely correlated to inflammation, were significantly lighter in infected WT mice compared to infected CD34 KO mice, showing that CD34 KO mice mount a weaker inflammatory response as compared with WT mice. H&E staining revealed that the caecum of WT mice had severe changes in pathology day-2 post-infection, with necrotic epithelial cells occupying the lumen, damaged crypt architecture, and extensive edema in the submucosa. Whereas, caecum of CD34 KO was not as inflamed: feces occupied the lumen, necrotic cells were scarce, and integrity of crypt architecture was mostly maintained, despite the invasion of the mucosa by inflammatory cells. Five days after infection, caecum of the WT mice was in a serious pathological state as the necrotic epithelial cells, and polymorphonuclear neutrophils were closely packed within the lumen, and inflammatory cells completely changed the

mucosal architecture. Whereas the lumen in CD34 KO mice caecum did not show many necrotic cells, and polymorphonuclear neutrophils, however, the mucosal structure did show severe changes like mucinous plugs, and crypt abscesses (Grassl et al., 2010). No difference was observed in the bacterial loads in two groups, thereby, suggesting that attenuated caecal inflammation in CD34 KO was due to the difference in the host inflammatory responses rather than the capacity to regulate the *S. Typhimurium* infection. Neutrophil recruitment after two and five days after infection with *S. Typhimurium* was significantly delayed in CD34 KO mice caecum as compared to WT mice caecum. The analysis was carried out using H&E staining, naphthol AS-D acetate esterase staining which highlights granulocytic cells like neutrophils and mast cells, and myeloperoxidase immunostaining, since neutrophils express a high amount of myeloperoxidase (Grassl et al., 2010).

In a mouse model of ulcerative colitis induced orally by dextran sulfate sodium (DSS), CD34 deficient mice showed significantly lesser colitis as compared with WT mice (Maltby et al., 2010). Flow cytometric analysis revealed that colon tissue of DSS-challenged WT mice had a significantly higher percentage of CD34 expressing eosinophils than CD34 KO mice. Furthermore, immunostaining against the eosinophil-specific major basic protein (MBP) showed that WT mice colon had a higher number of infiltrating eosinophils than the CD34 KO mice colon tissues on day-8 post-DSS administration. The bone marrow chimera experiments, whereby WT mice received the CD34 KO bone marrow, showed less colitis which was comparable to the response of CD34 KO mice to DSS treatment. Thereby, demonstrating the importance of expression of CD34 in eosinophils, which have a hematopoietic origin, in colitis development (Maltby et al., 2010).

Podocalyxin is a CD34-family protein and has been shown to be expressed in the vascular endothelia of rat lungs using immunohistochemistry (Tschernig et al., 2014). Previous studies using immunofluorescence and flow cytometry suggest expression of podocalyxin on the surface of activated rat platelets (Miettinen et al., 1999). Podocalyxin is also involved in the thrombogenic potential of platelets, and activated platelets are crucial in recruiting neutrophil in the vasculature during inflammation (Ma et al., 2008; Tschernig et al., 2014). It is an essential membrane protein of the glomerular epithelium and is necessary for the development of the kidney. In the developmental stage, *Podxl*-/- mice did not form foot processes because of their inability to soften tight junctions (Doyonnas et al., 2001). Takeda et al. used cell aggregation assay to show that podocalyxin functions as an anti-adhesion molecule and maintains an open filtration pathway

between adjacent foot processes in the glomerular epithelium by charge repulsion. Cell adhesion properties of transfected Chinese hamster ovary (CHO)-K1 and Madin-Darby canine kidney (MDCK) cells were studied with the help of cloned rat podocalyxin. CHO-K1 cells expressed high levels of podocalyxin, and showed complete inhibition of cell aggregation, and MDCK transfectants showed significantly decreased collection (~60–80%) compared with parental cells (Takeda et al., 2000).

Debruin et al. used a conditional knock-out mice model to show that podocalyxin expression in lung endothelial cells was responsible for the maintenance of vascular integrity. The selective deletion of podocalyxin in vascular endothelial cells (*PodxlΔEC*) using Cre-lox system under the control of *Cdh5* (VE-cadherin) promoter led to higher lung volume as well as higher levels of elastin-free collagen fibrils which point towards irregular lung growth in adult mice. Upon using Evan's blue dye vascular leakage assay, they found that *PodxlΔEC* mice lungs had significantly higher vascular permeability as compared to the control group mice, this difference magnified after LPS-induced lung inflammation. However, no apparent change in lung edema, vascular density or endothelial cell frequency was observed. The higher lung vascular permeability in *PodxlΔEC* mice can be attributed to abnormal laminin-dependent cell-matrix interactions as studied by plating the isolated endothelial cells on protein (collagen I, fibronectin or laminin) coated plates 90 min (static adhesion assay) or with protein coated well inserts for 48-hours (cell spreading assay) (Debruin et al., 2014).

In a recent study, Cait et al. used electrical cell substrate impedance sensing and live imaging to show that the human umbilical vein endothelial cells with siRNA silenced podocalyxin fail to form an efficient barrier when plated on extracellular matrix substrates. They also lacked adherence junctions as well as focal adhesions, along with disorganized cortical actin cytoskeleton (Cait et al., 2019).

2.6 CD34 and lung inflammation:

Mucosal dendritic cells have been shown to express CD34. CD34 KO DCs were unable to present antigen to T cells while preserving the innate inflammatory response (Blanchet, 2011). The researchers found that dendritic cells purified from the spleen of CD34 KO mice displayed defective migration in response to the chemotactic gradient (Blanchet, 2011). Ultimately, CD34 KO mice which were enabled with the human CD34 transgene expression gained the ability to develop hypersensitivity pneumonitis. In this murine hypersensitivity pneumonitis (Th1/Th17-dependent disease) model, CD34 KO mice were protected against the development of hypersensitivity pneumonitis.

In a mast cell and eosinophil-dependent asthma (Th2-dependent) model, eosinophils from CD34 KO mice show significantly less pulmonary migration compared with eosinophils from WT mice. CD34 KO and WT mice mount a comparable immune response. CD34 KO mice were resistant to allergic asthma development in this model. The data suggest that CD34 plays a vital role in the cell trafficking by acting as an anti-adhesive or pro-adhesive molecule, depending on the cell and tissue type (Blanchet et al., 2007).

Lo et al. showed that mice lungs lacking CD34 expression on the non-hematopoietic cells demonstrated higher sensitivity to bleomycin-induced lung injury. CD34 KO mice experienced extreme weight loss as well as early mortality compared to WT mice when challenged with bleomycin endotracheally. The response to was dose-dependent. At an early time point of three- and six-days post-bleomycin challenge, no difference was observed between the two groups in the total CD45+ leukocyte counts in the bronchoalveolar lavage fluid, or in the proinflammatory cytokine levels (IL-1β, CXCL1, IL-6, and TNF-α) in the lung tissues. However, Miles assay revealed that CD34 KO mice lungs experienced higher vascular leak than the WT mice six days after bleomycin challenge. Ultrastructural analysis using transmission electron microscopy (TEM) revealed exposed collagen in the interstitium suggesting widespread interstitial edema and delamination of the endothelium in the mice lungs lacking CD34. Thereby implicating CD34 in alveoli's structural integrity maintenance (Lo et al., 2017).

Nevertheless, to my knowledge, only one report is available on the expression and role of CD34 in neutrophil recruitment during acute lung inflammation (Lo et al., 2017). Considering the role of CD34 in cell shape and attachment (Delia et al., 1993; Ohnishi et al., 2013), and its role in leukocyte recruitment in allergic (Blanchet et al., 2007) and hypersensitivity models (Blanchet, 2011), it is hypothesised that CD34 KO mice will show altered vascular permeability, endothelial/leukocyte adhesion, and thus, transmigration in response to intranasal endotoxin (Lipopolysaccharide, LPS) compared with the WT mice.

2.7 Hypothesis and objectives

Hypothesis: CD34 KO mice will show lower vascular permeability, cytokine and chemokine release, and leukocyte transmigration in response to intranasal endotoxin (Lipopolysaccharide, LPS) compared with the WT mice

Objectives: To study LPS induced inflammatory response in the lungs of CD34 KO mice compared with WT mice

2.8 Rationale for experiments

Given CD34 expression on vascular endothelial cells and leukocytes and only one published report on the role of CD34 in acute lung inflammation (Lo et al., 2017), this possible relationship warrants further study. Considering the role of CD34 in cell shape and attachment (Delia et al., 1993; Ohnishi et al., 2013), and its role in leukocyte recruitment in allergic (Blanchet et al., 2007) and hypersensitivity models (Blanchet, 2011), we hypothesized that CD34 KO mice will show lower vascular permeability, cytokine and chemokine release, and lower leukocyte transmigration in response to intranasal endotoxin (Lipopolysaccharide, LPS) compared with the WT mice.

CHAPTER 3: MATERIALS AND METHODS

3.1 Animals:

Ten- to twelve-week-old C57BL/6 WT mice were purchased from Charles River (Montreal, QC, Canada). CD34 knock-out mice were received from Dr. McNagny lab at University of British Columbia and were bred at the Lab Animal Service Unit (LASU, University of Saskatchewan, SK, Canada). Age-matched mice were used in all experiments. All experiments were approved by University Committee on Animal Care and Supply (UCACS) and Animal Research Ethics Board (AREB) of the University of Saskatchewan (Saskatoon, SK, Canada).

Mice from each phenotype (i.e. WT and CD34 KO) were divided into five sub-groups comprising of 0, 3, 9, 15 and 24 h LPS treatment time-points (Fig.3.1). Each time-point had five-seven WT mice and five-seven CD34 KO mice. The 0 h time point reflects no LPS treatment. Both male and female mice were used for experiments. Each time point contained at least three mice of each gender for each phenotype. Sample size calculation was performed using OpenEpi online tool (http://www.openepi.com/), with two-sided confidence level (i.e. 1-α) set at 95% and power (i.e 1-β) set to 80%. The calculation yielded a sample size of 8-13 animals/phenotype (for each time-point).

3.2 Induction of lung injury:

Mice aged 12- to 16-week were anesthetized by isoflurane inhalation, and LPS (from Escherichia coli O55:B5; Sigma-Aldrich, Oakville, ON, Canada) diluted in sterile saline (1 g/L) was administered via intranasal route (50 µL/mice). Control mice at 0 h time point did not receive LPS. After 3, 9, 15 or 24 h, mice were sacrificed by cardiac puncture under deep terminal anesthesia induced by isoflurane. Blood was collected in acid citrate dextrose containing tubes. The blood

(100 µL) from each non-coagulated sample was taken to PDS (Prairie diagnostic services, Saskatoon, Canada), plasma from rest of the blood sample was stored at -80°C. PDS performed total and differential cell counts on the blood samples. Right lung was flash frozen in liquid nitrogen and stored in -80°C for MPO estimation to determine lung neutrophil migration. The left lung was fixed in 4% PFA, 0.1% glutaraldehyde and paraffin embedded.

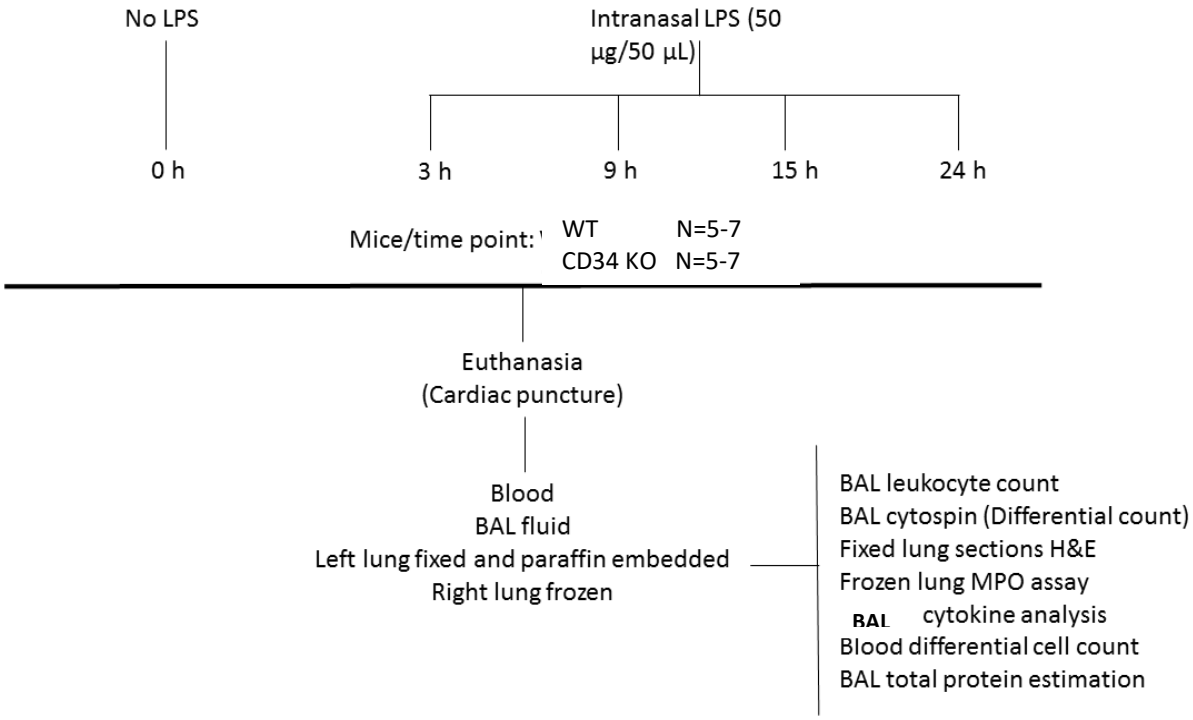

Fig.3.1: Experimental set-up: A schematic of the experimental set-up showing various time points of bronchoalveolar lavage (BAL), peripheral blood and tissue collection for various downstream assays from WT (N=6-7 per time-point) and CD34 KO (N=6-7 per time-point). The left lung was perfused with cold saline to get rid of circulating blood, fixed via tracheal intubation with 4% paraformaldehyde and 0.1% glutaraldehyde and paraffin embedded. The frozen tissue (using liquid nitrogen), BAL supernatant and plasma were stored at -80°C until further analysis.

3.3 Broncho-alveolar lavage (BAL) analysis:

Trachea was exposed through a midline incision and a sterile 23-gauge lavage tube was cannulated. Bilateral BAL was performed by instilling 0.5-ml sterile saline, thrice. Cytospin preparations were stained with Giemsa to obtain BAL differential cell counts (macrophage, neutrophil, monocyte and lymphocyte). Alveolar macrophages are bigger in size compared to monocyte. Thus, we differentiated them during counts based on size. The total BAL leukocyte count for each sample was calculated by adding the absolute differential counts (macrophage, neutrophil, monocyte and lymphocyte). BAL supernatant was stored at -80°C for cytokine analysis using ELISA.

3.4 Myeloperoxidase assay:

Myeloperoxidase (MPO) estimation was performed to indirectly quantify the number of neutrophils left behind in the lung tissue after BAL fluid removal. The right mouse lung sections stored at -80°C were mechanically homogenized in 500 µL of 50 mM HEPES (pH 8.0). Supernatant was discarded after centrifugation (10,000 g, 20 mins) and the pellet was resuspended in 500 µL of 0.5% CTAC. Resuspended pellets were homogenized and were centrifugated, the resultant supernatant was aliquoted into new tubes. A standard curve was made by using myeloperoxidase from human leukocytes (M6908- 5UN; Sigma-Aldrich). Sample (10 µl) was pipetted into separate wells of 96-wells microtiter plates in duplicates. Followed by 65 µL phosphate citrate. Lastly, 100 µL of TMB substrate was added and samples were incubated for 5 min to allow color development. After incubation, 150 µL stop solution was added to each well and absorbance were measured at O.D. 450 nm with a spectrophotometer.

3.5 Immunofluorescence staining (IF):

IF was performed to look at the neutrophil marker Gr1 and vWF, which is an endothelium marker, in WT and CD34 KO mice across different time-points. Tissue sections were deparaffinized with xylene and rehydrated in an ethanol series. Endogenous peroxidase activity was inactivated with

0.5% H_2O_2 in methanol in dark for 20 mins at room temperature. After washing, antigen retrieval was performed in two steps. Firstly, heat induced epitope retrieval (HIER) was performed by incubating sections in sodium citrate buffer (10 mM, pH 6.0) at 90°C-95°C for 20 minutes. Then, the sections were allowed to cool in distilled water, following which the sections were incubated with warmed pepsin (2 mg/ml in 0.01 N HCl) at 37°C for 20 min. After washing, they were blocked with 1% bovine serum albumin in 1% PBS for 30 min at room temperature. The sections were then incubated overnight at 4°C with 100 µL primary antibodies per section against Von Willebrand Factor (A0082, 1:300, Dako Denmark A/S, Glostrup, Denmark) and Gr-1 (rat anti-mouse, 1:100; 550291; BD Biosciences, ON, Canada. Next day, the slides were left at room temperature for 30 min followed by washing with PBS 1X thrice. After washing, they were incubated with 100 µL secondary antibody per section (AF488, green) for 30 min at room temperature (in dark). After washing, sections were counterstained with DAPI. Sections were then allowed to dry, and cover slips were mounted with Prolong gold mounting medium. Media was then allowed to cure for 24 hours before sealing the cover slip with nail varnish. Stained slides were stored in dark at 4°C.

3.6 Broncho-alveolar lavage (BAL) total protein estimation assay:

Total protein concentration estimation in the BAL supernatant was performed using a colorimetric assay, *DC*™ Protein Assay (Bio-Rad, *DC*™ Protein Assay, California, USA). The assay was performed to determine the amount of protein in the alveoli which was washed off with BAL. The amount of protein in the BAL supernatant is associated with the vascular permeability of the lungs. This assay is a modified version of Lowry assay. Standard or samples (5 µl each) of BAL fluid were pipetted into separate wells of 96-wells microtiter plates in duplicates. This was followed by adding 25 µl of Reagent A' (1 mL alkaline copper tartrate solution Reagent A + 20 µl surfactant solution Reagent S) to each well. Lastly, 200 µl of Reagent B (dilute Folin reagent) was added to each well. The samples were incubated for 15 minutes and the absorbance was measured at 750 nm by spectrophotometer.

3.7 Histology:

Left lung was harvested and fixed in 4% PFA, and 0.1% glutaraldehyde. Lungs were embedded in paraffin. Four-micrometer sections were stained with Hematoxylin and eosin (H&E) stain and analyzed by a pathologist who was blinded for groups. Lung perivascular, peribronchiolar and septal inflammation and damage was analyzed and semi-quantitatively scored. Inflammation levels were scored based on congestion, neutrophil infiltration, and endothelial damage. The higher level of congestion, endothelial damage and neutrophil infiltration correspond to a higher score for overall inflammation. Absence of inflammation was recorded as "0", minimal inflammation as, "1", moderate inflammation as, "2" and intense inflammation as, "3".

3.8 Cytokine analysis:

Cytokine studies were performed to characterize the differences in LPS induced inflammation among WT and CD34 KO mice. Cytokine levels were studied in BAL fluid supernatant using commercially available ELISA kit, Bio-Plex Pro™ Mouse Cytokine 23-plex Assay (#m60009rdpd, Bio-Rad, California, USA) which is based on fluorescent multiplex ELISA. The cytokines and chemokines included in the panel are TNFα, IL-6, IL-1β, MCP-1, KC, IL-10, IL-1α, IL-2, IL-3, IL-4, IL-5, IL-9, IL-12 p40, IL-12 p70, IL-13, IL-17A, G-CSF, GM-CSF, IFN-γ, MIP-1α, MIP-1β, RANTES, and Eotaxin. All procedures were carried out according to the manufacturer's instructions. Samples were loaded in duplicates, and signal detection was done using the Luminex Bio-Plex 200 system.

3.9 Statistical analyses:

Statistical analysis was performed using GraphPad Prism software version 8 (San Diego, CA, USA). Quantitative results were expressed as mean and error bars represented standard deviation. Normal distribution of residuals was tested by histogram and Shapiro-Wilk test. The datasets which

were lognormal (as per the Shapiro-Wilk test), were subjected to logarithmic transformation, followed by two-way ANOVA (Analysis of Variance) with Dunnett's multiple comparisons test. The critical value of α was set to 0.05 as a significant difference (two-tailed).

CHAPTER 4: RESULTS

4.1 Effect of CD34 on the peripheral blood counts:

Cell counts were performed on the blood samples using automatic cell counter to study if lack of CD34 had an effect on peripheral blood counts (Fig.4.1). Two-way ANOVA of total WBC show that interaction effect was significant (p=0.0349), while main effects were not significant. However, as shown in Fig.4.1, no difference was observed between WT and CD34 KO mice at any of the time-points. Segmented neutrophils (SEG) in blood samples were also analyzed with two-way ANOVA (Fig.4.2). Main effect of time-point post-LPS challenge was significant (p=0.0315), suggesting that intranasal LPS instillation induced a time-dependent response in the relative percentage of segmented neutrophils. Compared to CD34 KO at 0 h, CD34 KO at 15 h had a 3.5-fold increase in the relative percentage of SEG (p=0.0268). In comparison to WT at 0 h, no statistically significant difference was observed at any of the time points (p>0.05). Also, no difference was observed at any of the time-points in the SEG relative percentage between WT and CD34 KO mice (Fig.4.2, p>0.05). Eosinophil relative percentage data was analyzed by using two-way ANOVA (Fig.4.3.A). Main effect of time-point was significant (p<0.0001). Compared to CD34 KO at 0 h, CD34 KO at 3 h had a 1.9-fold decrease (p=0.0297), CD34 KO at 9 h had a 2.6-fold decrease (p=0.0197), CD34 KO at 15 h had a 7.9-fold decrease (p=0.0002), and CD34 KO at 24 h had a 10.5-fold decrease (p<0.0001). WT at 15 h had a 5.5-fold decrease (p=0.0212) and WT at 24 h had a 4.4-fold decrease (p=0.0112), compared to WT at 0 h. No difference was observed in the eosinophil relative percentage at any time-point for WT vs CD34 KO, p>0.05. As shown in Fig.4.3.B, for lymphocyte relative percentage in the blood samples, main effect of time-point was significant (p=0.0272). Indicating that the intranasal instillation of LPS induced time-dependent changes in the lymphocyte relative percentage in blood. Compared to CD34 KO at 0 h, CD34 KO at 15 h had a 2.5-fold decrease (p=0.0122) in the relative percentage of lymphocytes while there was no difference in WT. WT vs CD34 KO showed no difference at any of the time-points, p>0.05.

Lastly, platelet count data (Fig.4.4) in blood samples was evaluated using two-way ANOVA. Interaction effect was significant (p=0.0369); also both main effects, time and strain dependent, were significant. This indicates that the intranasal instillation of LPS induced a decrease in the number of platelets in peripheral blood at later time-points compared to baseline or 0 h. Significant interaction effect shows that the time-dependence is demonstrated by both WT and CD34 KO groups. Compared to WT at 0 h, WT at 3 h had a 1.9-fold decrease (p<0.0001), WT at 9 h had a 1.4-fold decrease (p=0.0385), WT at 15 h had a 1.6-fold decrease (p=0.0137), and WT at 24 h also had a 1.6-fold decrease (p=0.0020). CD34 KO at 15 h had a 1.5-fold decrease (p=0.0125) and CD34 KO at 24 h also had a 1.5-fold decrease (p=0.0027), compared to CD34 KO at 0 h. WT vs CD34 KO showed no difference at any of the time-points, p>0.05.

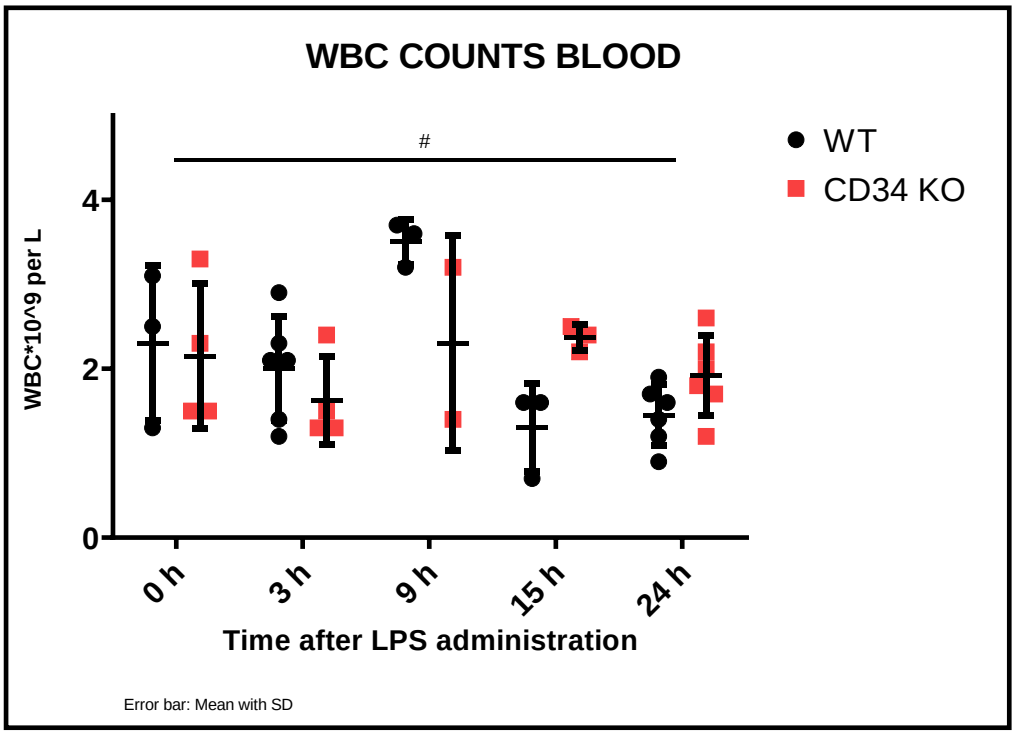

Fig.4.1: WBC Counts in blood samples: White blood cell counts in blood samples at various time points: 0-hour (no LPS; WT, N=3; CD34 KO, N=4), 3 h (WT, N=5; CD34 KO, N=4), 9 h (WT, N=3; CD34 KO, N=2), 15 h (WT, N=3; CD34 KO, N=3) and 24 h (WT, N=6; CD34 KO, N=6) post-LPS treatment with 50 µg LPS. The data is lognormal as per the Shapiro-Wilk test. Hence, logarithmic transformation was applied to the original data, followed by two-way ANOVA with Dunnett's multiple comparisons test. Interaction effect was significant #, F (4,30) = 2.978, p=0.0349; main effect of time-point was non-significant, F (4, 30) = 2.638, p=0.0533; main effect of mouse strain was non-significant F (1, 30) = 0.1153, p=0.7366. WT vs CD34 KO, p>0.05 at all time-points. Results are expressed as mean ± SD.

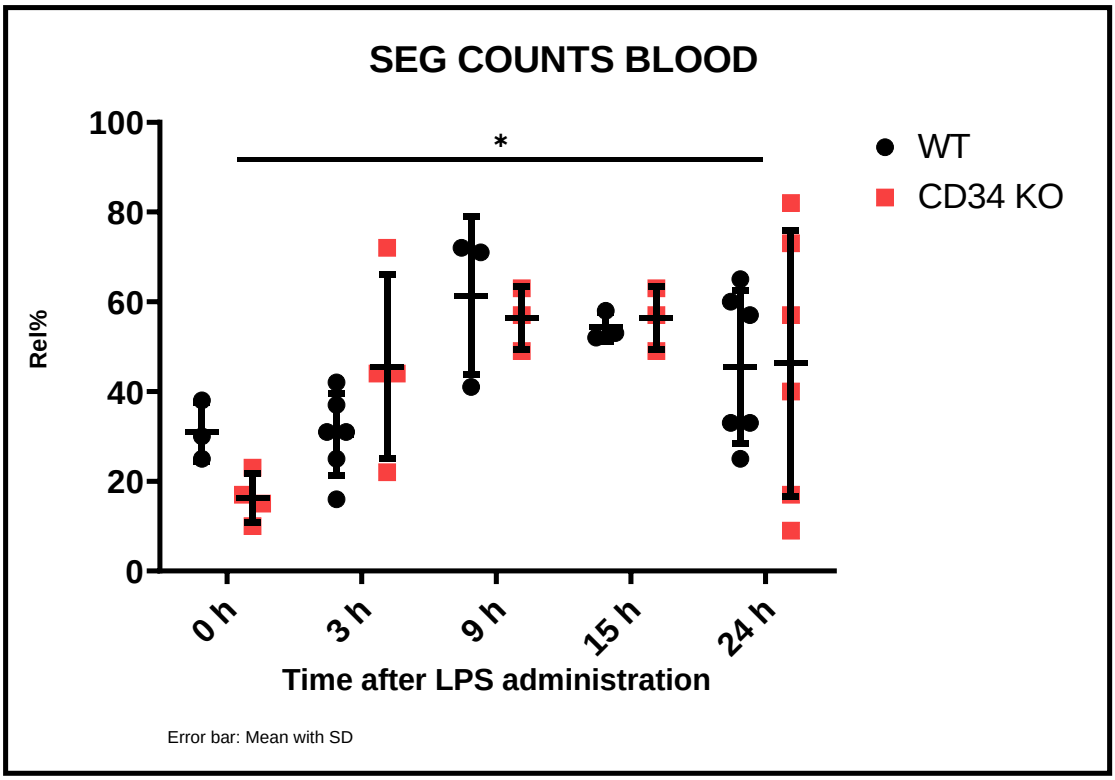

Fig.4.2: SEG Counts in blood samples: Mature (segmented) neutrophil counts in blood samples at various time points: 0-hour (no LPS; WT, N=3; CD34 KO, N=4), 3 h (WT, N=5; CD34 KO, N=4), 9 h (WT, N=3; CD34 KO, N=3), 15 h (WT, N=3; CD34 KO, N=3) and 24 h (WT, N=6; CD34 KO, N=6) post-LPS treatment with 50 µg LPS. The data was analyzed by using two-way ANOVA with Dunnett's multiple comparisons test. Interaction effect was non-significant, F (4,30) = 1.055, p=0.3957; main effect of time-point was significant (*), F (4, 30) = 3.061, p=0.0315; main effect of mouse strain was non-significant F (1, 30) = 3.061, p=0.5846. WT vs CD34 KO, p>0.05 at all time-points. Results are expressed as mean ± SD.

A

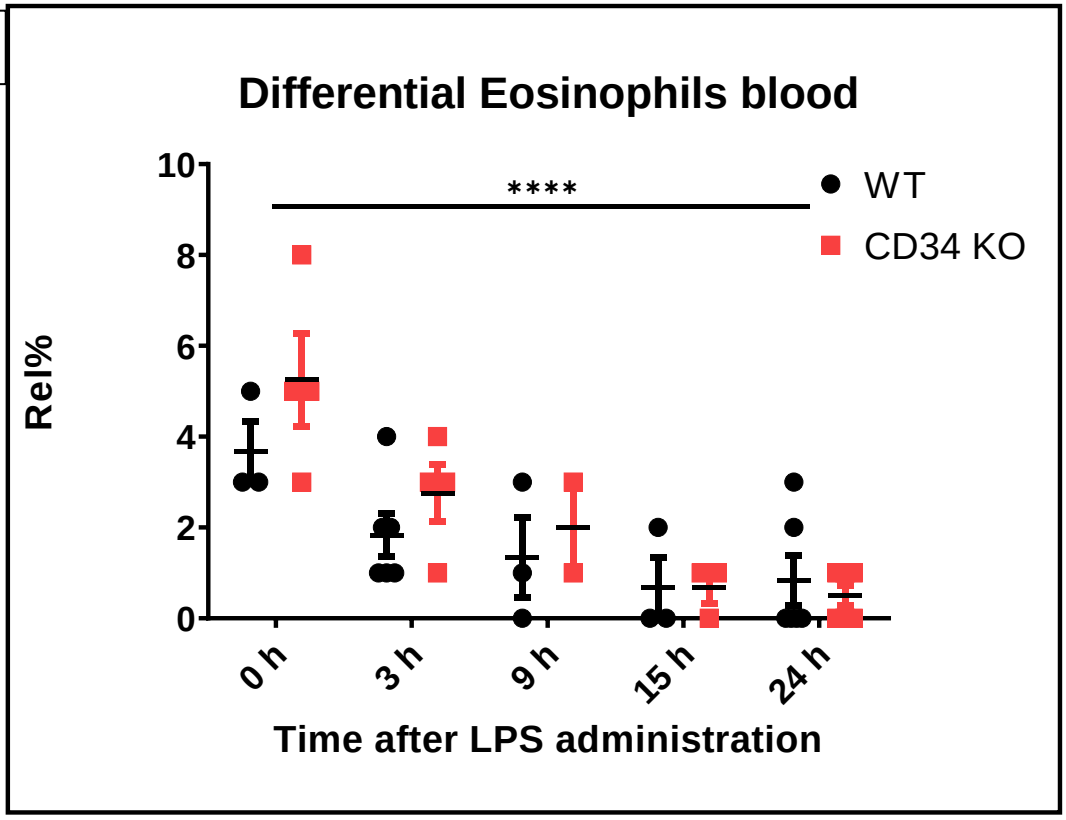
Differential Eosinophils blood
****
WT
CD34 KO
Rel%
10
8
6
4
2
0
0 h
3 h
9 h
15 h
24 h
Time after LPS administration

B

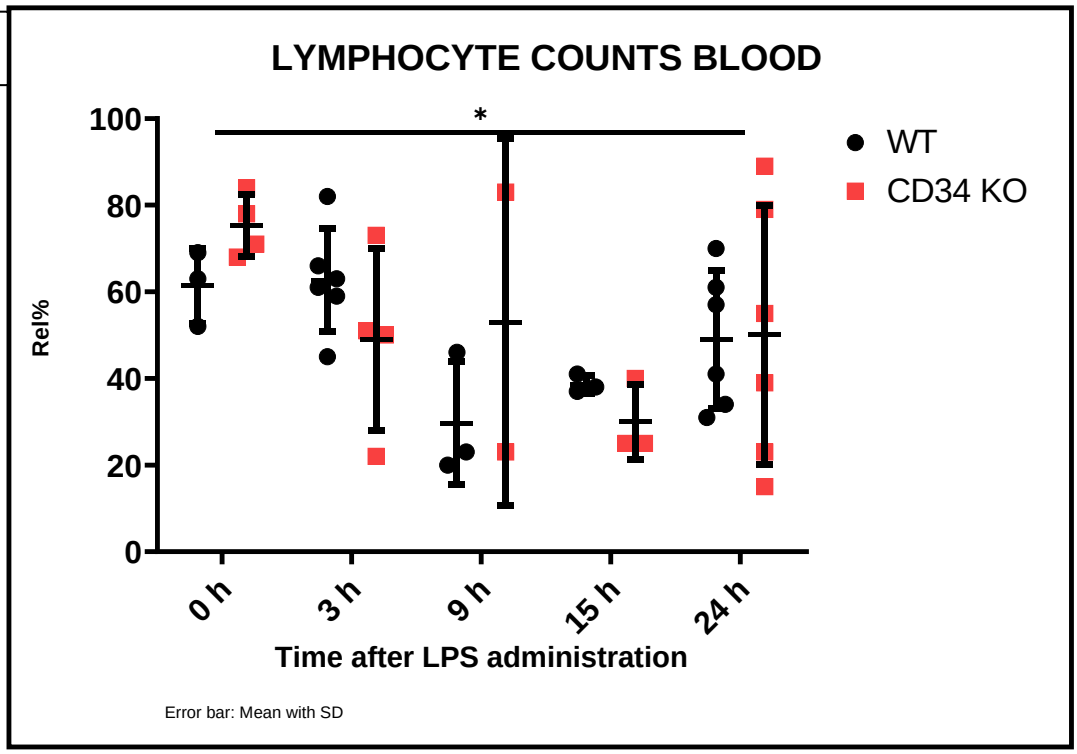
LYMPHOCYTE COUNTS BLOOD
*
WT
CD34 KO
Rel%
100
80
60
40
20
0
0 h
3 h
9 h
15 h
24 h
Time after LPS administration
Error bar: Mean with SD

Fig.4.3.A, B: Eosinophil and Lymphocyte Counts in blood samples: (A) Eosinophil counts in blood samples at various time points: 0-hour (no LPS; WT, N=3; CD34 KO, N=4), 3 h (WT, N=5; CD34 KO, N=4), 9 h (WT, N=3; CD34 KO, N=2), 15 h (WT, N=3; CD34 KO, N=3) and 24 h (WT, N=6; CD34 KO, N=6) post-LPS treatment with 50 µg LPS. The data was analyzed by using two-way ANOVA with Dunnett's multiple comparisons test. Interaction effect was non-significant, F (4,30) = 0.7790, p=0.5477; main effect of time-point was significant (*), F (4, 30) = 11.71, p<0.0001; and main effect of mouse strain was non-significant F (1, 19) = 1.796, p=0.1903. WT vs CD34 KO, p>0.05 at all time-points. (B) Lymphocyte counts in blood samples at various time points: 0-hour (no LPS; WT, N=3; CD34 KO, N=4), 3 h (WT, N=5; CD34 KO, N=4), 9 h (WT, N=3; CD34 KO, N=2), 15 h (WT, N=3; CD34 KO, N=3) and 24 h (WT, N=6; CD34 KO, N=6) post-LPS treatment with 50 µg LPS. The data was analyzed by using two-way ANOVA with Dunnett's multiple comparisons test. Interaction effect was non-significant, F (4,30) = 1.110, p=0.3702; main effect of time-point was significant (*), F (4, 30) = 3.181, p=0.0272; main effect of mouse strain was non-significant F (1, 30) = 0.2576, p=0.6155. WT vs CD34 KO, p>0.05 at all time-points. Results are expressed as mean ± SD.

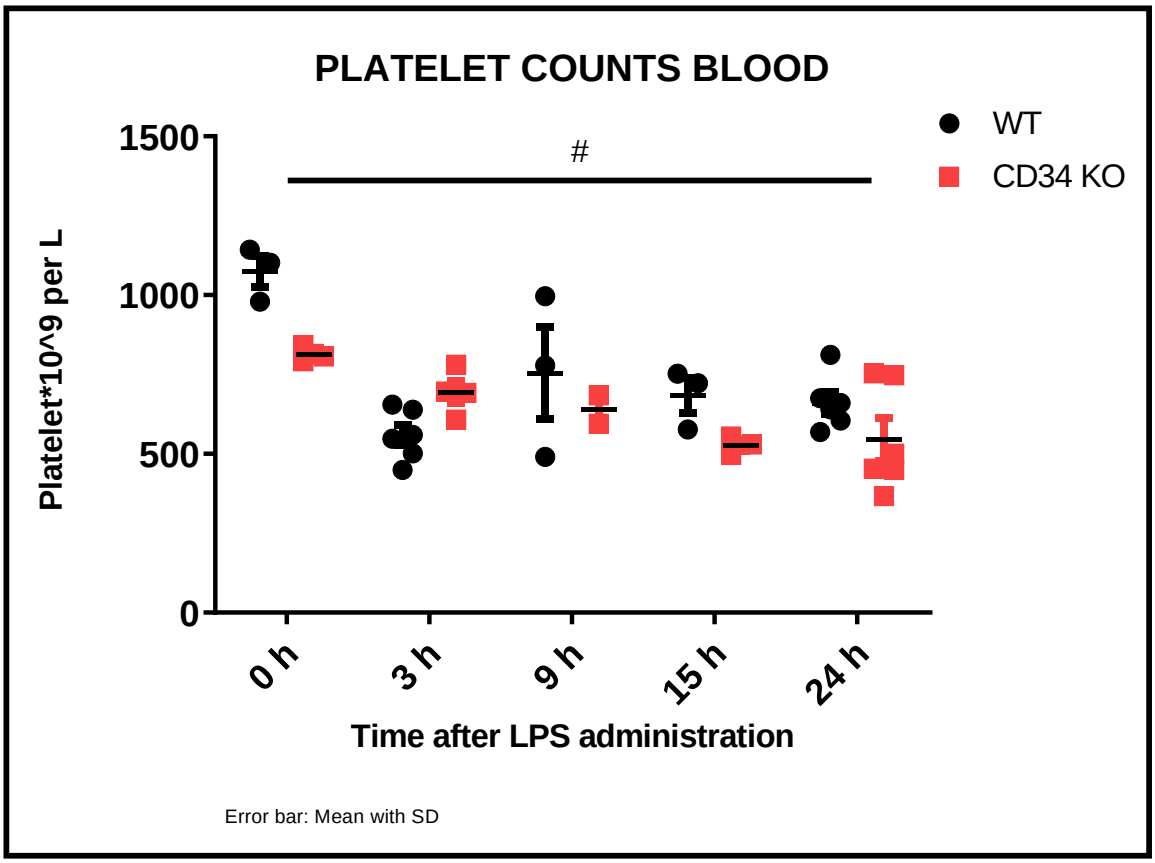

Fig.4.4: Platelet Counts in blood samples: Platelet counts in blood samples at various time points: 0-hour (no LPS; WT, N=3; CD34 KO, N=4), 3 h (WT, N=5; CD34 KO, N=4), 9 h (WT, N=3; CD34 KO, N=2), 15 h (WT, N=3; CD34 KO, N=3) and 24 h (WT, N=6; CD34 KO, N=6) post-LPS treatment with 50 µg LPS. The data is lognormal as per the Shapiro-Wilk test. Hence, logarithmic transformation was applied to the original data, followed by two-way ANOVA with Dunnett's multiple comparisons test. Interaction effect was significant (#), F (4, 30) = 2.934, p=0.0369; main effect of time-point was significant, F (4, 30) = 8.450, p=0.0001; main effect of mouse strain was also significant F (1, 30) = 4.725, p=0.0377. WT vs CD34 KO, p>0.05 at all time-points. Results are expressed as mean ± SD.

4.2 Inflammatory cell migration into the lungs of CD34 knock-out mice and WT mice upon LPS challenge:

To study the role of CD34 in acute lung inflammation, we used an LPS induced lung inflammation model of ALI. To study the development of lung inflammation, we first looked at the BAL cellular content. BAL total leukocyte counts were subjected to a two-way analysis of variance having five time-points (0 no LPS, 3, 9, 15, and 24 h) and two mouse strains (WT and CD34 KO). As shown in 4.5, the main effect of time-point post-LPS challenge was significant ($p<0.0001$), indicating that intranasal LPS instillation induced time-dependent lung leukocyte recruitment, in both WT and CD34 KO mice. Dunnett's multiple comparisons test revealed that there was no statistically significant difference between the total leukocyte counts at any of the post-LPS administration time-points in WT mice compared with CD34 knock-out mice ($p>0.05$).

Next, we looked at the total macrophage counts in BAL (Fig.4.6.A). A two-way ANOVA revealed that both the main effects of time-point post-LPS challenge ($p=0.0003$), and mouse strain ($p=0.0433$), were significant. However, interaction effect was non-significant ($p=0.1523$). Thereby implying that the intranasal instillation of LPS induced time-dependent changes in alveolar macrophage numbers but no difference between WT mice and CD34 KO mice at any of the time-points post-LPS administration ($p>0.05$). In comparison to WT at 0 h, WT at 3 h experienced a 5.9-fold decrease ($p=0.0008$), WT at 9 h had a 5.1-fold decrease ($p=0.0011$) and WT at 15 h had a 6.3-fold decrease ($p=.0066$). While there was a 2.5-fold decrease in CD34 KO at 24 h compared with CD34 KO at 0 h ($p=0.0261$), no difference was observed for rest of the time-points.

A two-way ANOVA of neutrophil numbers (Fig.4.6.B) revealed that there was no interaction effect ($p=0.4445$), but the main effect of time-point post-LPS challenge was significant ($p = 0.0068$), implying that intranasal LPS instillation induced time-dependent changes in neutrophil counts overall, but no difference between the number of neutrophils in the BAL fluid of WT mice and CD34 KO mice at any of the time-points post-LPS administration (Fig.4.6.B).

Myeloperoxidase (MPO) estimation was performed to quantify the number of neutrophils trapped in the lung (Fig.4.7). The main effect of time-point post-LPS challenge was significant ($p<0.0001$). In comparison to WT at 0 h, WT at 3 h experienced an 11.9-fold increase ($p=0.0001$), WT at 9 h

had a 9.4-fold increase (p=0.0008) and WT at 15 h had an 8.8-fold increase (p=.0036). While there was no difference between CD34 KO at 0 h compared with CD34 KO at 3 h, CD34 KO at 9 h had an 8.5-fold increase (p=0.0021) and CD34 KO at 15 h had a 5.6-fold increase (p=0.0065). At 3-hour post-LPS challenge, the MPO content was significantly higher in WT mice compared with CD34 knock-out mice (p=0.0308), but it was comparable in both groups for subsequent time points. Furthermore, immunofluorescence staining was performed with Gr-1 (red) which is a marker for polymorphonuclear leukocytes and certain inflammatory monocytes/macrophages (Fig.4.8); vWF, which is a marker for endothelium and platelets, is stained green; and DAPI, which stains for cell nuclei, is blue. We observed intravascular (within green stained vessels) adherent Gr1 positive neutrophils (red colored polymorphonuclear cells), especially at 9 h in post-LPS exposed WT mice compared to CD34 KO mice. CD34 KO mice show a different pattern of Gr1 positive cells, especially prevalent in alveolar septa (Fig.4.8). The alveolar staining for vWF (platelet aggregates) was not prominent in the CD34 KO mice at post-LPS exposure time-points, 9 h.

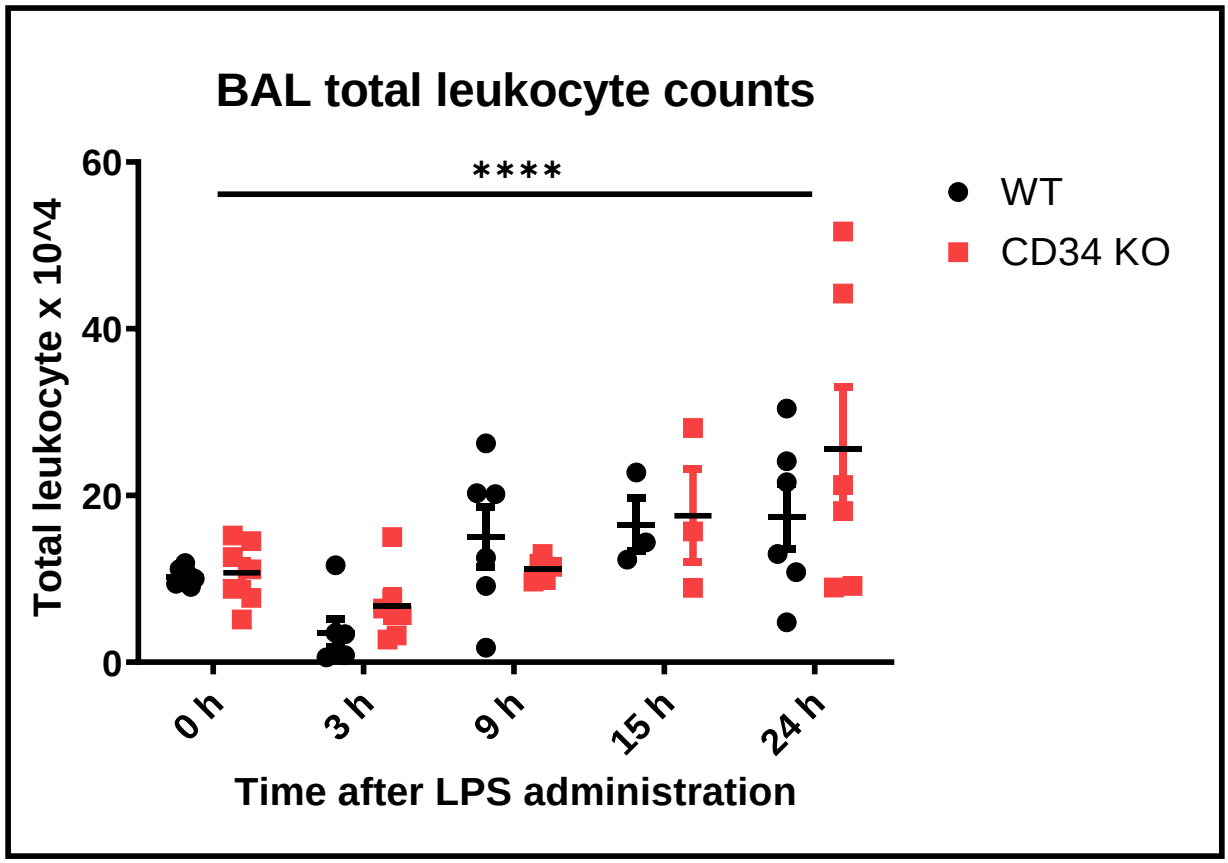

Fig.4.5: BAL Leukocyte Counts: Total Bronchoalveolar Lavage Fluid (BAL) leukocyte counts at 0-hour (no LPS; WT, N=7; CD34 KO, N=7), 3 h (WT, N=6; CD34 KO, N=6), 9 h (WT, N=6; CD34 KO, N=5), 15 h (WT, N=3; CD34 KO, N=3) and 24 h (WT, N=6; CD34 KO, N=6) post-LPS treatment with 50 µg LPS. Data analyzed using two-way ANOVA with Dunnett's multiple comparisons test. Interaction effect was non-significant, F (4,45) = 1.293, p=0.2872; main effect of time-point was significant (****), F (4, 45) = 10.44, p<0.0001; main effect of mouse strain was not significant F (1, 45) = 1.890, p=0.1760. WT vs CD34 KO, p>0.05 for each time-point Results are expressed as mean ± SD.

A

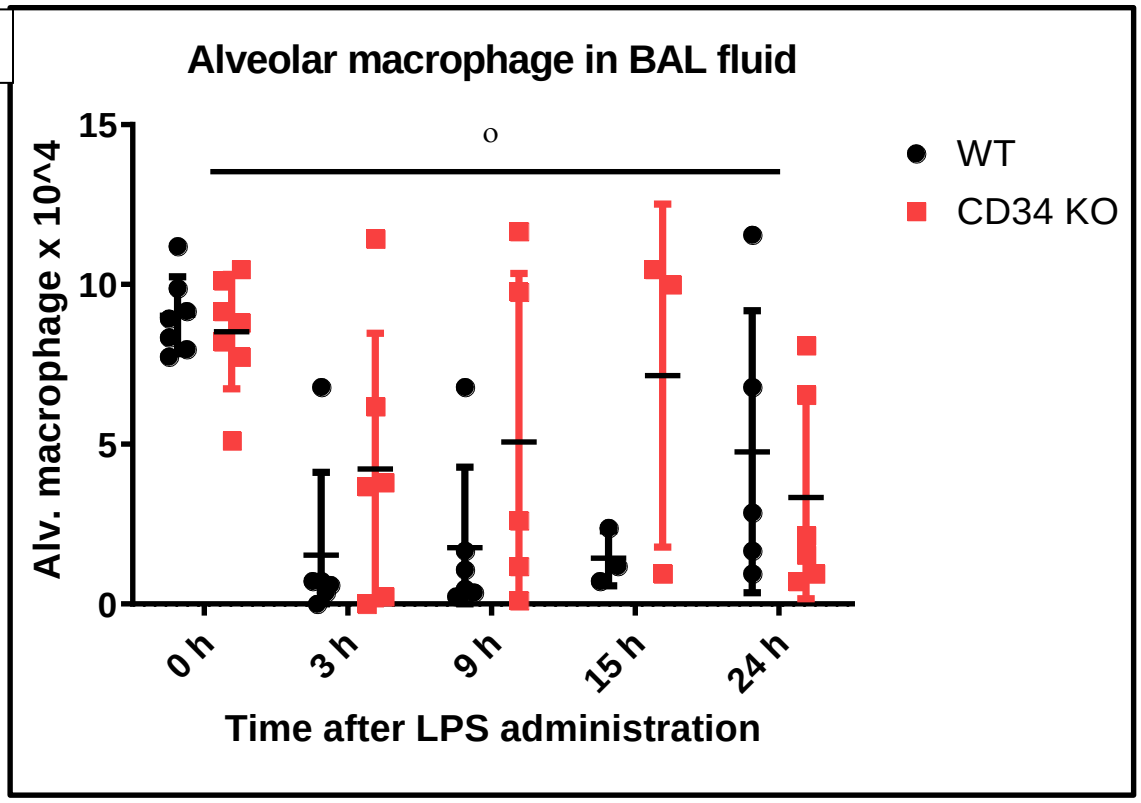
Alveolar macrophage in BAL fluid
o
WT
CD34 KO
Alv. macrophage x 10^4
15
10
5
0
0 h
3 h
9 h
15 h
24 h
Time after LPS administration

B

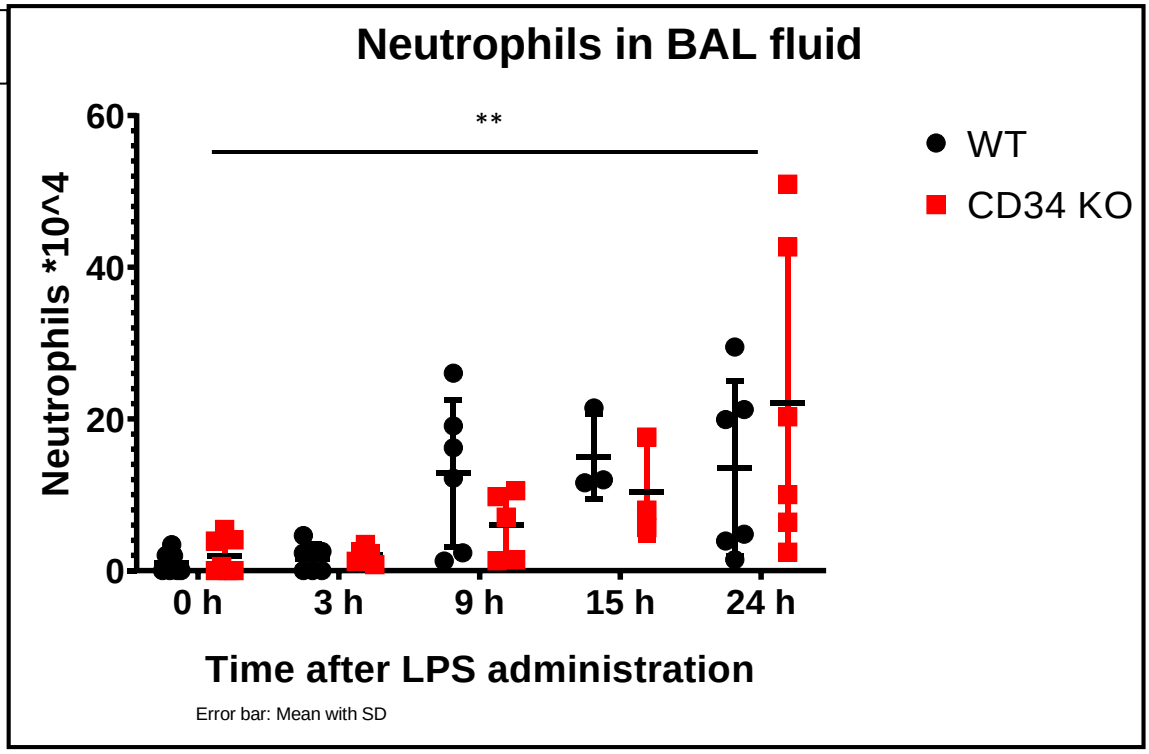
Neutrophils in BAL fluid
**
WT
CD34 KO
Neutrophils *10^4
60
40
20
0
0 h
3 h
9 h
15 h
24 h
Time after LPS administration
Error bar: Mean with SD

Fig.4.6.A,B: Bronchoalveolar Lavage (BAL) Differential Cell Counts: (A) Alveolar macrophage numbers at 0-hour (no LPS; WT, N=7; CD34 KO, N=7), 3 h (WT, N=6; CD34 KO, N=6), 9 h (WT, N=6; CD34 KO, N=5), 15 h (WT, N=3; CD34 KO, N=3) and 24 h (WT, N=6; CD34 KO, N=6) post-LPS treatment with 50 µg LPS. Data analyzed using two-way ANOVA with Dunnett's multiple comparisons test. Interaction effect was non-significant, F (4,44) = 1.769, p=0.1523; main effect of time-point was significant (***), F (4, 44) = 6.709, p=0.0003; main effect of mouse strain was significant (°) F (1, 44) = 4.331, p=0.0433. WT vs CD34 KO, p>0.05 for each time-point **(B)** Neutrophil numbers at 0-hour (no LPS; WT, N=7; CD34 KO, N=7), 3 h (WT, N=6; CD34 KO, N=6), 9 h (WT, N=6; CD34 KO, N=5), 15 h (WT, N=3; CD34 KO, N=3) and 24 h (WT, N=6; CD34 KO, N=6) post-LPS treatment with 50 µg LPS. Data analyzed using two-way ANOVA with Dunnett's multiple comparisons. Interaction effect was non-significant, F (4,38) = 0.954, p=0.4445; main effect of time-point was significant (**), F (4, 38) = 4.167, p = 0.0068; main effect of mouse strain was not significant F (1, 38) = 0.0030, p=0.9562. WT vs CD34 KO, p>0.05 for each time-point. All results are expressed as mean ± SD.

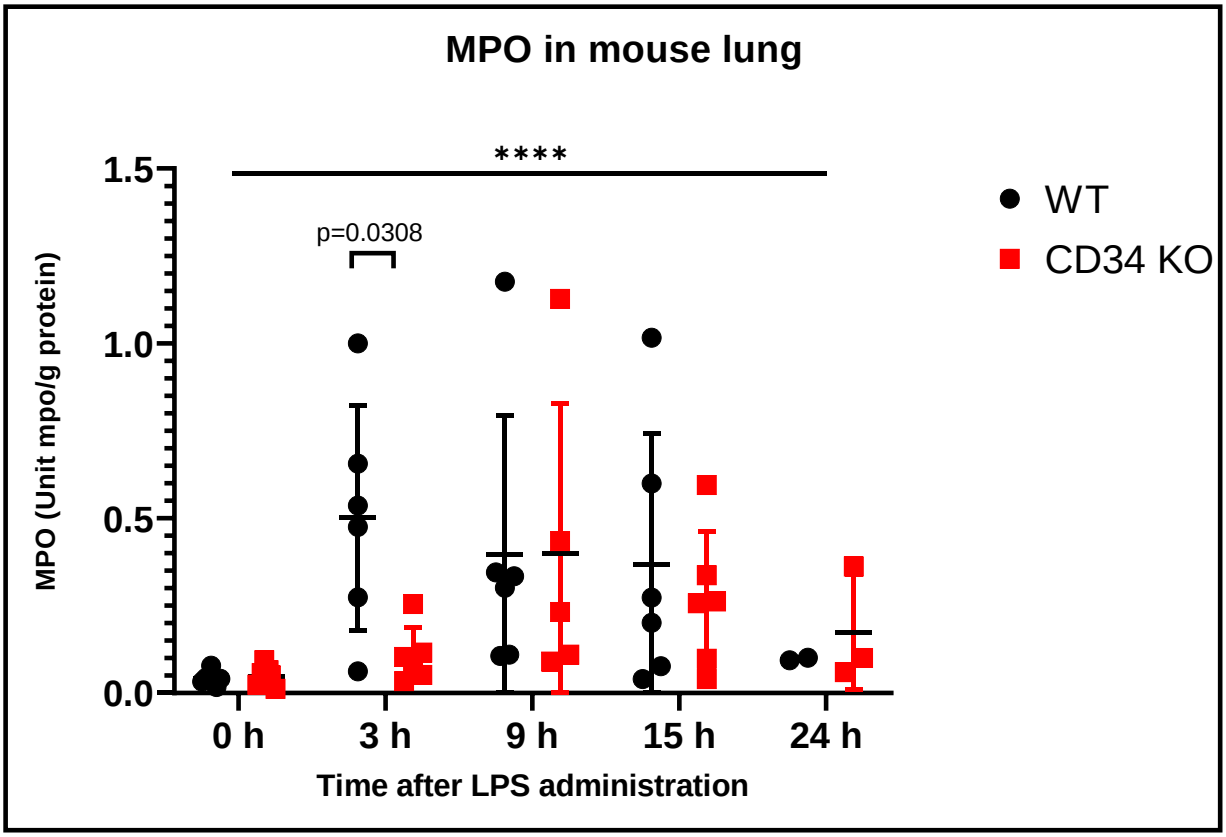

Fig.4.7: Myeloperoxidase estimation in mouse lungs: MPO amount per gram protein at various time points: 0-hour (no LPS; WT, N=7; CD34 KO, N=7), 3 h (WT, N=6; CD34 KO, N=6), 9 h (WT, N=6; CD34 KO, N=5), 15 h (WT, N=6; CD34 KO, N=6) and 24 h (WT, N=2; CD34 KO, N=3) post-LPS treatment with 50 µg LPS. The data is lognormal as per the Shapiro-Wilk test. Hence, logarithmic transformation was applied to the original data, followed by two-way ANOVA with Dunnett's multiple comparisons test. Interaction effect was non-significant, F (4,44) = 1.601, p=0.1910; main effect of time-point was significant (****), F (4, 44) = 9.982, p<0.0001; main effect of mouse strain was not significant F (1, 44) = 1.134, p=0.2927. WT vs CD34 KO at 3 h, p=0.0308. Experiment was performed in duplicates. Results are expressed as mean ± SD.

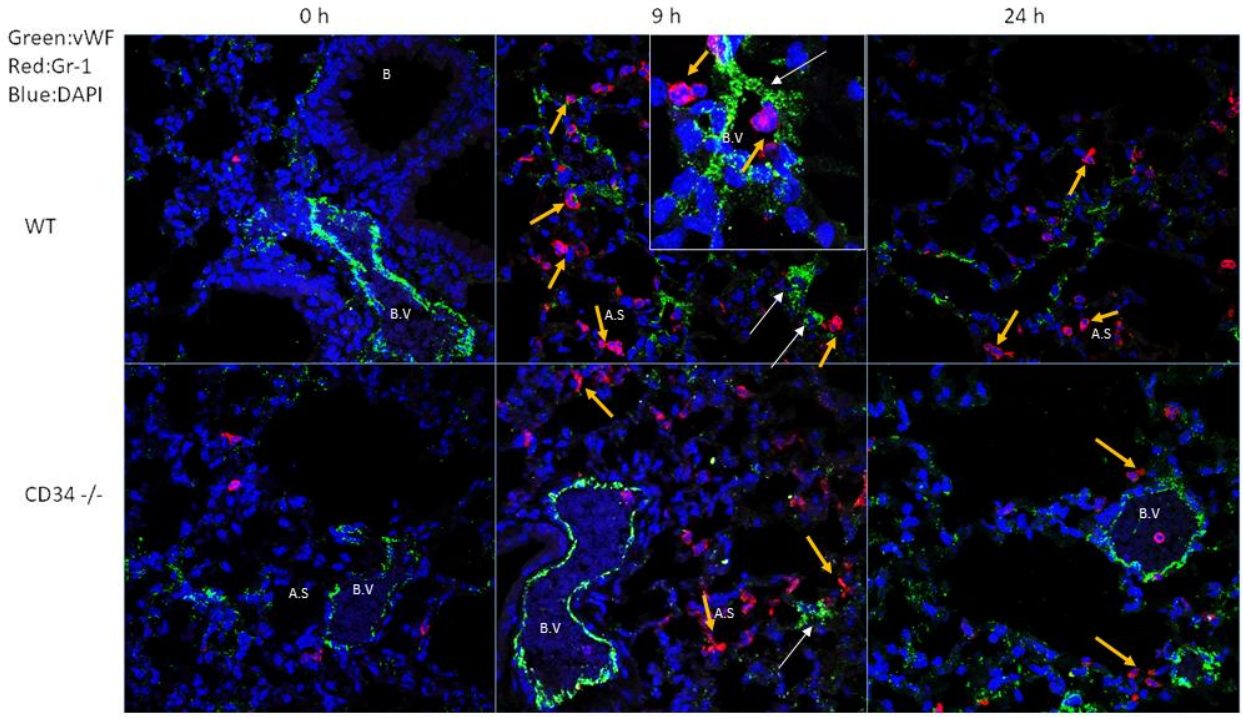

Fig.4.8: Immunofluorescence staining in mouse lung sections: Immunofluorescence staining on mouse lungs was performed for various time points: 0 (no LPS), 9 and 24h in WT (WT, N=2) and CD34 KO (N=2) mice exposed to 50 µg LPS. Red: Gr-1, marker for polymorphonuclear cells or neutrophil granulocytes; Green: vWF, marker for endothelium and platelets; Blue: DAPI, staining for cell nucleus. Representative images from three independent experiments. Note the presence of intravascular Gr1 positive (red colored) polymorphonuclear cell (neutrophils) marked with yellow arrows in WT mice at 9 h post-LPS exposure time-point. CD34 KO mice show a different pattern of Gr1 positive cells, especially prevalent in alveolar septa. Platelet aggregates can be seen (white arrows) as vWF positive (green stained) clusters in alveolar septal post-LPS exposure. B: Bronchiole; B.V.: Blood vessel, A.S.: Alveolar septum. Scale: 50µm, inset 25µm

4.3 CD34 knock-out mice show altered lung pathology upon LPS challenge compared with the WT mice:

Total protein concentration in BAL samples was quantified as a surrogate marker for pulmonary vascular permeability. Two-way ANOVA analysis indicated that main effects of time-point post-LPS challenge ($p<0.0001$) and mouse strain ($p=0.0017$) were significant. Thereby implying that the intranasal instillation of LPS induced time-dependent changes in pulmonary vascular permeability. In comparison to WT at 0 h, WT at 3 h experienced a 4-fold increase ($p=0.0006$), WT at 9 h had a 3.4-fold increase ($p=0.0050$) WT at 15 h had a 5.5-fold increase ($p<0.0001$), and WT at 24 h showed a 3.1-fold increase ($p=0.0026$). While there was a 3-fold increase in CD34 KO at 15 h compared with CD34 KO at 0 h ($p=0.0065$), no difference was observed for rest of the time-points. As shown in Fig.4.9, WT mice have a higher total protein content in the BAL supernatant at 3-hour post-LPS administration compared to the CD34 knock-out mice ($p=0.0452$). The difference in BAL total protein amounts between the two groups was seen at 24 h time-point as well ($p=0.0113$), pointing towards an attenuated vascular permeability in the CD34 knock-out compared to WT mice in response to LPS.

H & E staining was performed on the lung samples from time points 0, 3, 9, 15 and 24 hours. Lungs were congested, and perivascular space was infiltrated with leukocytes as shown at 3 h in WT mice compared to CD34 KO mice (Fig.4.10). At 9, 15 and 24 h post-LPS administration, lungs in the WT mice were congested and perivascular space was infiltrated with leukocytes compared with the CD34 knock-out mice (Fig.4.11). Note at 24 h, there are leukocytes adhering to the large blood vessel (BV) despite perfusion of lungs; alveolar infiltration near a bronchus (B) is significant in both strains showing dissemination of inflammation. Semi-quantitative scoring of lung inflammation was also performed on H & E stained lung sections (Fig.4.12). Two-way ANOVA with Dunnett's multiple comparisons test showed that for perivascular inflammation score, the main effects of time-point ($p<0.0001$) and mouse strain ($p=0.0030$) were significant. For peribronchiolar inflammation score, the main effects of time-point ($p<0.0001$) and mouse strain were ($p=0.0050$). For Septal inflammation score, the main effects of time-point ($p<0.0001$) and mouse strain ($p=0.0009$) were significant. This indicates that LPS induced time-dependent changes in perivascular, peribronchiolar, and septal inflammation in both groups. No difference

between WT and CD34 KO groups was observed in perivascular, peribronchiolar, and septal inflammation scores (Fig.4.12).

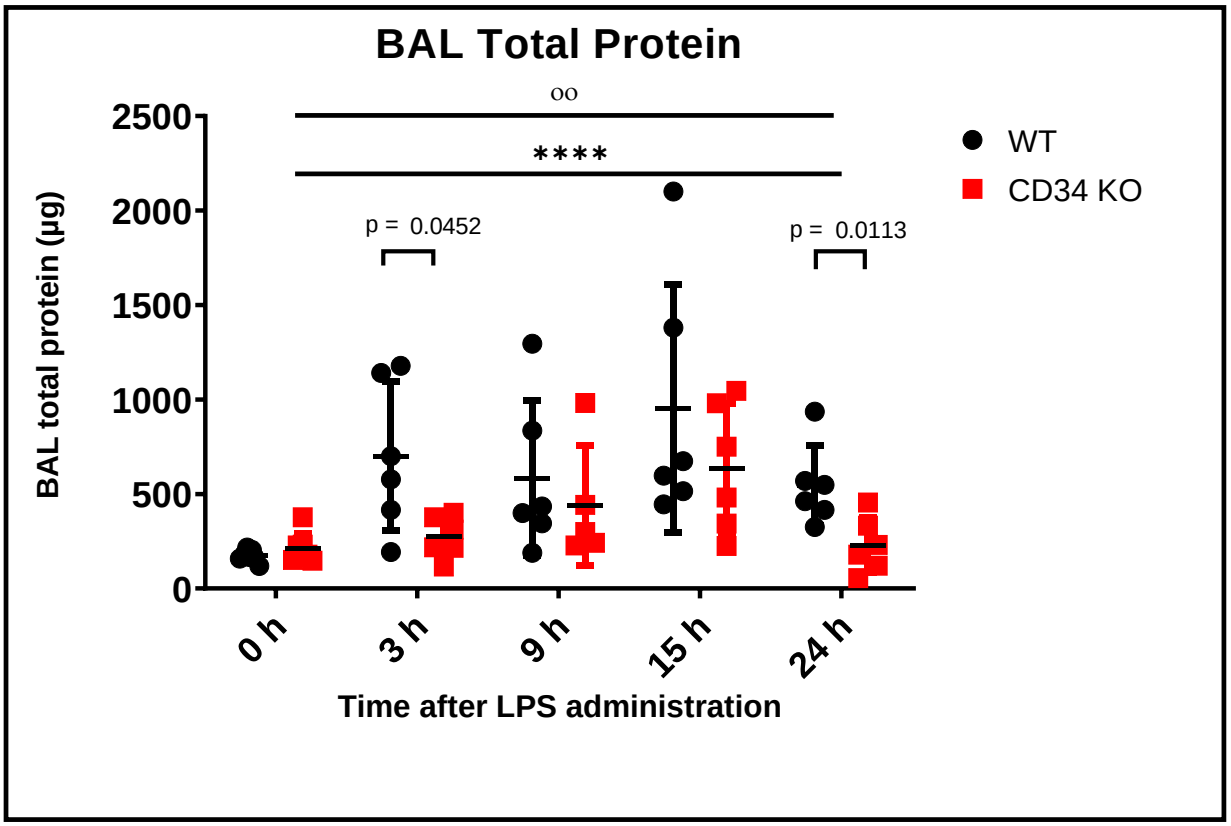

Fig.4.9: BAL Total Protein (µg) estimation assay: Total protein estimation in the BAL samples at various time points: 0-hour (no LPS; WT, N=7; CD34 KO, N=7), 3 h (WT, N=6; CD34 KO, N=6), 9 h (WT, N=6; CD34 KO, N=5), 15 h (WT, N=6; CD34 KO, N=6) and 24 h (WT, N=6; CD34 KO, N=6) post-LPS treatment with 50 µg LPS. The data is lognormal as per the Shapiro-Wilk test. Hence, logarithmic transformation was applied to the original data, followed by two-way ANOVA with Dunnett's multiple comparisons test. Interaction effect was non-significant, F (4,51) = 2.436, p=0.0589; main effect of time-point was significant (****), F (4, 51) = 9.404, p<0.0001; main effect of mouse strain was significant (°°) F (1,51) = 10.95, p=0.0017. WT vs CD34 KO at 3 h (p=0.0452), at 24 h (p=0.0113). Experiment was performed in duplicates. All results are expressed as mean ± SD.

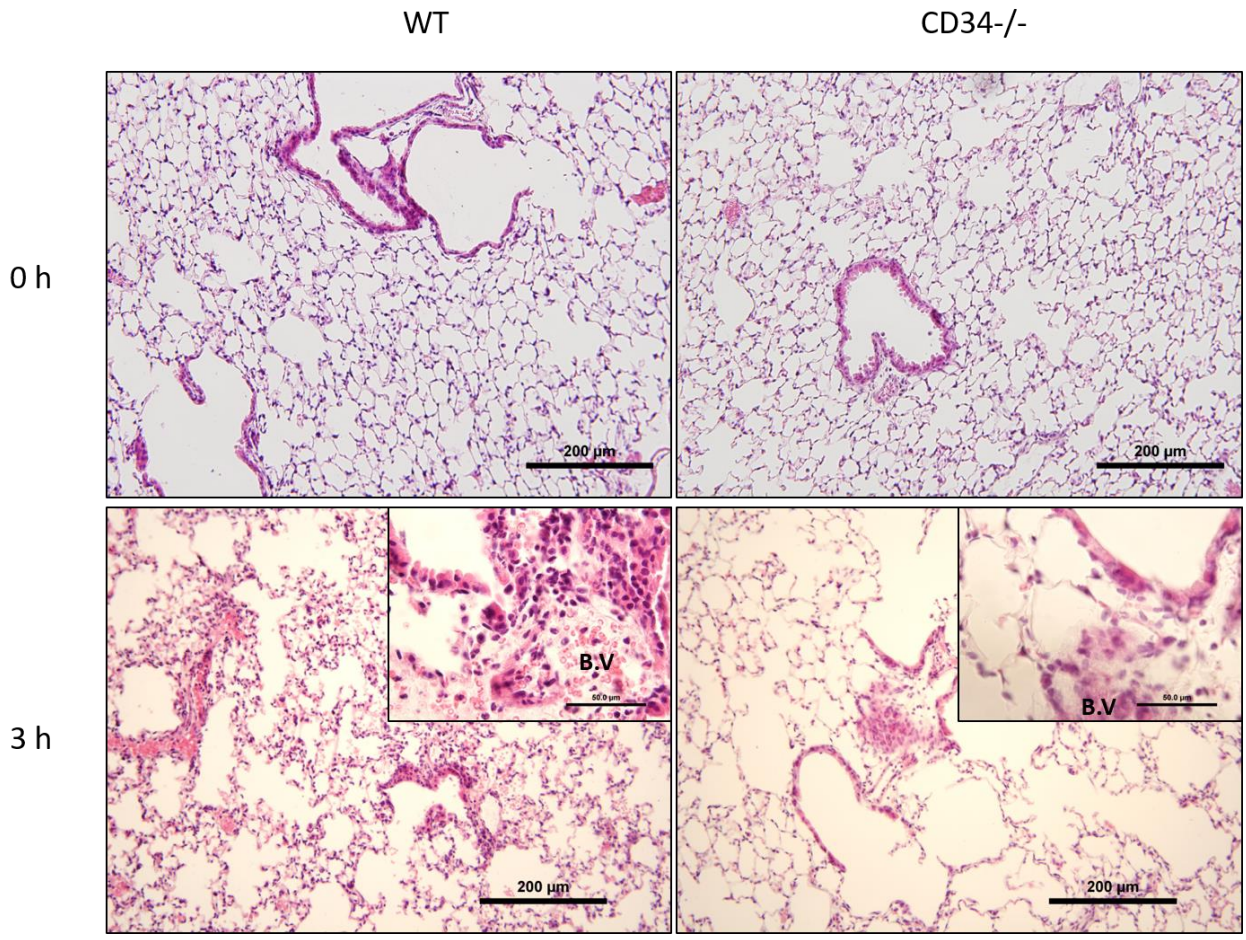

Fig.4.10: Lung H&E Histology (0, 3 h): Representative images from H&E stained perfused left lung from 0-hour (no LPS; WT, N=7; CD34 KO, N=7), and 3 h (WT, N=6; CD34 KO, N=6) post-LPS treatment with 50 µg LPS. Scale bar: 200 µm, inset 50 µm

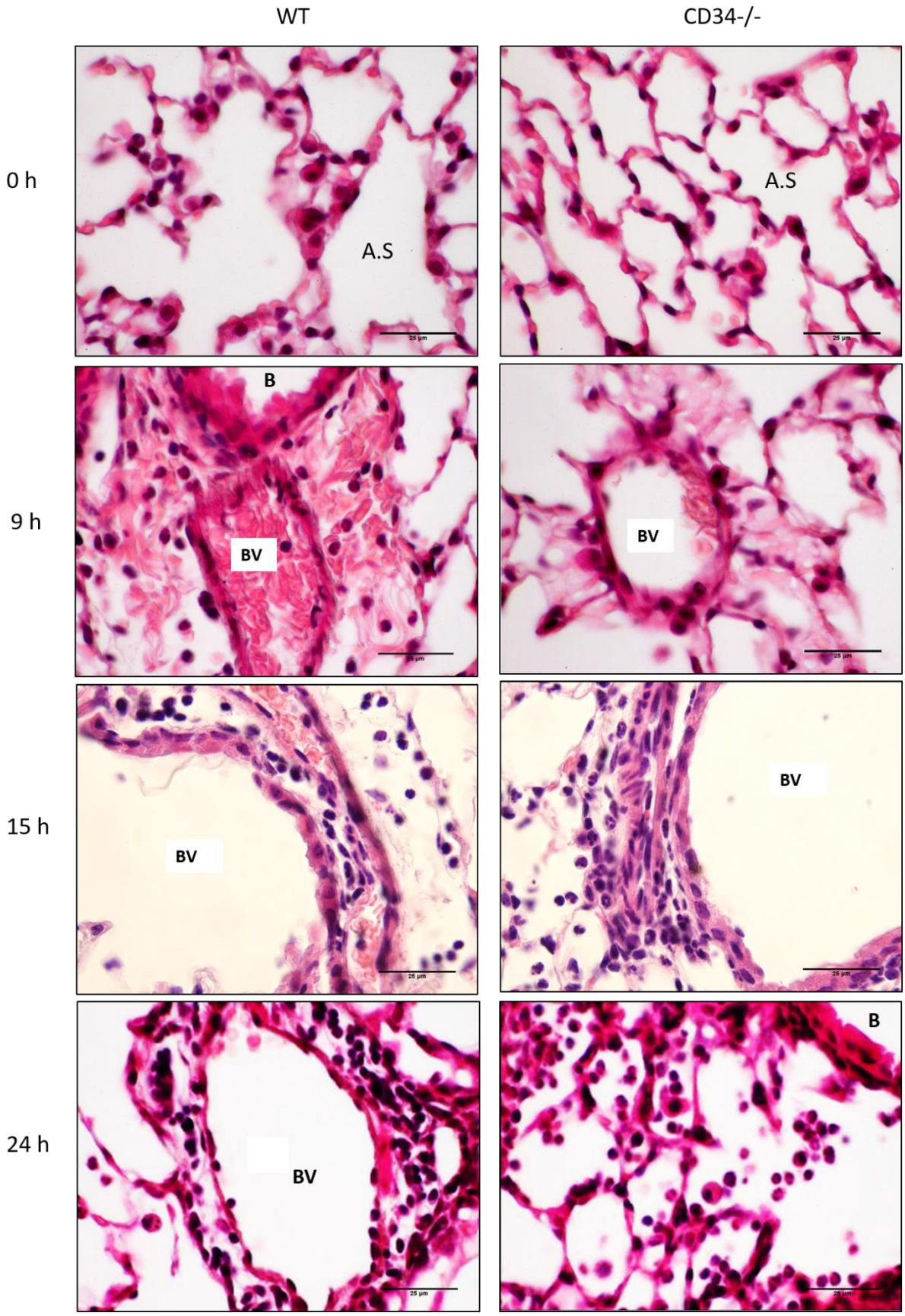
WT
CD34-/-
0 h
9 h
15 h
24 h
A.S
A.S
B
BV
BV
BV
BV
BV
B

Fig.4.11: Lung H&E Histology (0, 9, 15, 24 h): Representative images from H&E stained perfused left lung from 0-hour (no LPS; WT, N=7; CD34 KO, N=7), 9 h (WT, N=6; CD34 KO, N=5), 15 h (WT, N=3; CD34 KO, N=4) and 24 h (WT, N=6; CD34 KO, N=6) post-LPS treatment with 50 µg LPS. Note at 24 h, there are leukocytes adhering to the large blood vessel (BV) despite perfusion of lungs; alveolar infiltration near a bronchus (B) is significant in both strains showing dissemination of inflammation. Scale bar: 25 µm

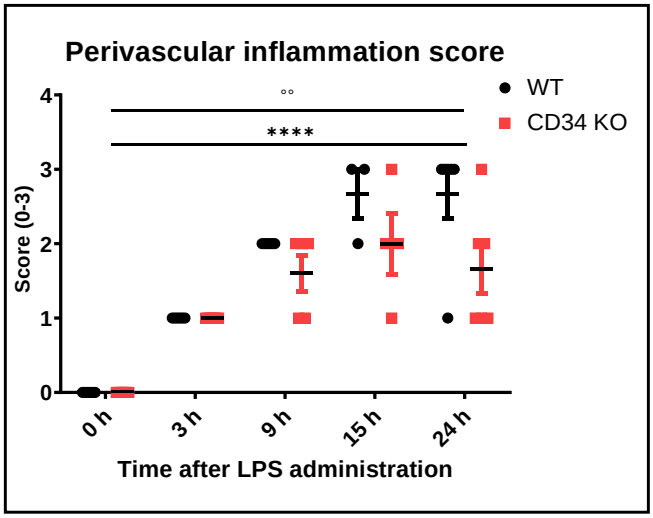
Perivascular inflammation score
WT
CD34 KO
°°
****
Score (0-3)
0
1
2
3
4
0 h
3 h
9 h
15 h
24 h
Time after LPS administration

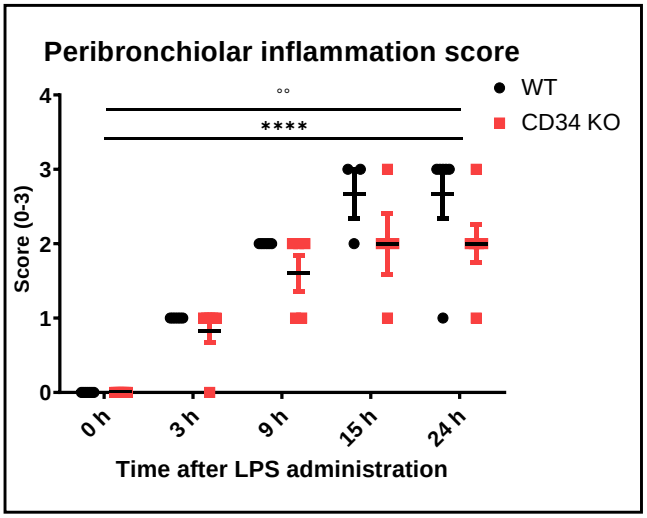
Peribronchiolar inflammation score
WT
CD34 KO
°°
****
Score (0-3)
0
1
2
3
4
0 h
3 h
9 h
15 h
24 h
Time after LPS administration

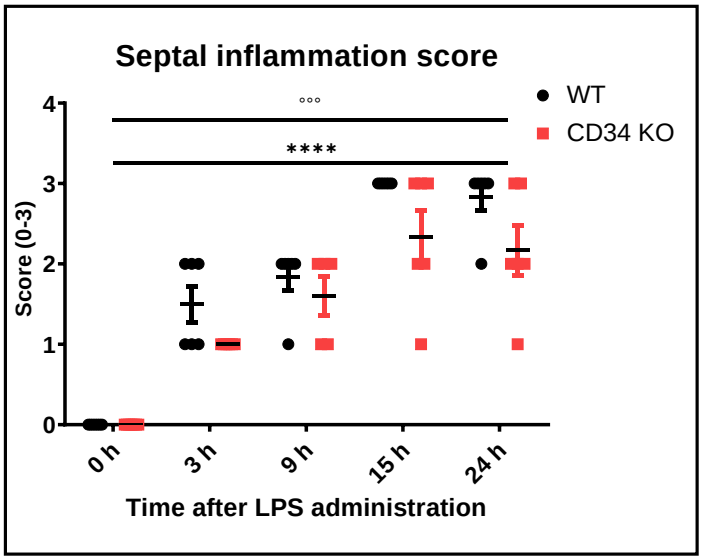
Septal inflammation score
WT
CD34 KO
°°°
****
Score (0-3)
0
1
2
3
4
0 h
3 h
9 h
15 h
24 h
Time after LPS administration

Fig.4.12: Histological Scoring of Inflammation in lung sections: Perivascular, peribronchiolar and septal inflammation scores from H&E stained left lung from 0-hour (no LPS; WT, N=7; CD34 KO, N=7), 3 h (WT, N=6; CD34 KO, N=6), 9 h (WT, N=6; CD34 KO, N=5), 15 h (WT, N=3; CD34 KO, N=4) and 24 h (WT, N=6; CD34 KO, N=6) post-LPS treatment with 50 µg LPS. Two-way ANOVA with Dunnett's multiple comparisons test was used to analyze the data. For perivascular inflammation score, interaction effect was non-significant, F (4,46) = 2.438, p=0.0603; main effect of time-point was significant (****), F (4, 46) = 47.80, p<0.0001; main effect of mouse strain was significant (°°) F (1,46) = 9.805, p=0.0030. For peribronchiolar inflammation score, interaction effect was non-significant, F (4,46) = 1.155, p=0.3430; main effect of time-point was significant (****), F (4, 46) = 55.25, p<0.0001; main effect of mouse strain was significant (°°) F (1,46) = 8.700, p=0.0050. For Septal inflammation score, interaction effect was non-significant, F (4,51) = 1.322, p=0.2743; main effect of time-point was significant (****), F (4, 51) = 73.57, p<0.0001; main effect of mouse strain was significant (°°°) F (1,51) = 12.52, p=0.0009. No difference in perivascular, peribronchiolar, and septal inflammation score in WT vs CD34 KO at any of the time-points. All results are expressed as mean ± SD.

4.4 CD34 knock-out mice show reduced expression of TNF-α, IL-1β, KC, IL-6, IL-10, and MIP-1α upon LPS challenge compared with the WT mice:

We looked at the level of various cytokines and chemokines associated with ALI in BAL fluid to study the inflammatory response induced by LPS. The 2-way ANOVA interaction effect between time-point and mouse strain was significant in TNF-α (p<0.0001), IL-1β (p=0.0235), KC (p<0.0001), IL-6 (p=0.0197) (Fig.4.13.A, B, C, and D, respectively). This indicates that the intranasal instillation of LPS induced time-dependent change in the levels of TNF-α, IL-1β, KC, and IL-6 in both WT and CD34 KO groups. LPS induces early (3 h) release of BAL TNF-α, IL-1β, KC, and IL-6 in WT mice when compared to no LPS at baseline (0 h) or later time-points at 9, 15 and 24 h (Fig.4.13.A, B, C, and D). WT mice show increased expression of pro-inflammatory cytokines, TNF-α (p<0.0001), IL-1β (p=0.0008), KC (p<0.0001) and IL-6 (p=0.0004), in BAL supernatant 3-hour post-LPS administration compared with the CD34 knock-out mice (Fig.4.13.A, B, C, and D). Two-way ANOVA on IL-10 (p=0.0423) and MIP-1α (p=0.0066) data shows that significant interaction effect between time-points and strain (Fig.4.14.A, B). This indicates that the intranasal instillation of LPS induced time-dependent change in the levels of IL-10 and MIP-1α in both WT and CD34 KO groups. LPS induces early (3 h) release of BAL IL-10 and MIP-1α in WT mice when compared to no LPS at baseline (0 h) or later time-points at 9, 15 and 24 h (Fig.4.14.A, B). Fig.4.14.A shows higher expression of anti-inflammatory cytokine IL-10 in WT mice at 3-hour post-LPS challenge, compared to CD34 knock-out mice (p=0.0017). As shown in Fig.4.14.B, MIP-1α is upregulated in WT group compared to CD34 knock-out group, 3-hour after LPS administration (p<0.0001). Two-way ANOVA on IL-12(p40) (Fig.4.15) shows that the main effects of time-point (p=0.0018) and mouse strain (p=0.0010) were significant. This indicates a time-dependent effect of LPS on IL-12(p40) levels in BAL in both WT and CD34 KO groups. However, no difference was observed between WT and CD34 KO groups at any of the time-points (p>0.05). Two-way ANOVA on IFN-γ (Fig.4.16.A) shows that the interaction effect not significant. Two-way ANOVA on G-CSF (Fig.4.16.B) both the main effects of time-point (p=0.0008), and mouse strain (p=0.0010.) were significant. But no difference was observed at any of the time-points in the expression levels of IFN-γ (Fig.4.16.A) and G-CSF (Fig.4.16.B) in BAL samples between the two groups. Two-way ANOVA on MIP-1b (Fig.4.17.A**)** shows that interaction effect (p=0.0034), and the main effect of time-point was significant as well (p=0.0013).

This indicates that the intranasal instillation of LPS induced time-dependent change in the levels of MIP-1b in both WT and CD34 KO groups. At 3 h post-LPS challenge, WT had a higher level of MIP-1b compared with CD34 KO ($p<0.0001$). Two-way ANOVA on MCP-1 (Fig.4.17.B**)** indicates that the main effect of time-point was significant ($p=0.0019$). There was no difference in MCP-1 levels in BAL between WT and CD34 KO at any of the time-points ($p>0.05$). Two-way ANOVA on RANTES (Fig.4.18**)** shows that the main effect of time-point was significant ($p=0.0090$), indicating LPS induced time-dependent change in the levels of RANTES. Compared to WT at 15 h, CD34 KO at 15 h group had low RANTES levels in BAL ($p=0.0403$).

A

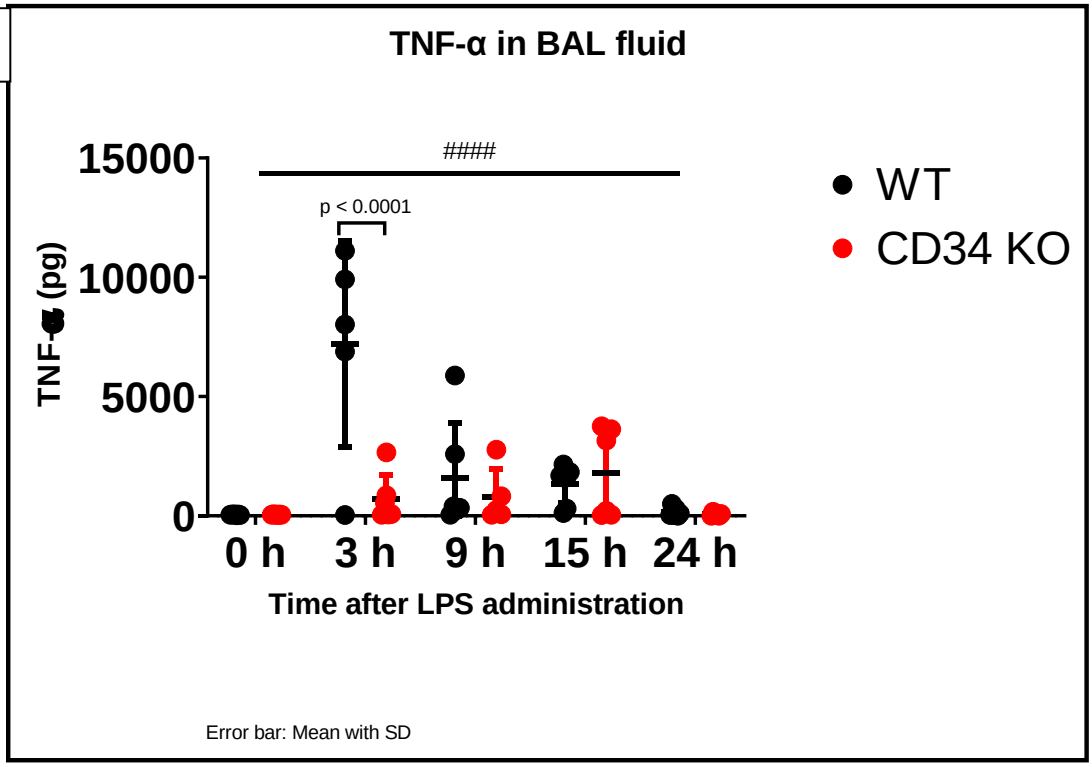
TNF-α in BAL fluid
####
p < 0.0001
15000
10000
5000
0
TNF-α (pg)
0 h
3 h
9 h
15 h
24 h
Time after LPS administration
WT
CD34 KO
Error bar: Mean with SD

B

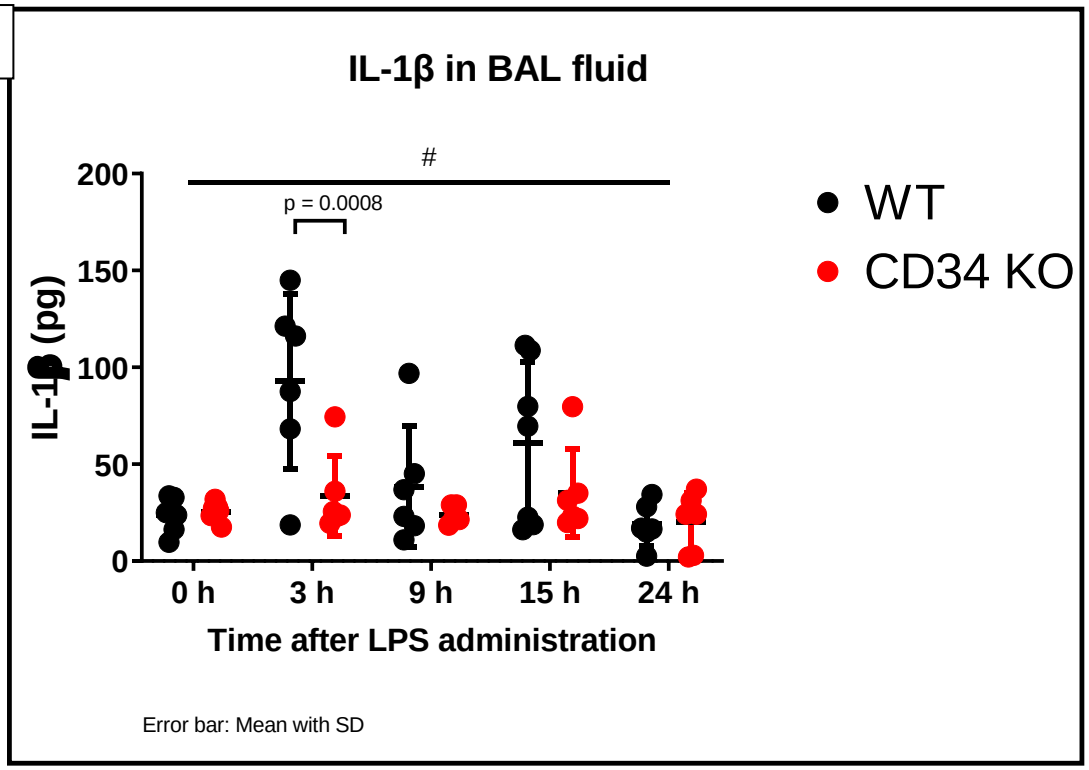
IL-1β in BAL fluid
#
p = 0.0008
200
150
100
50
0
IL-1β (pg)
0 h
3 h
9 h
15 h
24 h
Time after LPS administration
WT
CD34 KO
Error bar: Mean with SD

C

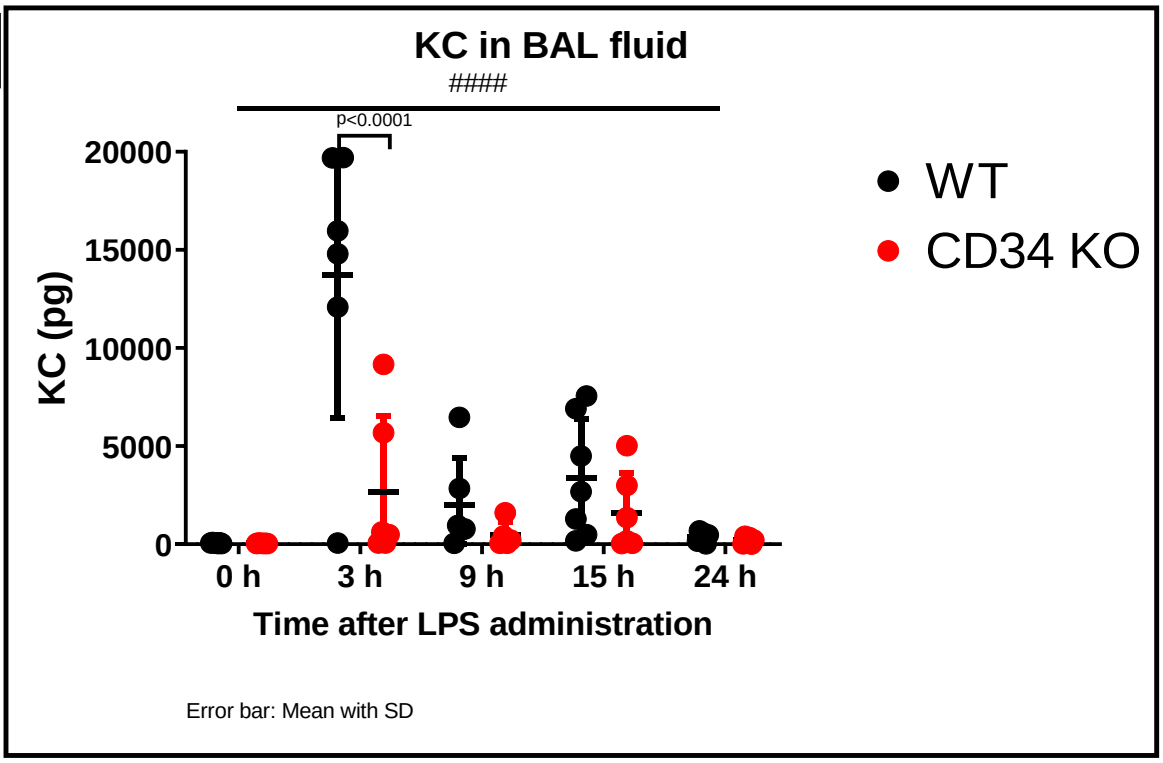
KC in BAL fluid
####
p<0.0001
20000
15000
10000
5000
0
KC (pg)
0 h
3 h
9 h
15 h
24 h
Time after LPS administration
WT
CD34 KO
Error bar: Mean with SD

D

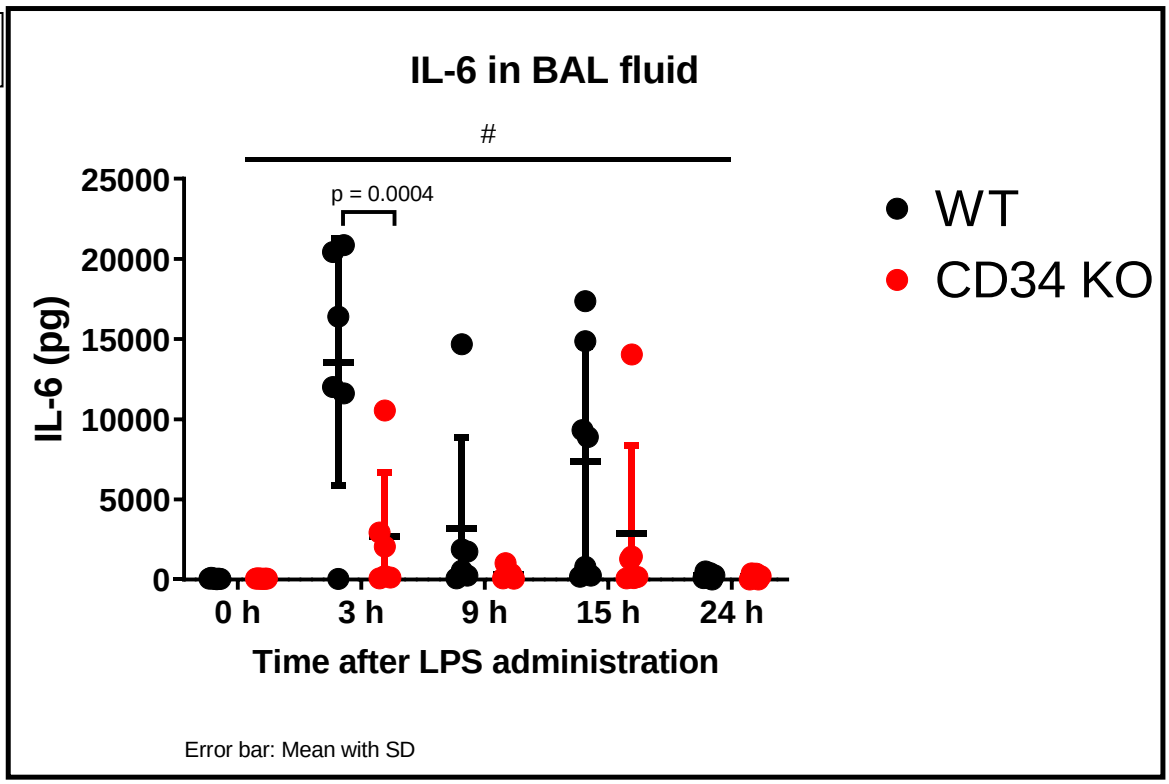
IL-6 in BAL fluid
#
p = 0.0004
25000
20000
15000
10000
5000
0
IL-6 (pg)
0 h
3 h
9 h
15 h
24 h
Time after LPS administration
WT
CD34 KO
Error bar: Mean with SD

Fig.4.13.A, B, C, D: TNF-α, IL-1β, KC and IL-6 content in BAL fluid: TNF-α, IL-1β, KC and IL-6 in the BAL samples at various time points: 0-hour (no LPS; WT, N=7; CD34 KO, N=7), 3 h (WT, N=6; CD34 KO, N=6), 9 h (WT, N=6; CD34 KO, N=5), 15 h (WT, N=7; CD34 KO, N=6) and 24 h (WT, N=6; CD34 KO, N=6) post-LPS treatment with 50 µg LPS. Data sets were analyzed using two-way ANOVA with Dunnett's multiple comparisons test. (A) TNF-α: Interaction effect was significant (####), F (4,51) = 9.028, p<0.0001; main effect of time-point was significant, F (4, 51) = 11.13, p<0.0001; main effect of mouse strain was significant F (1, 51) = 10.92, p=0.0017. WT vs CD34 KO at 3 h, p<0.0001; (B) IL-1β: Interaction effect was significant (#), F (4, 52) = 3.087, p=0.0235; main effect of time-point was significant, F (4, 52) = 6.353, p=0.0003; main effect of mouse strain was significant F (1, 52) = 9.111, p=0.0039. WT vs CD34 KO at 3 h, p=0.0008; (C) KC: Interaction effect was significant (####), F (4, 52) = 7.554, p<0.0001; main effect of time-point was significant, F (4, 52) = 16.01, p<0.0001; main effect of mouse strain was significant F (1, 52) = 15.01, p=0.003. WT vs CD34 KO at 3 h, p<0.0001; (D) IL-6: Interaction effect was significant (#), F (4, 52) = 3.213, p=0.0197; main effect of time-point was significant, F (4, 52) = 7.818, p<0.0001; main effect of mouse strain was significant F (1, 52) = 10.72, p=0.0019. WT vs CD34 KO at 3 h, p=0.0004. Results are expressed as mean ± SD. Experiment was performed in duplicates.

A

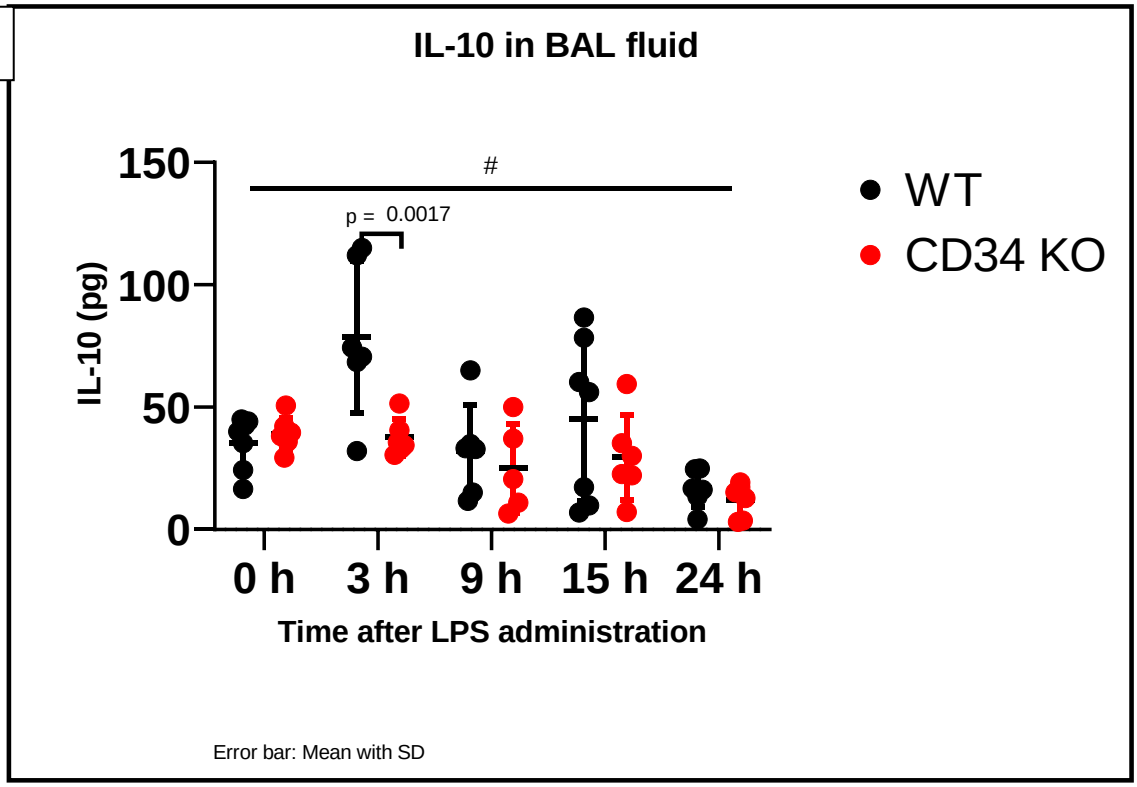
IL-10 in BAL fluid
150
100
50
0
IL-10 (pg)
#
p = 0.0017
0 h
3 h
9 h
15 h
24 h
Time after LPS administration
WT
CD34 KO
Error bar: Mean with SD

B

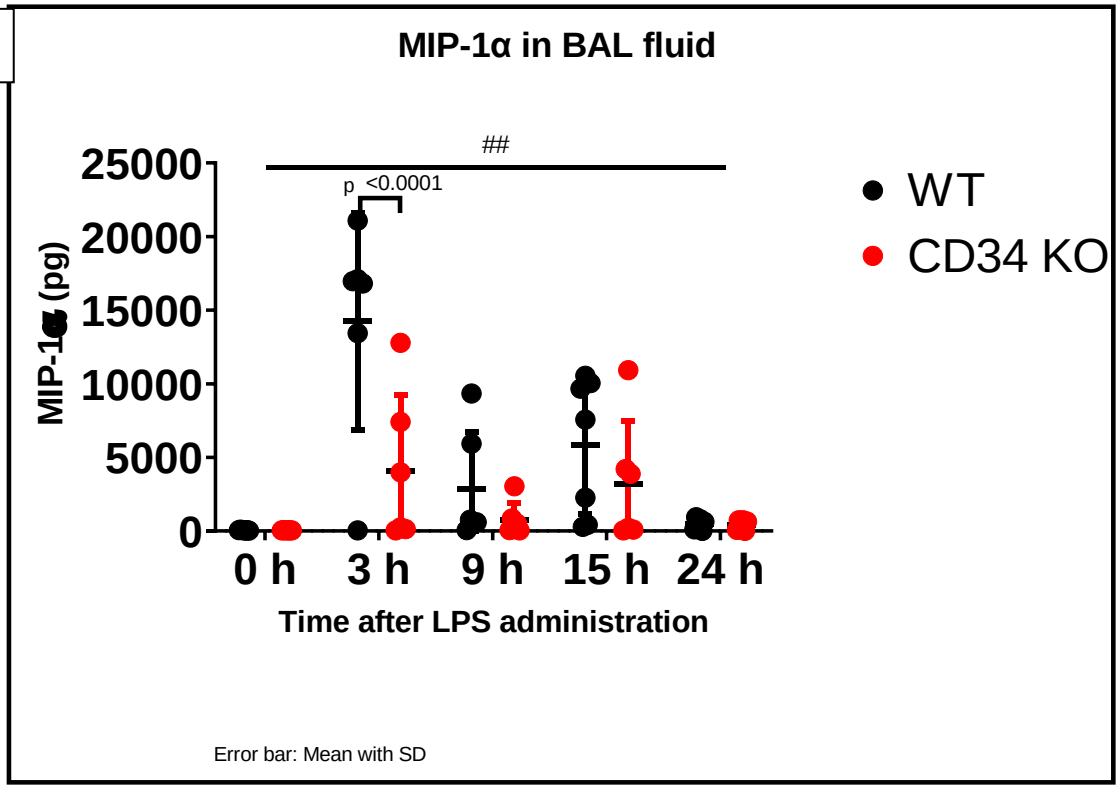
MIP-1α in BAL fluid
25000
20000
15000
10000
5000
0
MIP-1α (pg)
##
p <0.0001
0 h
3 h
9 h
15 h
24 h
Time after LPS administration
WT
CD34 KO
Error bar: Mean with SD

Fig.4.14.A, B: IL-10 and MIP-1α content in BAL fluid: IL-10 and MIP-1α in the BAL samples at various time points: 0-hour (no LPS; WT, N=7; CD34 KO, N=7), 3 h (WT, N=6; CD34 KO, N=6), 9 h (WT, N=6; CD34 KO, N=5), 15 h (WT, N=7; CD34 KO, N=6) and 24 h (WT, N=6; CD34 KO, N=6) post-LPS treatment with 50 µg LPS. Data sets were analyzed using two-way ANOVA with Dunnett's multiple comparisons test. (A) IL-10: Interaction effect was significant (#), F (4, 52) = 2.669, p=0.0423; main effect of time-point was significant, F (4, 52) = 8.844, p<0.0001; main effect of mouse strain was significant F (1, 52) = 7.529, p=0.0083. WT vs CD34 KO at 3 h, p=0.0017. (B) MIP-1α: Interaction effect was significant (##), F (4, 53) = 3.995, p=0.0066; main effect of time-point was significant, F (4, 53) = 13.18, p<0.0001; main effect of mouse strain was significant F (1, 53) = 10.44, p=0.0021. WT vs CD34 KO at 3 h, p<0.0001. Results are expressed as mean ± SD. Experiment was performed in duplicates.

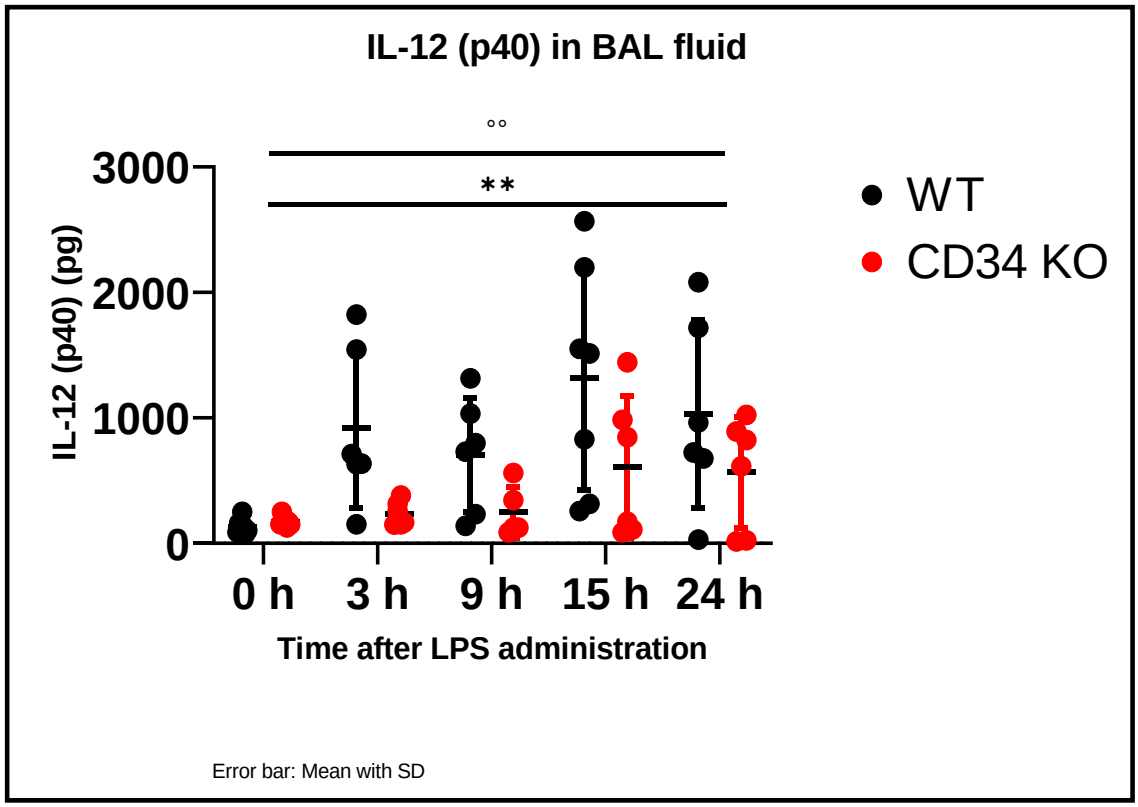

Fig.4.15: IL-12(p40) content in BAL fluid: IL-12(p40) in the BAL samples at various time points: 0-hour (no LPS; WT, N=7; CD34 KO, N=7), 3 h (WT, N=6; CD34 KO, N=6), 9 h (WT, N=6; CD34 KO, N=5), 15 h (WT, N=7; CD34 KO, N=6) and 24 h (WT, N=6; CD34 KO, N=6) post-LPS treatment with 50 µg LPS. Data sets were analyzed using two-way ANOVA with Dunnett's multiple comparisons test. Interaction effect was non-significant, F (4, 52) = 1.188, p=0.3271; main effect of time-point was significant (**), F (4, 52) = 4.977, p=0.0018; main effect of mouse strain was significant (°°) F (1, 52) = 12.27, p=0.0010. WT vs CD34 KO, p>0.05 at all time-points. All results are expressed as mean ± SD. Experiment was performed in duplicates.

A

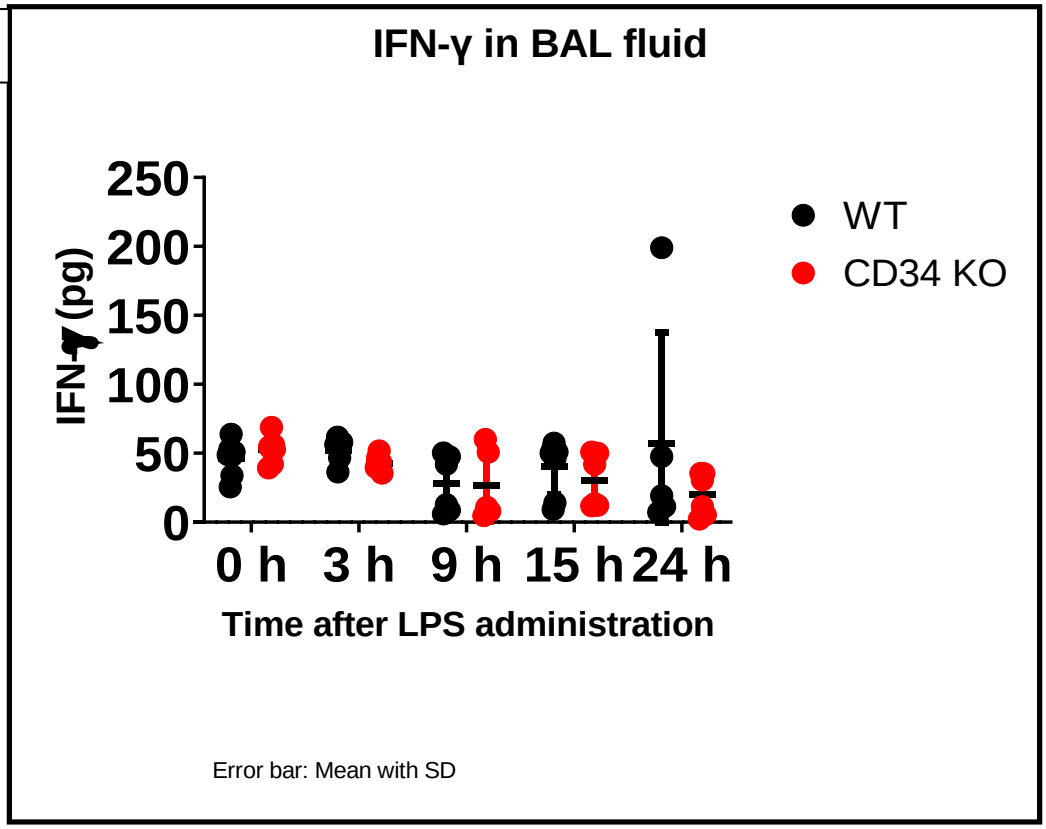
IFN-γ in BAL fluid
IFN-γ (pg)
250
200
150
100
50
0
0 h
3 h
9 h
15 h
24 h
Time after LPS administration
WT
CD34 KO
Error bar: Mean with SD

B

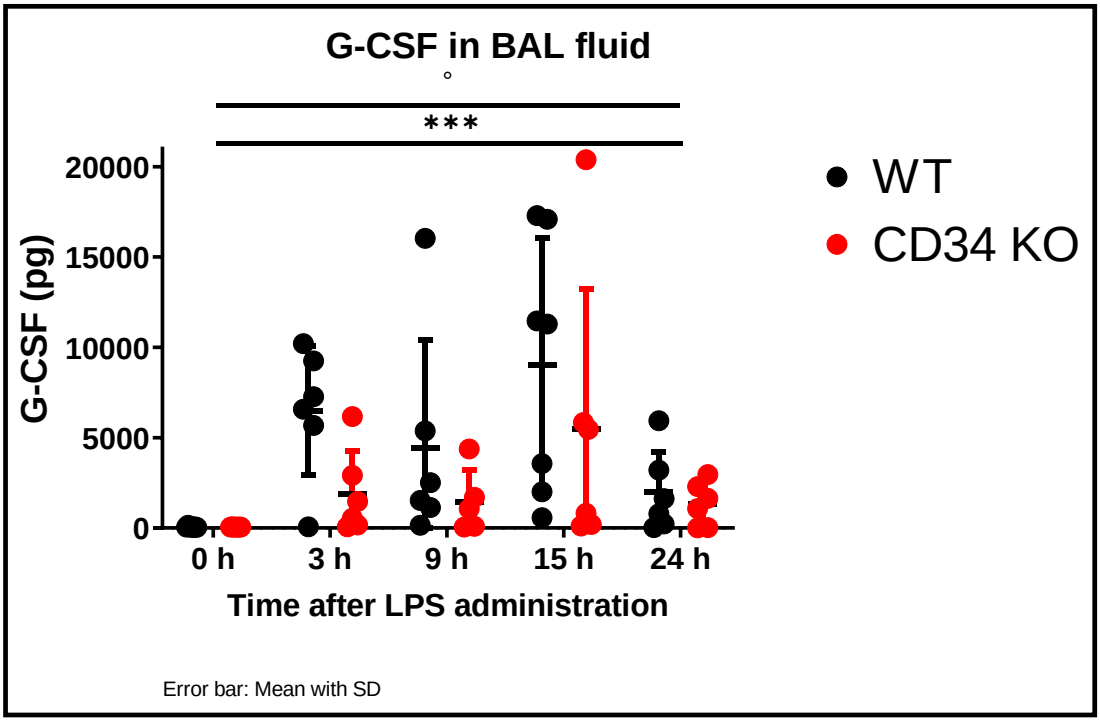
G-CSF in BAL fluid
°
***
G-CSF (pg)
20000
15000
10000
5000
0
0 h
3 h
9 h
15 h
24 h
Time after LPS administration
WT
CD34 KO
Error bar: Mean with SD

Fig.4.16.A, B: IFN-γ and G-CSF content in BAL fluid: IFN-γ and G-CSF in the BAL samples at various time points: 0-hour (no LPS; WT, N=7; CD34 KO, N=7), 3 h (WT, N=6; CD34 KO, N=6), 9 h (WT, N=6; CD34 KO, N=5), 15 h (WT, N=7; CD34 KO, N=6) and 24 h (WT, N=6; CD34 KO, N=6) post-LPS treatment with 50 µg LPS. Data sets were analyzed using two-way ANOVA with Dunnett's multiple comparisons test. (A) IFN-γ: Interaction effect was non-significant, F (4, 51) = 1.023, p=0.4043; main effect of time-point was non-significant, F (4, 51) = 1.308, p=0.2797; main effect of mouse strain was non-significant F (1, 51) = 2.055, p=0.1578. WT vs CD34 KO, p>0.05 at all time-points. (B) G-CSF: Interaction effect was non-significant, F (4, 52) = 0.7037, p=0.5930; main effect of time-point was significant (***), F (4, 52) = 5.597, p=0.0008; main effect of mouse strain was significant (°) F (1, 52) = 4.911, p=0.0311. WT vs CD34 KO, p>0.05 at all time-points. All results are expressed as mean ± SD. Experiment was performed in duplicates.

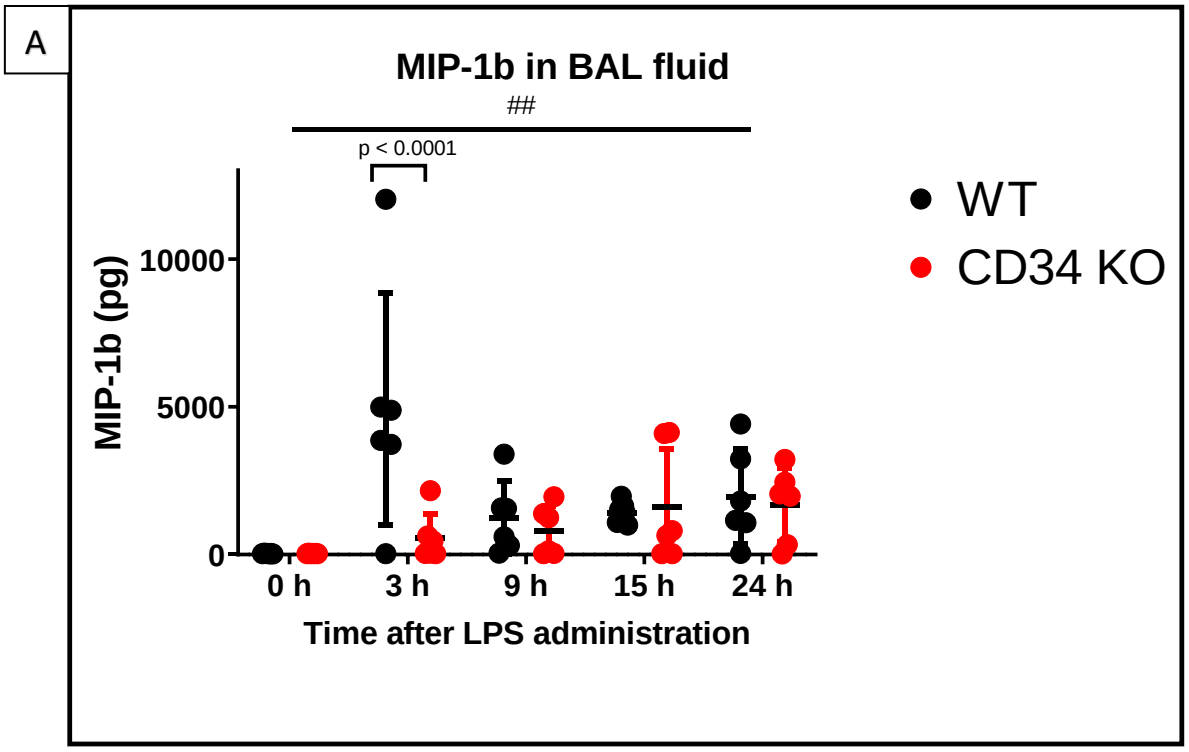
A
MIP-1b in BAL fluid
##
p < 0.0001
MIP-1b (pg)
10000
5000
0
0 h
3 h
9 h
15 h
24 h
Time after LPS administration
WT
CD34 KO

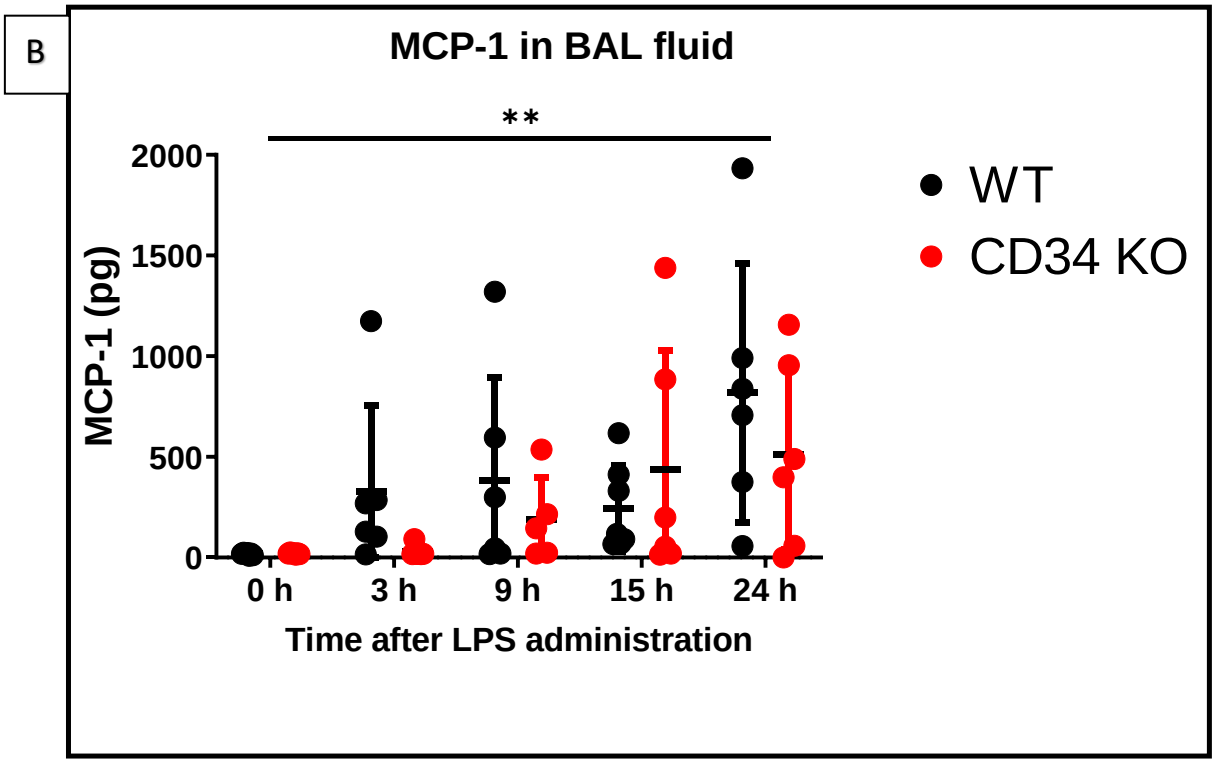
B
MCP-1 in BAL fluid
**
MCP-1 (pg)
2000
1500
1000
500
0
0 h
3 h
9 h
15 h
24 h
Time after LPS administration
WT
CD34 KO

Fig.4.17.A, B: MIP-1b and MCP-1 content in BAL fluid: MIP-1b and MCP-1 in the BAL samples at various time points: 0-hour (no LPS; WT, N=7; CD34 KO, N=7), 3 h (WT, N=6; CD34 KO, N=6), 9 h (WT, N=6; CD34 KO, N=5), 15 h (WT, N=7; CD34 KO, N=6) and 24 h (WT, N=6; CD34 KO, N=6) post-LPS treatment with 50 µg LPS. Data sets were analyzed using two-way ANOVA with Dunnett's multiple comparisons test. (A) MIP-1b: Interaction effect was significant (##), F (4, 53) = 4.477, p=0.0034; main effect of time-point was significant, F (4, 53) = 5.283, p=0.0013; main effect of mouse strain was significant F (1, 53) = 5.959, p=0.0180. WT vs CD34 KO at 3 h, p<0.0001; (B) MCP-1: Interaction effect was non-significant, F (4, 52) = 0.9960, p=0.4181; main effect of time-point was significant (**), F (4, 52) = 4.931, p=0.0019; main effect of mouse strain was non-significant F (1, 52) = 1.556, p=0.2178. WT vs CD34 KO, p>0.05 at all time-points. All results are expressed as mean ± SD. Experiment was performed in duplicates.

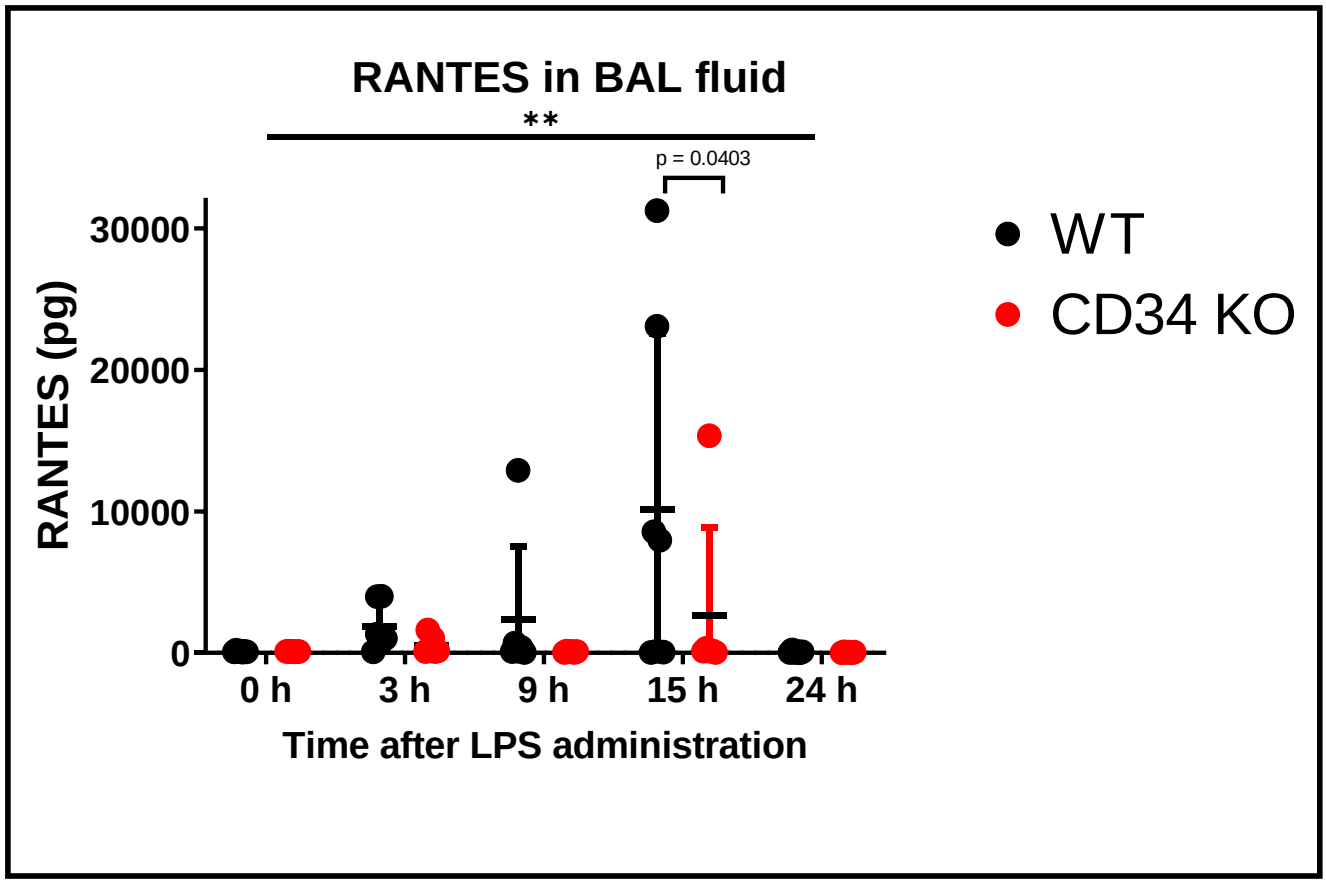

Fig.4.18: RANTES content in BAL fluid: RANTES in the BAL samples at various time points: 0-hour (no LPS; WT, N=7; CD34 KO, N=7), 3 h (WT, N=6; CD34 KO, N=6), 9 h (WT, N=6; CD34 KO, N=5), 15 h (WT, N=7; CD34 KO, N=6) and 24 h (WT, N=6; CD34 KO, N=6) post-LPS treatment with 50 µg LPS. Data set was analyzed using two-way ANOVA with Dunnett's multiple comparisons test. Interaction effect was non-significant, F (4, 53) = 1.236, p=0.2874; main effect of time-point was significant (**), F (4, 53) = 3.773, p=0.0090; main effect of mouse strain was non-significant F (1, 53) = 3.254, p=0.0769. WT vs CD34 KO at 15 h, p=0.0403. All results are expressed as mean ± SD. Experiment was performed in duplicates.

CHAPTER 5: DISCUSSION

In this study, we have used a mouse model with 12- to 16-wk-old mice and administered intranasal LPS (50 µL/mice) from Escherichia coli O55:B5 (diluted in sterile saline at 1 g/L). This LPS model shows neutrophilic inflammation response as well as increase in intrapulmonary cytokines which are similar to ARDS (Matute-Bello, 2008). While CD34 KO mice have been utilized previously in studying various inflammatory conditions as well as in one study of ALI in a bleomycin model (Lo et al., 2017), our project is novel in terms of studying LPS induced pattern recognition receptor, TLR4 mediated acute lung injury in CD34 KO mice.

Our results show that intranasal LPS challenge induced time-dependent changes in both groups in the total WBC counts in peripheral blood, relative percentages of mature/segmented neutrophil, eosinophil, lymphocyte, and platelet counts in peripheral blood samples from mice. Similarly, LPS induced changes across different time-points in BAL total leukocyte counts, alveolar macrophage counts, neutrophil counts, MPO activity, BAL total protein content. TNF-α, IL-1β, KC, IL-6, IL-10, MIP-1a, and MIP-1b levels in BAL demonstrated post-LPS time-dependent changes in both the strains. IL-12(p40), MCP-1, G-CSF and RANTES levels demonstrated post-LPS time-dependent behaviour as well.

Acute LPS exposure induces mobilization of leukocytes from storage sites like the bone marrow and spleen. Our results show no difference between WT and CD34 KO mice total white blood cell counts. Compared to CD34 KO at 0 h, CD34 KO at 15 h had a 3.5-fold increase in the relative percentage of SEG, but it was not observed in WT mice. Blood eosinophil counts dropped from baseline (0 h) in CD34 KO group, starting at 3 h with 1.9-fold drop up to 10.9-fold drop at 24 h. Blood eosinophil counts dropped from baseline (0 h) in WT group, 5.5-fold at 15 h and 4.4-fold at 24 h. Further, compared to CD34 KO at 0 h, CD34 KO at 15 h had a 2.5-fold decrease in the relative percentage of lymphocytes while there was no difference in WT. Lastly, platelet counts decreased in both WT and CD34 KO groups for subsequent time-points, compared to baseline (0 h) of respective groups. WT at 15 h had a 1.6-fold decrease, and WT at 24 h also had a 1.6-fold

decrease, compared to WT at 0 h. CD34 KO at 15 h had a 1.5-fold decrease and CD34 KO at 24 h also had a 1.5-fold decrease, compared to CD34 KO at 0 h. This drop in platelet counts could be due to the migration of platelets in lung vasculature, where platelets can form P-selectin dependent aggregates with neutrophils (Zarbock et al., 2006). Due to coagulation of a number of blood samples immediately after cardiac puncture, the sample sizes at different time-points were reduced. There was no difference observed between the two groups at different time-points, most likely due to reduced sample size for multiple time points.

Our results showed no statistically significant difference between the total leukocyte counts at any of the post-LPS administration time-points in WT mice compared with CD34 KO mice. This is a similar result to the bleomycin model study (Lo et al., 2017). Similarly, no difference was observed in the alveolar macrophage counts between WT and CD34 KO group at any of the post-LPS administration time-points. However, in WT group, compared to baseline (WT, 0 h) the alveolar macrophage counts dropped 5.9-fold at 3 h, 5.1-fold at 9 h and 6.3-fold at 15 h. In contrast, in CD34 KO group, alveolar macrophage counts dropped 2.5-fold at 24 h, compared to baseline (CD34 KO, 0 h). The drop could be because of more adherent macrophage post-LPS instillation not washing away during BAL. Another possible reason could be the apoptosis of macrophage after phagocytosis. No difference was observed in the neutrophil counts between WT and CD34 KO group at any of the post-LPS administration time-points. The reason behind lack of neutrophils in BAL of WT at 3-hour time-point compared to no LPS WT group could be due to either spurious counts or the effect of including both male and female mice in the study.

In this study, I had used both male and female mice due to lack of knowledge between the gender differences in lung disease. But for each group, I tried to keep the male to female ratio as close to 1 as possible within the constraints of experimental animal numbers. While there have been studies showing a difference in inflammatory response between male and female mice, the exact response varies depending on the model used (Card et al., 2006). Card et al. showed that males had significantly severe hypothermia and greater airway hyperresponsiveness than females post-intratracheal LPS administration, as well as higher BALF total cells, neutrophils, and TNF-α levels 6 h post-LPS challenge. We looked at the data in order to understand if the gender difference might be responsible in our study for not achieving significant results, however there was no clear pattern based on gender, with both the genders contributing to outliers. This can be attributed to the low

number of animals from each gender (N=1-3 per group for each gender, for each time-point), and thus the inability to statistically analyse the data based on gender.

The number of leukocytes in the BAL samples account for the cells that had migrated into the alveoli of the mice upon LPS-administration and subsequently washed off with bronchoalveolar lavage procedure. However, most neutrophils get trapped in the vasculature or interstitial space of inflamed lungs (Reutershan et al., 2005). Lung MPO in our experimental design, is thus an indicator of the number of adherent neutrophils left in the lung after lavage and vascular lung perfusion. Interestingly, our results show that the lung MPO content was significantly higher at 3-hour time-point in WT mice compared with CD34 knock-out mice. CD34 KO mice showed a delayed rise in MPO, starting at 9 h. Furthermore, immunofluorescence staining results show prominent alveolar staining with Gr-1, a marker for polymorphonuclear leukocytes and a subset of inflammatory monocytes/macrophages. We also noted a lower vWF alveolar septal expression in CD34 KO mice post-LPS exposure, which points to a plausible suppression of LPS induced platelet activation in CD34 KO mice. Platelet activation is essential for heterotypic leukocyte adherence to pulmonary capillaries (Ma et al., 2008). I did not quantify the regional lung Gr1 and vWF expression from confocal microscopy, but quantification might help support the lung MPO and BAL protein data where CD34 KO mice have significantly lower MPO levels at 3 h time-point compared to WT mice.

Our immunofluorescence results show presence of CD34 in the bronchiolar epithelium, in addition to alveolar septa, in WT mice at 0 h (No LPS).To my knowledge, these observations are reported for the first time in the lung tissues with the use of a novel antibody, EP373Y, which is reactive to the conserved C-terminal sequence of human CD34 protein. The same antibody also detected CD34 in the lung tissues of dogs and pigs (Appendix B, Fig.B.1, Fig.B.3), showing expression of CD34 on bronchiolar epithelia as well as alveolar septa. Our observations of CD34 expression in the bronchiolar epithelium and given the pan-selectin affinity of CD34 (Felschow et al., 2001; Alfaro et al., 2011; Ohnishi et al., 2013; AbuSamra et al., 2017), reinforce a plausible role of CD34 in lung neutrophil adherence as indicated by higher lung MPO as well as BAL neutrophils in LPS exposed WT mice when compared to CD34 KO, whereby CD34 might be facilitating the interaction between lung epithelium and neutrophils.

WT mice also had a significantly higher total protein content in the BAL supernatant at 3-hour post-LPS administration compared to the CD34 KO mice, which shows that WT mice had increased vascular permeability. The significant difference in BAL total protein amounts between the two groups was seen at 24 h time-point as well, pointing towards vascular barrier protection as indicated by attenuated vascular permeability in the CD34 KO mice. Thus, CD34 KO mice display delays in lung neutrophil recruitment kinetics (lung MPO content) and loss of lung vascular barrier properties (BAL total protein content).

Cytokine expression levels were studied using 23-plex ELISA in order to characterize the lung inflammatory response in our model. WT mice showed increased expression of pro-inflammatory cytokines, TNF-α and IL-1β in BAL supernatant 3-hour post-LPS administration compared with the CD34 knock-out mice. Our results are similar to previous study, where TNF-α levels begin to rise as early as 30 min post intratracheal LPS challenge and peak at 1 h in WT rats, the levels remain high for up to 4 h (Xing et al., 1994; Li et al., 1998). Mice do not express IL-8 but they have KC chemokine, which is a mouse homologue of human IL-8. IL-8 is induced by pro-inflammatory cytokines TNF-α, IL-6, IFN-γ and IL-1β, and acts as a neutrophil chemoattractant (Brat et al., 2005; Matute-Bello, 2008). KC expression was also elevated in WT mice at 3-hour post-LPS challenge, compared to CD34 knock-out mice. IL-6 activates leukocytes, and IL-6 levels correlate with severity of ARDS (Stapleton et al., 2019). IL-6 expression was 5-fold higher in WT mice at 3-hour post-LPS challenge, compared to CD34 knock-out mice. IL-6 levels in rats have been shown to peak within 6 h post-intratracheal LPS challenge and it was not detected in BAL until an hour post-LPS challenge (Xing et al., 1994). There was higher expression of anti-inflammatory cytokine IL-10 in WT mice at 3-hour post-LPS challenge, compared to CD34 knock-out mice. IL-10 has been associated with high mortality rate in ARDS (Stapleton et al., 2019). MIP-1α is a pro-inflammatory chemokine which plays a role in neutrophil chemotaxis in mice (Gao et al., 1997). MIP-1α is upregulated in WT group compared to CD34 knock-out group, 3-hour after LPS administration. IL-12 p40 subunit of IL-12 is secreted early on by the antigen-presenting cells like macrophages, when they interact with PAMPs (Abdi, 2002). IL-12 p40 levels in BALF had no difference between WT and CD34 KO at any of the time-points. G-CSF is a principal cytokine involved in the proliferation, differentiation and mobilization of neutrophilic granulocytes (Panopoulos et al., 2008). RANTES is actively involved in recruitment of leukocytes such as macrophages, basophils, and eosinophils to the site of inflammation (Aldinucci et al., 2014). No

difference was observed in the expression levels of IFN-γ, G-CSF and RANTES in BAL samples between the two groups. LPS induces innate immune (TLR4) mediated NF-κB activation, IL-1β inflammasome activation as well as cell-death induced cytokine/chemokine responses (Takeda et al., 2004). WT mice released peak cytokines and chemokines such as, TNF-α, IL-1β, KC, MIP-1α, IL-6, IL-10 and IL-12 p40 sub-unit, at 3 h post-LPS exposure when compared to no LPS (0 h), which is in-line with previous reports (Bosmann et al., 2012). CD34 KO mice released negligible TNF-α and IL-12 p40 sub-unit. Moreover, there was negligible LPS induced IL-1β or IL-10 release in CD34 KO mice. These results indicate that CD34 KO mice potentially lack in TLR4 mediated IL-1β inflammasome activation when compared to WT mice. LPS induced an early (3 h) and a later (15 h) peak in IL-6 concentrations in WT mice compared to 5-fold lower concentrations in CD34 KO mice (at 3 h).

Collectively, the lung histology, MPO, BAL protein content and BAL cytokine/chemokine analysis indicate that CD34 KO mice show delays in lung vascular permeability and neutrophil adhesion kinetics and a suppression of IL-1β and TNFα dependent innate immune response. Our results propose novel role of CD34 in neutrophil adherence as well as activation and corroborate with the recent *in vivo* studies showing L-selectin mediated neutrophil adherence, activation as well as clearance from the inflammation site (McEver, 2015; Liu et al., 2017). I have summarized the effects of LPS on mouse lungs and possible roles of CD34 in neutrophil adherence, and activation, as well as in TLR4 mediated inflammasome activation in Fig.5.1. This figure was adopted from a doctoral thesis (Zhao, 2009).

As our study was designed to understand the early phase of immune activation, it will be interesting to study the later time-points as innate immune activation precedes the repair or immune cell clearance pathways, which in the intranasal LPS model can last up to a few weeks. It is quite probable that the CD34 KO mice show defective repair or lung leukocyte clearance due to impaired immune activation.

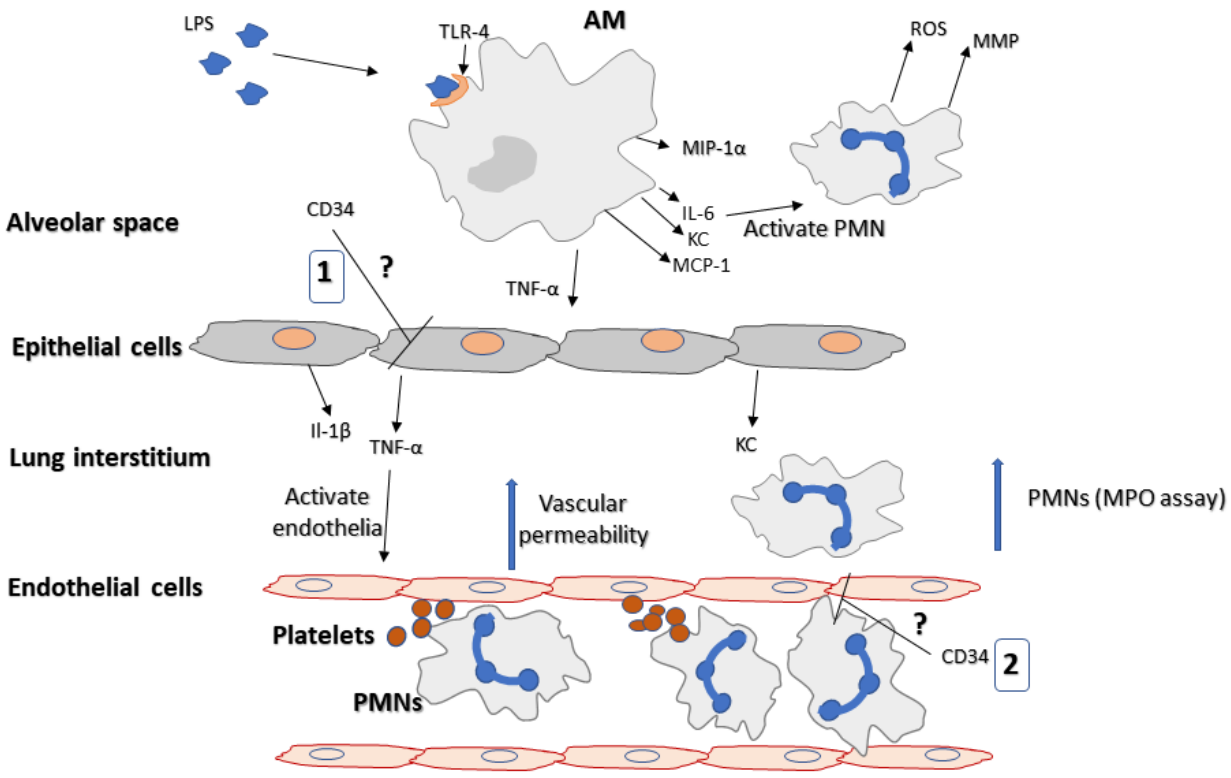
LPS
TLR-4
AM
ROS
MMP
MIP-1α
IL-6
KC
MCP-1
Activate PMN
Alveolar space
CD34
1
?
TNF-α
Epithelial cells
Il-1β
TNF-α
KC
Lung interstitium
Activate endothelia
Vascular permeability
PMNs (MPO assay)
Endothelial cells
Platelets
PMNs
?
CD34
2

Fig.5.1 Role of CD34 in LPS-induced acute lung injury in mice: TLR4 on alveolar macrophages (AM) can bind to LPS which leads to activation of AM via TLR4 signaling. Activated AMs and epithelial cells release early pro-inflammatory cytokines, TNF-α and IL-1β. Both lead to expression of IL-6 and KC, which is a functional homologue of human IL-8 in mouse. KC is an essential chemotactic factor and plays a role in the development of ALI. Chemokines activate β2 integrin and L-selectin expression which play an important role in neutrophil migration across the endothelia and activation of PMNs by IL-6 leads to increased vascular damage because of degranulation of activated PMNs, releasing toxic chemicals like ROS, and proteinases. Our results suggest that CD34 might be involved in: 1) L-selectin mediated neutrophil adherence, activation as well as clearance from the site of inflammation, since CD34 KO mice display delays in lung neutrophil recruitment kinetics (lung MPO content) and delays in loss of lung vascular barrier properties (BAL total protein content), 2) IL-1β and TNFα dependent innate immune response, since CD34 KO mice display impaired production of ALI associated cytokines and chemokines, TNF-α, IL-1β, KC, MIP-1α, IL-6, IL-10 and IL-12 p40 sub-unit, compared to their levels in BAL samples of WT mice at 3 h post-LPS administration.

CHAPTER 6: CONCLUSION AND FUTURE DIRECTIONS

The objective of this project was to study the intranasal LPS induced inflammatory response in the lungs of CD34 knock-out mice compared with WT (C57BL/6N) mice. To that end, we carried out experiments at different time-points post LPS challenge, to look at several factors associated with an inflammatory response in the lungs of mice, including peripheral blood cell counts, total and differential leukocyte cell counts in BALF, adherent neutrophils left in the lung after lavage (MPO levels, Gr-1 IF staining), lung vascular permeability (BAL total protein), inflammation scoring (H&E staining), and cytokine and chemokine levels in BALF.

Our results demonstrate a time-dependent inflammatory response in WT mice and CD34 knock-out mice in response to intranasal LPS challenge. While there was no difference in the total or differential leukocyte counts, including, alveolar macrophages and neutrophils, lung MPO content in CD34 KO was lower than WT group at 3 h time-point. Additionally, CD34 KO mice MPO levels begin to rise at 9 h, as opposed to early 3 h rise in WT mice. Suggesting that CD34 KO mice display delays in lung neutrophil recruitment kinetics. In addition, immunofluorescence staining images show distinct alveolar staining with Gr-1, a marker for polymorphonuclear leukocytes and a subset of inflammatory monocytes/macrophages. Our immunofluorescence staining image in WT mice at 0 h (No LPS) also show presence of CD34 in the bronchiolar epithelium, in addition to alveolar septa. Our observations of CD34 expression in the bronchiolar epithelium and given the pan-selectin affinity of CD34 (Felschow et al., 2001; Alfaro et al., 2011; Ohnishi et al., 2013; AbuSamra et al., 2017), reinforce a plausible role of CD34 in lung neutrophil adherence as indicated by higher lung MPO in LPS exposed WT mice when compared to CD34 KO. CD34 KO mice display loss of lung vascular barrier properties as suggested by lower total protein in BAL supernatant in CD34 KO mice at 3 h and 24 h time-points.

LPS induces innate immune (TLR4) mediated NF-κB activation, IL-1β inflammasome activation as well as cell-death induced cytokine/chemokine responses (Takeda et al., 2004). In WT mice cytokines and chemokines such as, TNF-α, IL-1β, KC, MIP-1α, IL-6, IL-10 and IL-12 p40 sub-unit, peaked at 3 h, which is in-line with previous reports (Bosmann et al., 2012). While CD34 KO mice released negligible TNF-α, IL-1β, IL-10 and IL-12 p40 sub-unit. These results indicate that CD34 KO mice potentially lack in TLR4 mediated IL-1β inflammasome activation when compared to WT mice.

Together, the lung histology, MPO, BAL protein content and BAL cytokine/chemokine analysis suggest that CD34 KO mice show delayed lung vascular permeability and neutrophil adhesion kinetics, and a suppression of IL-1β and TNFα dependent innate immune response. Our study was designed to understand the early phase of immune activation, lasting up to 24 h. Future experiments can be conducted to study the later time-points as innate immune activation precedes the repair or immune cell clearance pathways, which in the intranasal LPS model can last up to a few weeks. It is quite probable that the CD34 KO mice will show defective repair or lung leukocyte clearance due to impaired immune system activation.

Further, quantification of the regional lung Gr1 and vWF expression from confocal microscopy, might help support the lung MPO and BAL protein data where CD34 KO mice have significantly lower MPO levels at 3 h time-point compared to WT mice.

One of the limitations of this study is that both male and female mice were used due to lack of knowledge between the gender differences in lung disease. While there have been studies showing a difference in inflammatory response between male and female mice, the exact response varies depending on the model used (Card et al., 2006). Card et al. showed that males had significantly severe hypothermia and greater airway hyperresponsiveness than females post-intratracheal LPS administration, as well as higher BALF total cells, neutrophils, and TNF-α levels 6 h post-LPS challenge. Future studies can be conducted with either a larger sample size to include equal number of male and female in each group or conducting experiments with exclusively male or female animals.

While intranasal LPS mouse model of ALI provides the advantage of reproducibility, with some similarities to human ARDS symptoms, especially with respect to increase in intrapulmonary cytokines. LPS, however, does not cause extensive epithelial and endothelial damage in mice. This damage can be seen in human ARDS patients. The dose response in mice also differs since they lack PIM. Mice require higher dose of LPS (mg/kg range) to develop lung injury features, whereas humans can develop severe inflammation with a much smaller dose (μg/kg range). It is also important to note that mice and humans have evolved under widely different environmental pressures over the past millions of years. This has resulted in some changes in their immune systems to face specific pathogenic challenges endemic to their environments. One such difference is lack of IL-8 in mice, however, mice have KC which is a functional homologue of IL-8. Our protein of interest, CD34, also shares high sequence similarity across different species and the C-terminal of CD34 is a highly conserved region across species, including humans and mice. In conclusion, a mice model of ALI can be seen as an acceptable animal model in understanding the role of CD34 in LPS-induced acute lung inflammation.

APPENDIX A: BAL MONOCYTE AND LYMPHOCYTE COUNTS

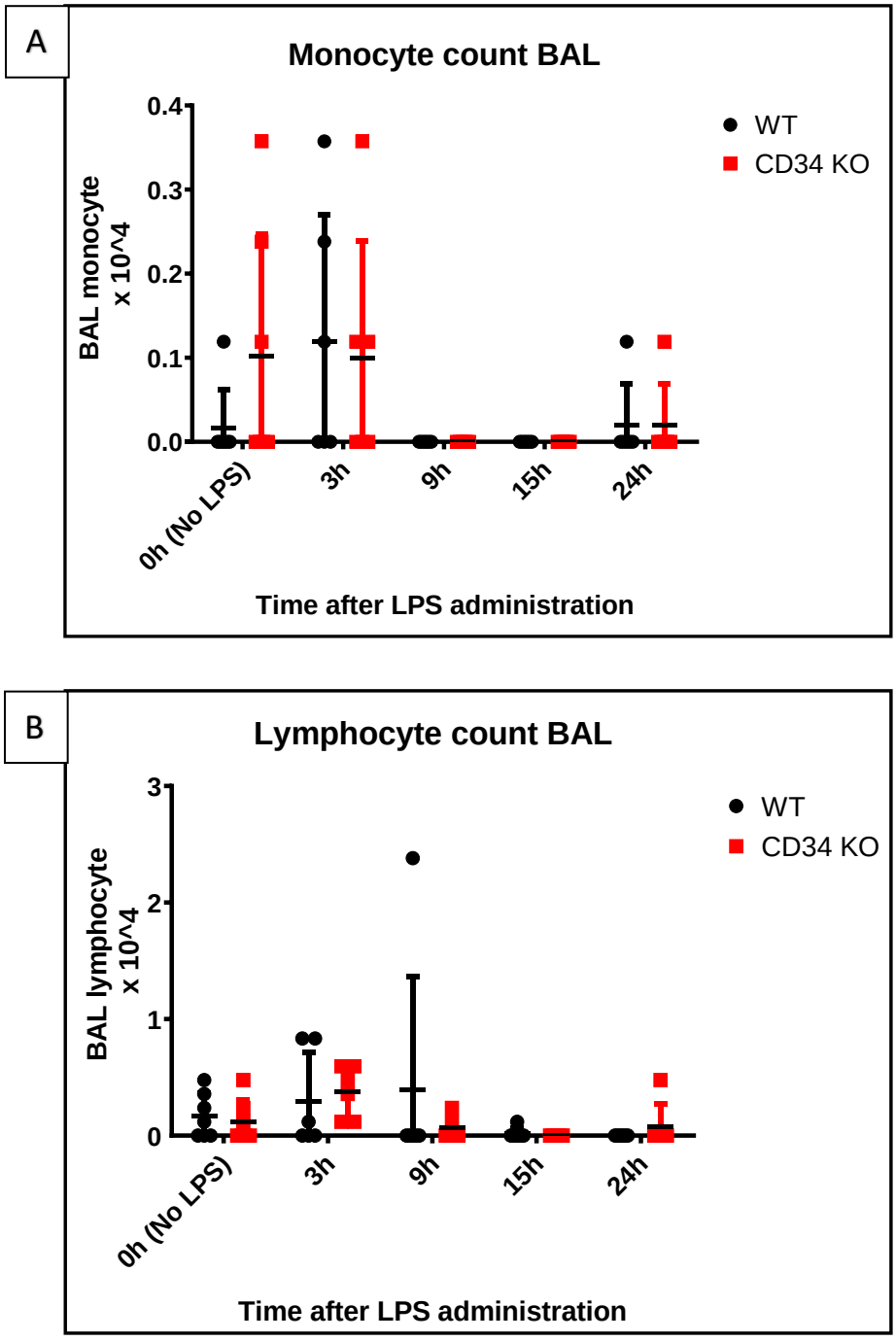

Fig.A.1.A, B: BAL Monocyte and Lymphocyte Counts: Total Bronchoalveolar Lavage Fluid (BAL) monocyte counts(A) and lymphocyte counts(B) at various time points (0 h, 3, 9, 15, 24 h) in WT (WT, N=5-7; at 15h, N=3) and CD34 KO (N=5-7; at 15h, N=3) mice. The data is lognormal as per the Shapiro-Wilk test. Hence, logarithmic transformation was applied to the original data, followed by two-way ANOVA with Dunnett's multiple comparisons test. Results are expressed as mean ± SD. WT vs CD34 $p>0.05$, ns

APPENDIX B: EXPRESSION OF CD34 IN DOG AND PIG LUNG TISSUE

INTRODUCTION

The cell surface protein CD34 has been observed to be expressed in various human tissues and cells including hematopoietic stem cells (2), vascular endothelial cells (3), mucosal dendritic cells (4), mast cells (5), eosinophils (6,7), microglia (8), fibrocytes (9), muscle satellite cells (10) and inactivated platelets (11). In canine models, CD34 expression has been observed in hematopoietic stem cells in bone marrow (12), peripheral blood and the hair follicle.

The cytoplasmic region of CD34, encoded by exons 7 and 8, contains the highest degree of sequence similarity between human, murine, and canine CD34.There is greater than 90% amino acid identity, and approximately 92% nucleotide identity within this region. This region contains several known or potential protein kinase phosphorylation sites (13). In case of complete CD34 protein, there is 70% amino acid identity between human and canine CD34.

There is a lack of literature and studies related to the expression of CD34 in various organs and cells of canine and porcine models. Therefore, it would be appropriate to initiate the project with Immunohistochemistry experiments to observe CD34 expression in blood (various cells), liver and lungs in canine and porcine models. CD34 monoclonal antibodies for relevant species are available and can be arranged.

MATERIALS AND METHODS

Western Blot: Western blots were performed on dog lungs. Protein extracts were separated by SDS-PAGE and transferred onto PVDF membranes. They were probed with antibodies against CD34 (Rabbit mAb, ab81289, 1: 10,000, Abcam Inc., Cambridge, MA, USA) and β-actin (Mouse mAb, ab8224, 1:1000, Abcam Inc., Cambridge, MA, USA). Proteins of interest were detected with fluorescein-conjugated bovine anti-mouse IgG-FITC antibody (sc-2366, 1: 1000, Santa Cruz Biotechnology, Inc., Dallas, Texas, USA) and Cy5-conjugated goat anti-rabbit IgG antibody (ab97077, 1: 1000, Abcam Inc., Cambridge, MA, USA).

Immunohistochemistry: Tissue sections were deparaffinized with xylene and rehydrated in an ethanol series. Endogenous peroxidase activity was inactivated with 0.5% H_2O_2 in methanol in dark for 20 mins at room temperature. After washing, antigen retrieval was performed by incubating sections with warmed pepsin (2 mg/ml in 0.01N HCl) at 37°C for 40 min. After washing, they were blocked with 1% bovine serum albumin (BSA) in 1% PBS for 30 min at room temperature. The sections were then incubated overnight at 4°C with either primary antibodies against CD34 (rabbit monoclonal EP373Y, ab81289, 1:500, Abcam Inc., Cambridge, MA, USA), Von Willebrand Factor (A0082, 1:300, Dako Denmark A/S, Glostrup, Denmark) or 1% BSA (negative control). After washing, they were incubated with secondary antibody (HRP-conjugated goat anti-rabbit IgG antibody, P0448, 1:500, Dako Denmark A/S, Glostrup, Denmark) for 30 min at room temperature. The sections were developed with VECTOR VIP Peroxidase (HRP) substrate kit (SK-4600, VECTOR Laboratories Inc., Burlingame, CA, USA) at room temperature for 5 min and counterstained with methyl green. Sections were then dehydrated in an ethanol series and cover slips were mounted with mounting medium.

Immunofluorescence staining (IF): IF was performed to look at the CD34 expression in WT mice lungs at 0h time-point. Tissue sections were deparaffinized with xylene and rehydrated in an ethanol series. Endogenous peroxidase activity was inactivated with 0.5% H_2O_2 in methanol in dark for 20 mins at room temperature. After washing, antigen retrieval was performed in two steps. Firstly, heat induced epitope retrieval (HIER) was performed by incubating sections in sodium citrate buffer (10mM, pH 6.0) at 90°C-95°C for 20 minutes. Then, the sections were allowed to

cool in distilled water, following which the sections were incubated with warmed pepsin (2 mg/ml in 0.01N HCl) at 37°C for 20 min. After washing, they were blocked with 1% bovine serum albumin in 1% PBS for 30 min at room temperature. The sections were then incubated overnight at 4°C with 100 µL primary antibodies per section against CD34 (rabbit anti-mouse, EP373Y, ab81289, 1:500, Abcam Inc., Cambridge, MA, USA). Next day, the slides were left at room temperature for 30 min followed by washing with PBS 1X thrice. After washing, they were incubated with 100 µL secondary antibody per section (AF488, green) for 30 min at room temperature (in dark). After washing, sections were counterstained with DAPI. Sections were then allowed to dry, and cover slips were mounted with Prolong gold mounting medium. Media was then allowed to cure for 24 hours before sealing the cover slip with nail varnish. Stained slides were stored in dark at 4°C.

RESULTS

vWF ab

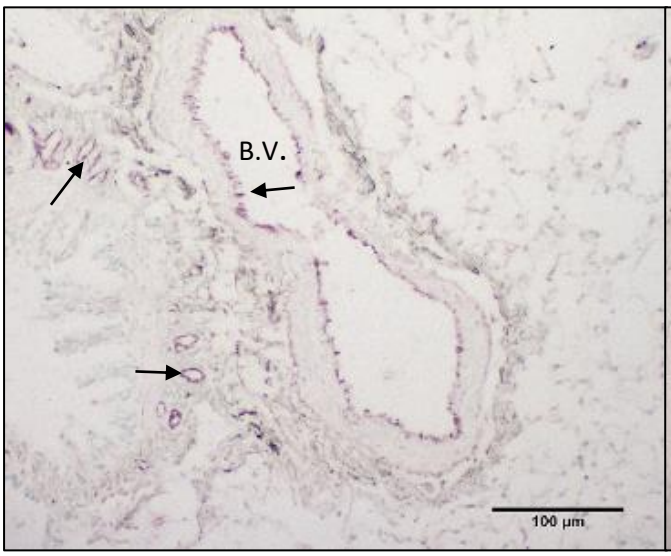

CD34 ab

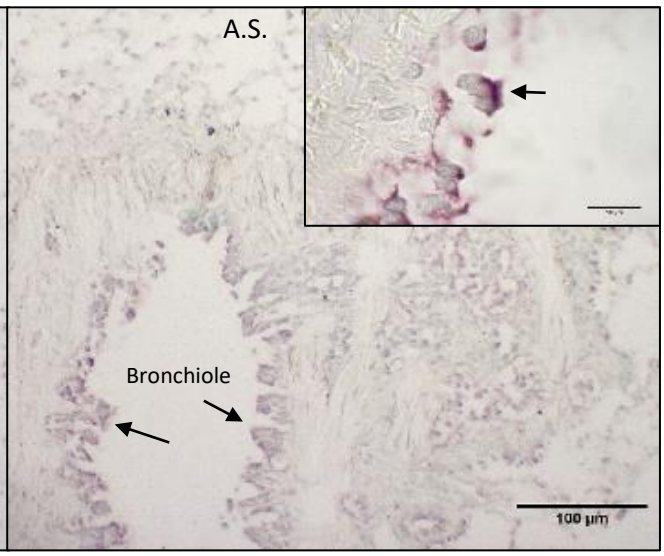

CD34 ab

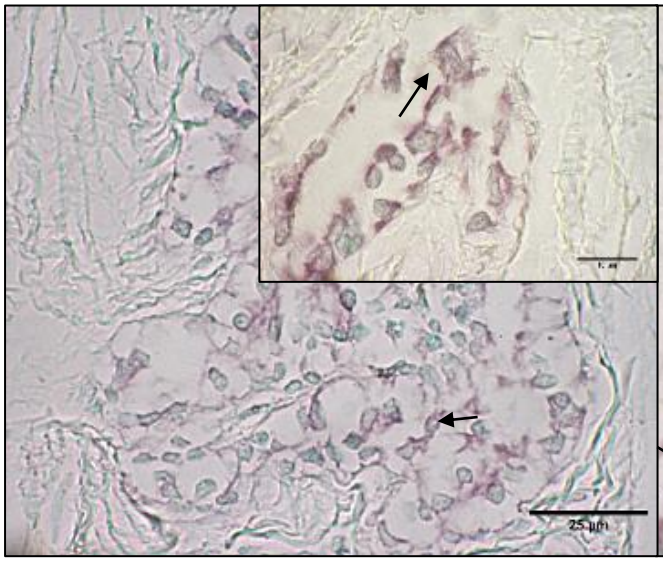

CD34 ab

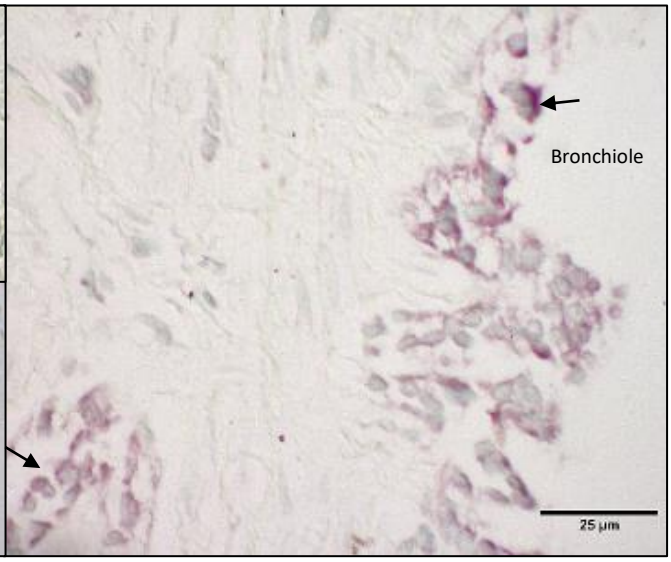

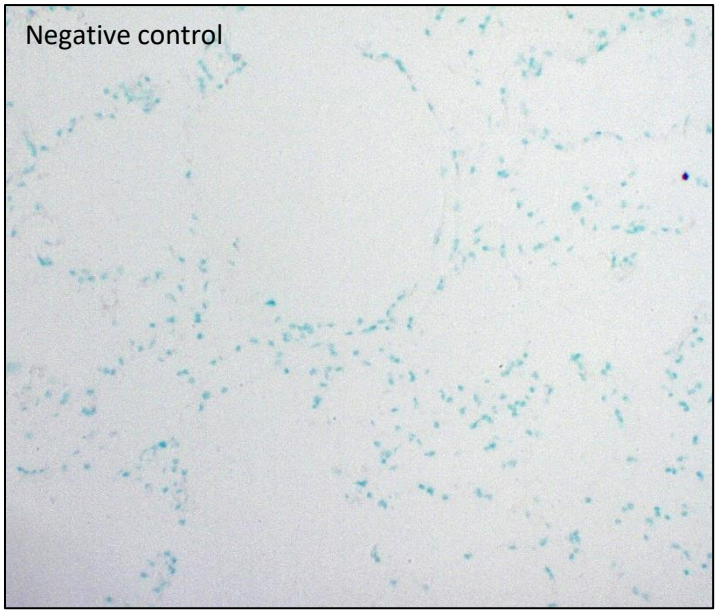

Fig.B.1: Immunohistochemical staining in dog lung sections: Immunohistochemistry was performed on normal dog lungs (N=2). Black arrows pointing at positive staining for CD34 antibody. B.V: Blood vessel; E: Epithelia; i: Interstitium; L: Leukocyte; A.S: Alveolar space. Positive control: vWF, marker for endothelium.

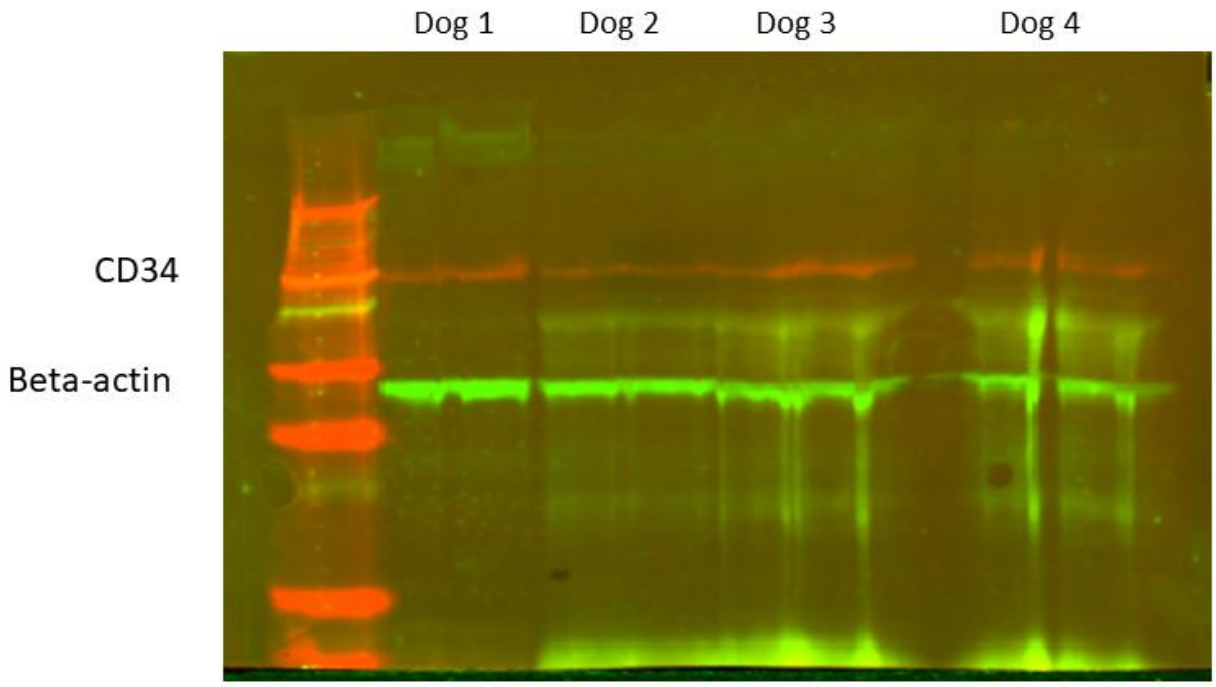

Fig.B.2: Western Blot analysis in dog lung sections: Western blot was performed on normal dog lungs (N=4). Visible red band positive staining detected corresponds to CD34. Control: Beta-actin, green band

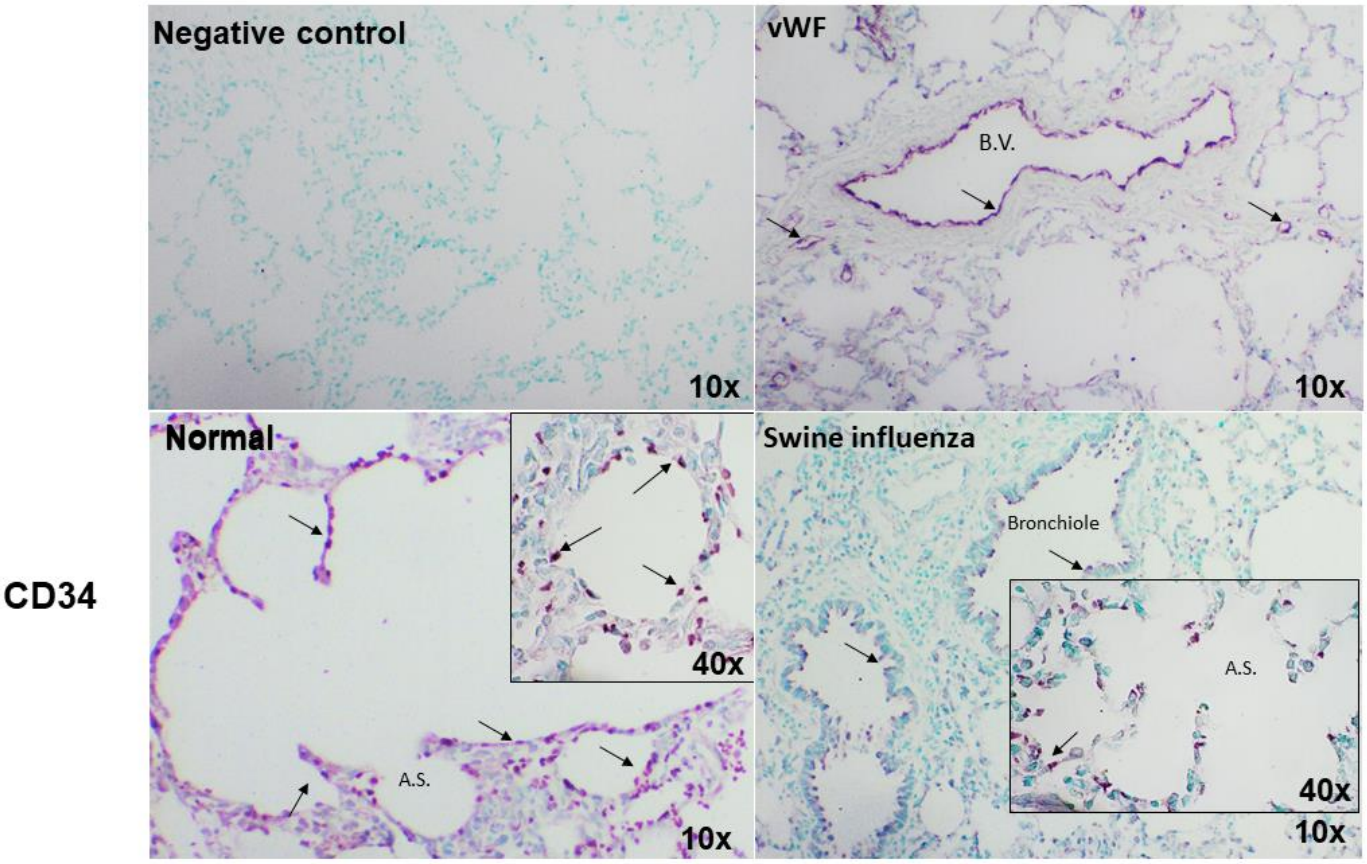

Fig.B.3: Immunohistochemical staining in pig lung sections: Immunohistochemistry was performed on normal pig lungs (N=2) and Swine influenza pig lungs (N=2). Black arrows pointing at positive staining for CD34 antibody. B.V: Blood vessel; A.S: Alveolar space. Positive control: vWF, marker for endothelium.

Green: CD34
Blue: DAPI

WT

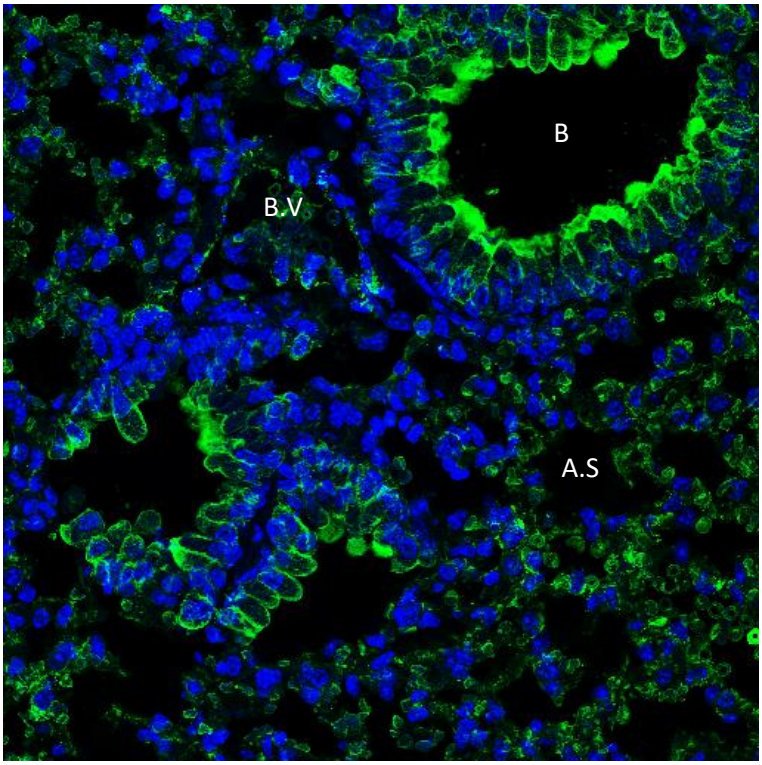

Fig.B.4: CD34 immunofluorescence staining in WT mouse lung section: Immunofluorescence staining on WT mouse lungs was performed for various time points: 0 (no LPS), 9 and 24h in WT (WT, N=2) mice exposed to 50 µg LPS. Green: CD34; Blue: DAPI, staining for cell nucleus. B: Bronchiole; B.V.: Blood vessel, A.S.: Alveolar septum. Scale: 50µm

APPENDIX C: CYTOKINES AND CHEMOKINES

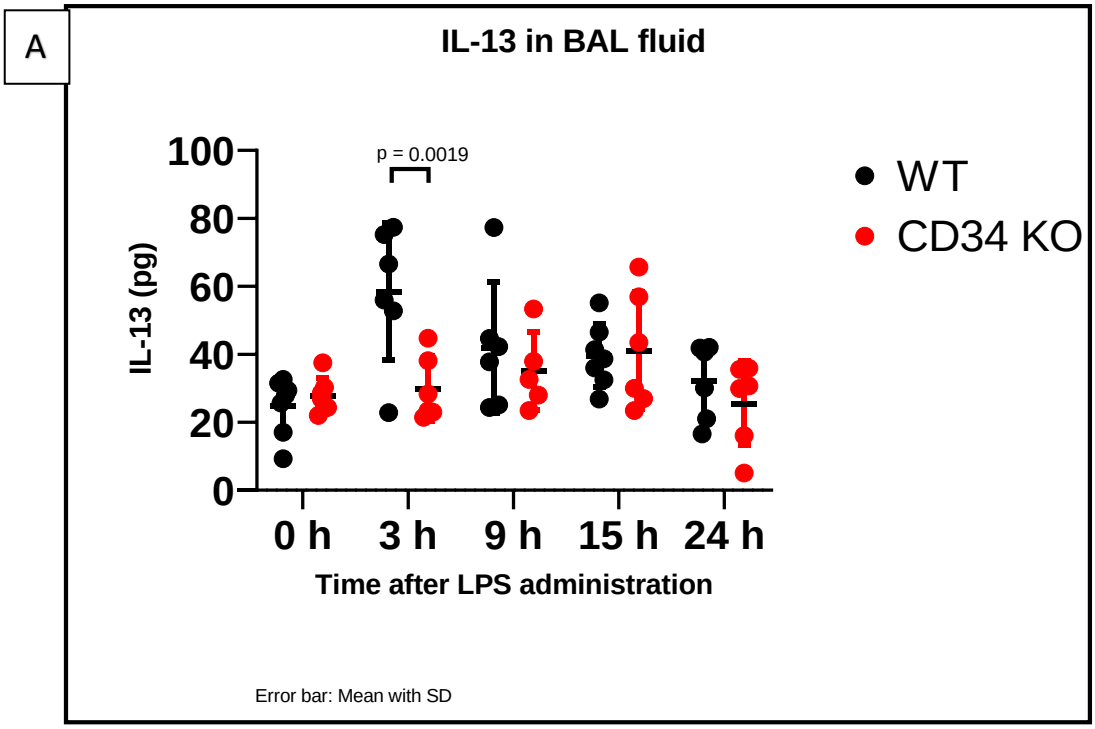

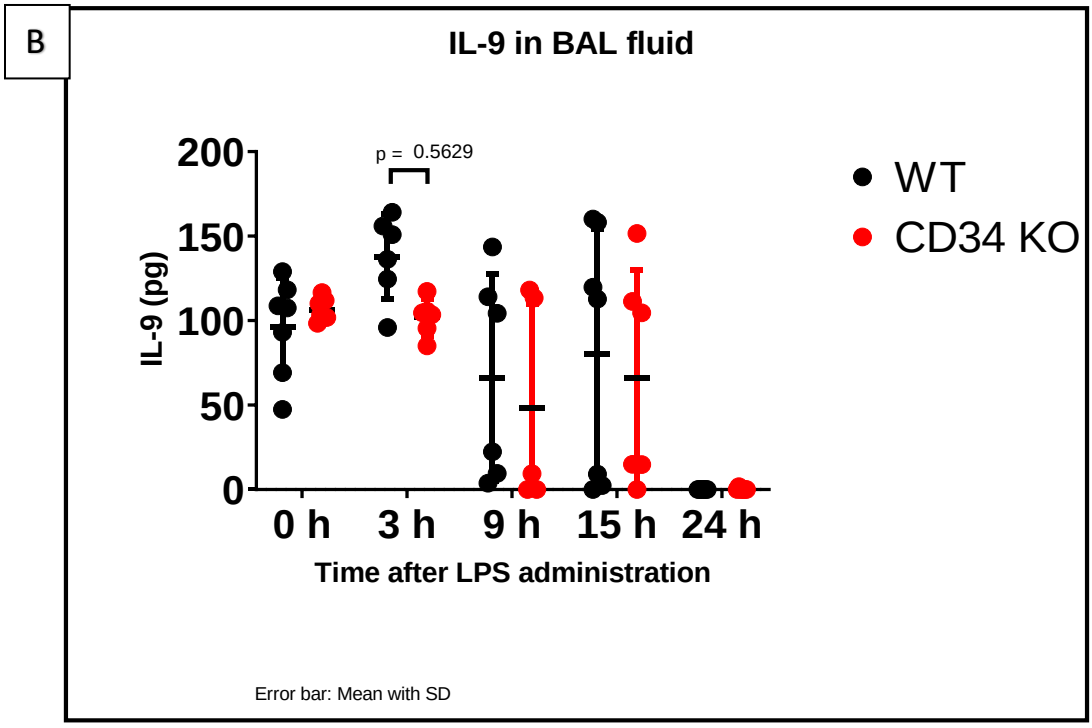

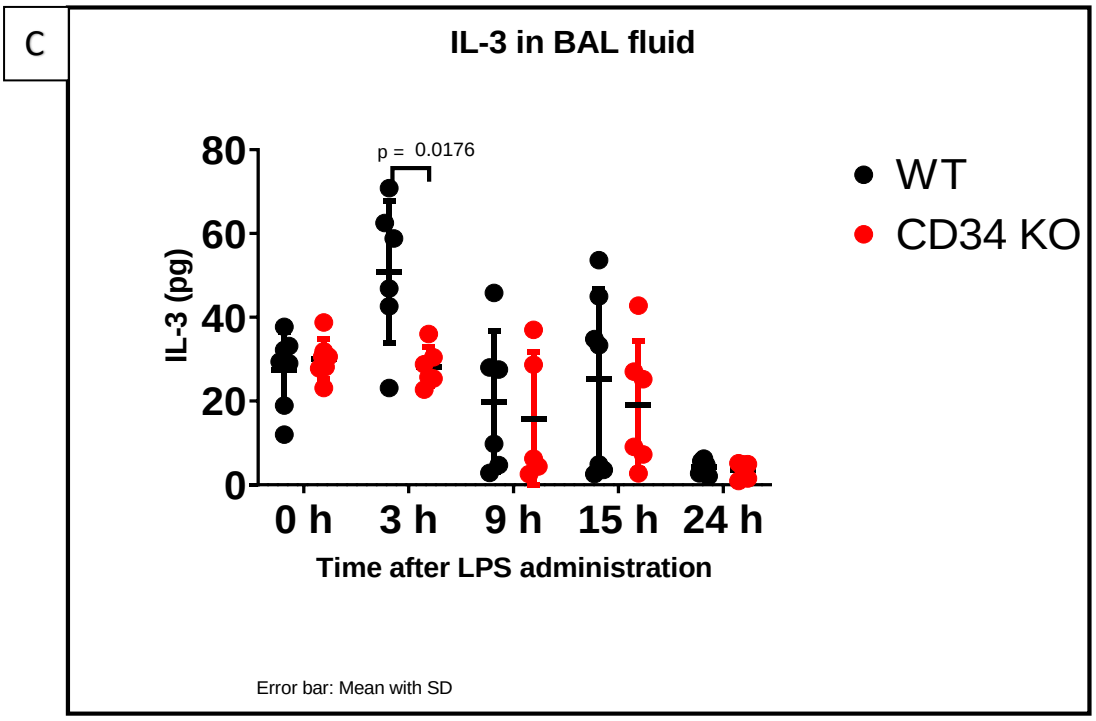

Fig.C.1.A, B, C: ***IL-13, IL-9 and IL-3 content in BAL fluid:*** IL-13, IL-9 and IL-3 in the BAL samples at various time points (0 h, 3, 9, 15, 24 h) in WT (WT, N=5-7) and CD34 KO (N=5-7) mice. Data sets were analyzed using two-way ANOVA with Dunnett's multiple comparisons test (p-values shown in the graph above). All results are expressed as mean ± SD

A

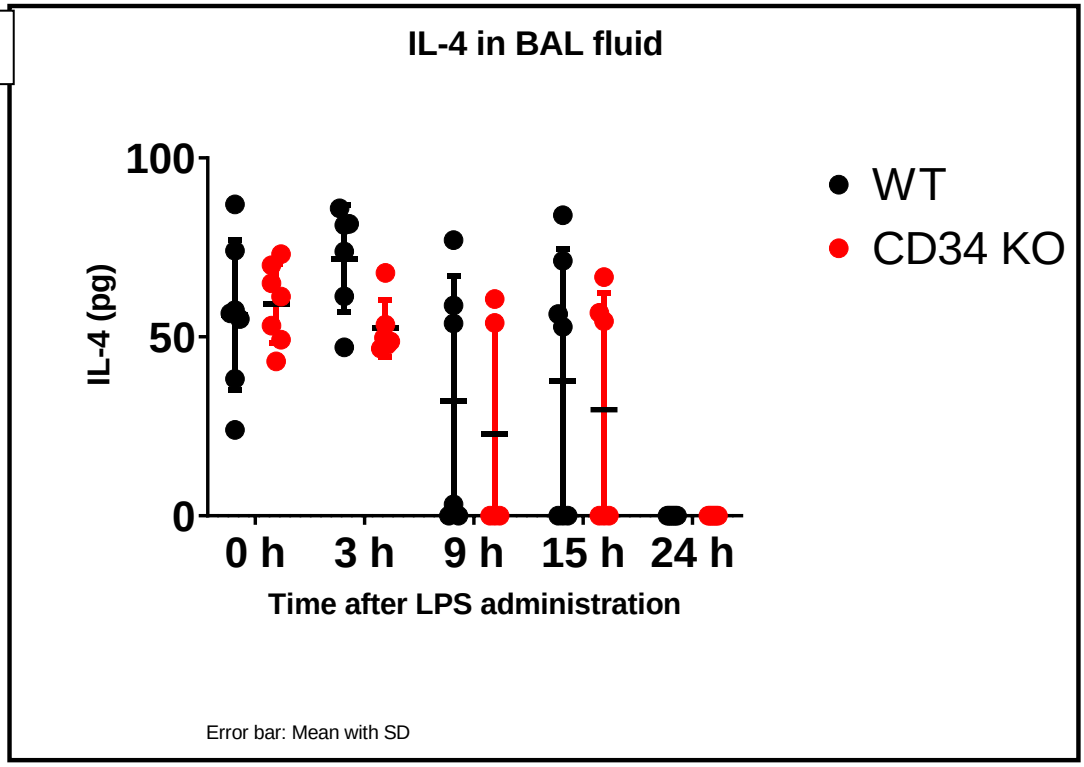
IL-4 in BAL fluid
100
50
0
IL-4 (pg)
0 h
3 h
9 h
15 h
24 h
Time after LPS administration
WT
CD34 KO
Error bar: Mean with SD

B

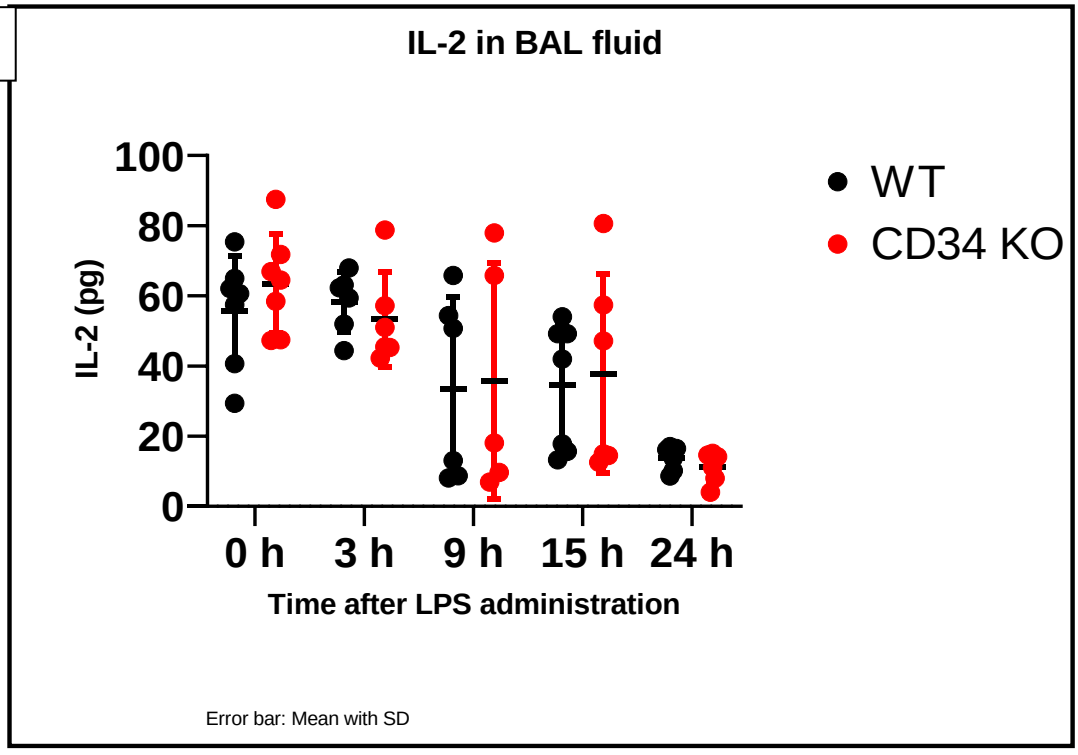
IL-2 in BAL fluid
100
80
60
40
20
0
IL-2 (pg)
0 h
3 h
9 h
15 h
24 h
Time after LPS administration
WT
CD34 KO
Error bar: Mean with SD

Fig. C.2.A, B: ***IL-4 and IL-2 content in BAL fluid:*** IL-4 and IL-2 in the BAL samples at various time points (0 h, 3, 9, 15, 24 h) in WT (WT, N=5-7) and CD34 KO (N=5-7) mice. Data sets were analyzed using two-way ANOVA with Dunnett's multiple comparisons test (p-values shown in the graph above). All results are expressed as mean ± SD

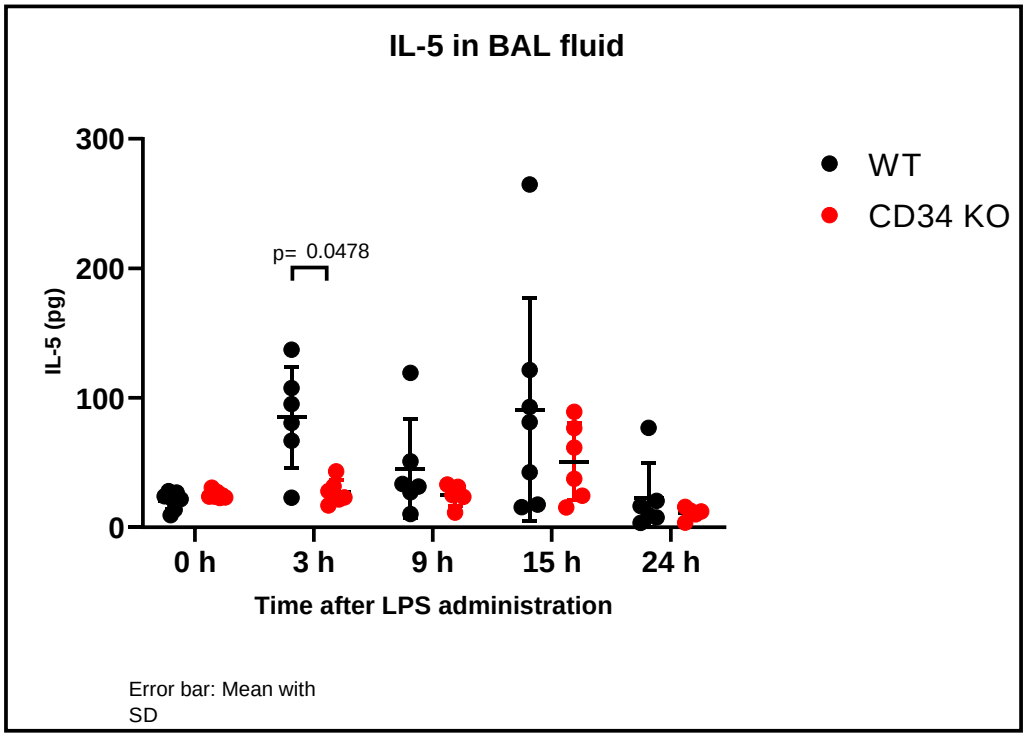

Fig. C.3: ***IL-5 content in BAL fluid:*** IL-5 in the BAL samples at various time points (0 h, 3, 9, 15, 24 h) in WT (WT, N=5-7) and CD34 KO (N=5-7) mice. Data sets were analyzed using two-way ANOVA with Dunnett's multiple comparisons test (p-values shown in the graph above). All results are expressed as mean ± SD

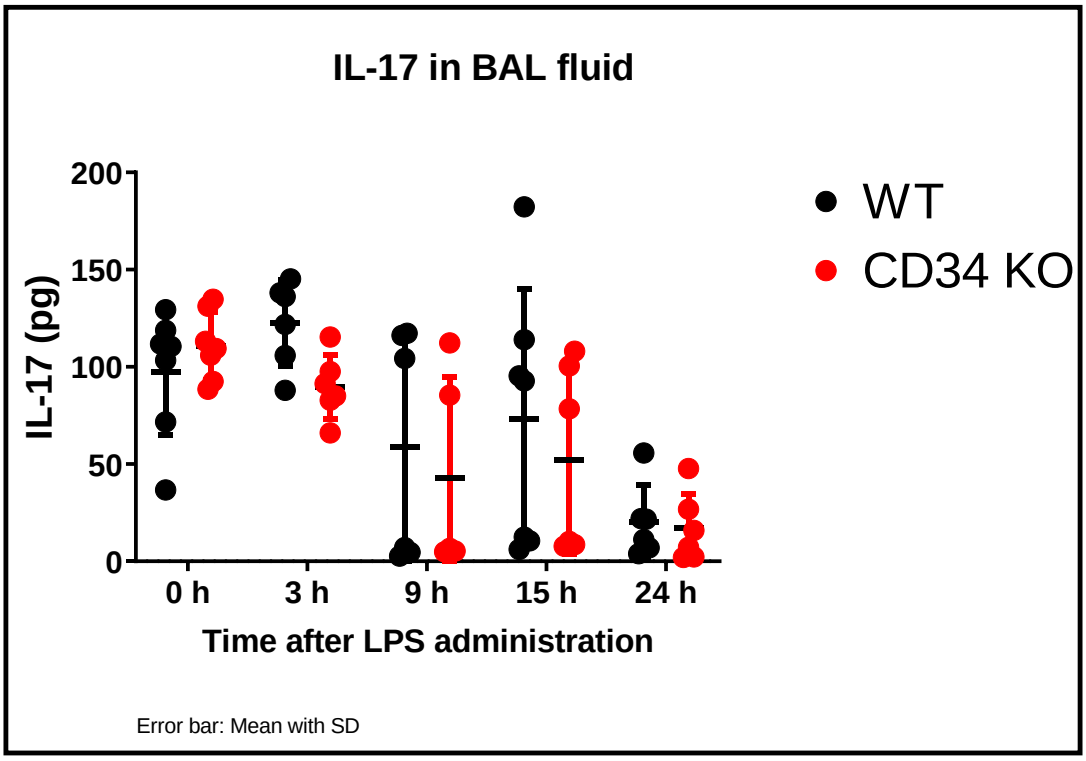

Fig.C.4: ***IL-17 content in BAL fluid:*** IL-17 in the BAL samples at various time points (0 h, 3, 9, 15, 24 h) in WT (WT, N=5-7) and CD34 KO (N=5-7) mice. Data sets were analyzed using two-way ANOVA with Dunnett's multiple comparisons test (p-values shown in the graph above). All results are expressed as mean ± SD

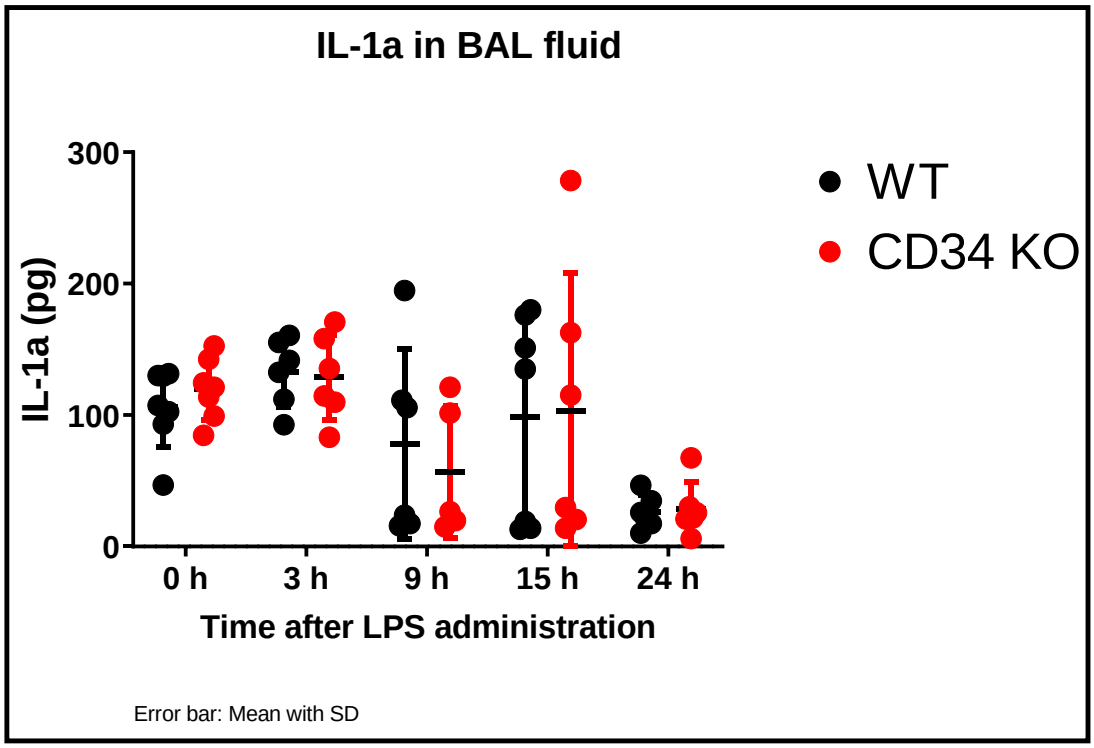

Fig.C.5: ***IL-1a content in BAL fluid:*** IL-1a in the BAL samples at various time points (0 h, 3, 9, 15, 24 h) in WT (WT, N=5-7) and CD34 KO (N=5-7) mice. Data sets were analyzed using two-way ANOVA with Dunnett's multiple comparisons test (p-values shown in the graph above). All results are expressed as mean ± SD

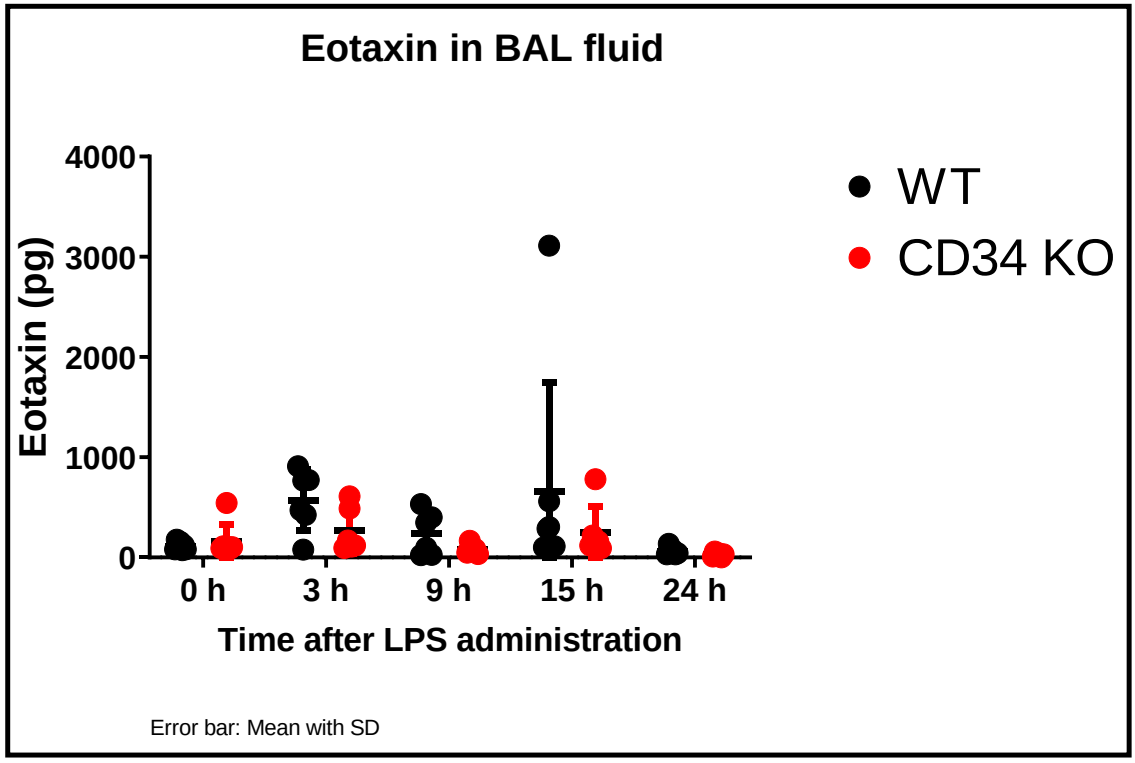

Fig.C.6: ***Eotaxin content in BAL fluid***: RANTES in the BAL samples at various time points (0 h, 3, 9, 15, 24 h) in WT (WT, N=5-7) and CD34 KO (N=5-7) mice. Data sets were analyzed using two-way ANOVA with Dunnett's multiple comparisons test (p-values shown in the graph above). All results are expressed as mean ± SD

REFERENCES

Haslett, C., Savill, J.S., & Meagher, L. (1989). The neutrophil. *Current opinion in immunology, 2*(1), 10-18.

Haslett, C. (1999). Granulocyte Apoptosis and Its Role in the Resolution and Control of Lung Inflammation. *American Journal of Respiratory and Critical Care Medicine, 160*(5), S5-S11.

Matute-Bello, G., & Martin, T.R. (2003). Science review: Apoptosis in acute lung injury. *Critical care, 7*, 355-358.

Matute-Bello, G., Charles W. Frevert,and Thomas R. Martin. (2008). Animal models of acute lung injury. *Am J Physiol Lung Cell Mol Physiol., 295*, L379-L399.

Grommes, J., & Soehnlein, O. (2011). Contribution of neutrophils to acute lung injury. *Mol Med, 17*(3-4), 293-307. doi:10.2119/molmed.2010.00138

Inagawa, H., Kohchi, C., & Soma, G.-i. (2011). Oral Administration of Lipopolysaccharides for the Prevention of Various Diseases: Benefit and Usefulness. *Anticancer Research, 31*(7), 2431-2436.

Alexander. C., E.T.R. (2001). Invited review: Bacterial lipopolysaccharides and innate immunity. *Journal of endotoxin research, 7*, 168-202.

Maas, S.L., Soehnlein, O., & Viola, J.R. (2018). Organ-Specific Mechanisms of Transendothelial Neutrophil Migration in the Lung, Liver, Kidney, and Aorta. *Frontiers in Immunology, 9*(2739). doi:10.3389/fimmu.2018.02739

Ashley, N., Zachary M. Weil, and Randy J. Nelson. (2012). Inflammation: Mechanisms, Costs, and Natural Variation. *Annual Review of Ecology, Evolution, and Systematics, 43*, 385-406.

De Filippo, K., Henderson, R.B., Laschinger, M., & Hogg, N. (2008). Neutrophil Chemokines KC and Macrophage-Inflammatory Protein-2 Are Newly Synthesized by Tissue Macrophages Using Distinct TLR Signaling Pathways. *The Journal of Immunology, 180*(6), 4308-4315. doi:10.4049/jimmunol.180.6.4308

Hackett, T.-L., Holloway, R., Holgate, S.T., & Warner, J.A. (2008). Dynamics of pro-inflammatory and anti-inflammatory cytokine release during acute inflammation in chronic obstructive pulmonary disease: an ex vivo study. *Respiratory Research, 9*(1), 47-61. doi:10.1186/1465-9921-9-47

Ley, K., Laudanna, C., Cybulsky, M.I., & Nourshargh, S. (2007). Getting to the site of inflammation: the leukocyte adhesion cascade updated. *Nature reviews.Immunology, 7*(9), 678-689. doi:10.1038/nri2156

Phillipson, M., Kaur, J., Colarusso, P., Ballantyne, C.M., & Kubes, P. (2008). Endothelial domes encapsulate adherent neutrophils and minimize increases in vascular permeability in paracellular and transcellular emigration. *PLoS One, 3*(2), e1649. doi:10.1371/journal.pone.0001649

Petri, B., Kaur, J., Long, E.M., Li, H., Parsons, S.A., Butz, S., et al. (2011). Endothelial LSP1 is involved in endothelial dome formation, minimizing vascular permeability changes during neutrophil transmigration in vivo. *Blood, 117*(3), 942-952. doi:10.1182/blood-2010-02-270561

Niggli, V. (2003). Microtubule-disruption-induced and chemotactic-peptide-induced migration of human neutrophils: implications for differential sets of signalling pathways. *Journal of Cell Science, 116*(Pt 5), 813-822.

Niggli, V., & Rossy, J. (2008). Ezrin/radixin/moesin: versatile controllers of signaling molecules and of the cortical cytoskeleton. *Int J Biochem Cell Biol, 40*(3), 344-349. doi:10.1016/j.biocel.2007.02.012

Nielsen, J.S., McNagny, Kelly M. . (2008). Novel functions of the CD34 family. *Journal of Cell Science, 121*, 3683-3692.

Andrews, R., Singer JW, Bernstein ID. (1989). Precursors of colony-forming cells in humans can be distinguished from colony-forming cells by expression of the CD33 and CD34 antigens and light scatter properties. *J Exp Med., 169*, 1721-1731.

Lewandowska, K., Kaplan, D., & Husel, W. (2003). CD34 expression on platelets. *Platelets, 14*(2), 83-87. doi:10.1080/0953710031000080577

Delia, D., Lampugnani, M.G., Resnati, M., Dejana, E., Aiello, A., Fontanella, E., et al. (1993). CD34 expression is regulated reciprocally with adhesion molecules in vascular endothelial cells in vitro. *Blood, 81*(4), 1001-1008.

Ohnishi, H., Sasaki, H., Nakamura, Y., Kato, S., Ando, K., Narimatsu, H., et al. (2013). Regulation of cell shape and adhesion by CD34. *Cell Adh Migr, 7*(5), 426-433. doi:10.4161/cam.25957

Tan, P.C., Furness, S.G., Merkens, H., Lin, S., McCoy, M.L., Roskelley, C.D., et al. (2006). Na+/H+ exchanger regulatory factor-1 is a hematopoietic ligand for a subset of the CD34 family of stem cell surface proteins. *Stem Cells, 24*(5), 1150-1161. doi:10.1634/stemcells.2005-0426

Blanchet, M.R., Maltby, S., Haddon, D.J., Merkens, H., Zbytnuik, L., & McNagny, K.M. (2007). CD34 facilitates the development of allergic asthma. *Blood, 110*(6), 2005-2012. doi:10.1182/blood-2006-12-062448

Blanchet, M.R., Jami L. Bennett, Matthew J. Gold, Elena Levantini, Daniel G. Tenen, Melissa Girard, Yvon Cormier and Kelly M. McNagny (2011). CD34 Is Required for Dendritic Cell Trafficking and Pathology in Murine Hypersensitivity Pneumonitis. . *Am. J. Respir. Crit. Care Med., 184*, 687-698.

Lo, B.C., Gold, M.J., Scheer, S., Hughes, M.R., Cait, J., Debruin, E., et al. (2017). Loss of Vascular CD34 Results in Increased Sensitivity to Lung Injury. *American Journal of Respiratory cell and molecular biology, 57*(6), 651-661. doi:10.1165/rcmb.2016-0386OC

Williams, A.E., and Rachel C. Chambers. (2014). The mercurial nature of neutrophils: still an enigma in ARDS? *Am J Physiol Lung Cell Mol Physiol., 306*, L217-L230.

Han, S., & Mallampalli, R.K. (2015). The Acute Respiratory Distress Syndrome: From Mechanism to Translation. *The Journal of Immunology, 194*(3), 855-860. doi:10.4049/jimmunol.1402513

Medzhitov, R. (2008). Origin and physiological roles of inflammation. *Nature, 454*, 428-435.

Matute-Bello, G., Downey, G., Moore, B.B., Groshong, S.D., Matthay, M.A., Slutsky, A.S., et al. (2011). An Official American Thoracic Society Workshop Report: Features and Measurements of Experimental Acute Lung Injury in Animals. *American Journal of Respiratory cell and molecular biology, 44*(5), 725-738. doi:10.1165/rcmb.2009-0210ST

Brat, D.J., Bellail, A.C., & Van Meir, E.G. (2005). The role of interleukin-8 and its receptors in gliomagenesis and tumoral angiogenesis. *Neuro-oncology, 7*(2), 122-133. doi:10.1215/S1152851704001061

Muller, W.A. (2013). Getting Leukocytes to the Site of Inflammation. *Vet Pathology, 50*, 7-22.

McEver, R.P. (2015). Selectins: initiators of leucocyte adhesion and signalling at the vascular wall. *Cardiovascular Research, 107*(3), 331-339. doi:10.1093/cvr/cvv154

Liu, Z., Yago, T., Zhang, N., Panicker, S.R., Wang, Y., Yao, L., et al. (2017). L-selectin mechanochemistry restricts neutrophil priming in vivo. *Nature communications, 8*, 15196-15196. doi:10.1038/ncomms15196

Phillipson, M., Heit, B., Colarusso, P., Liu, L., Ballantyne, C.M., & Kubes, P. (2006). Intraluminal crawling of neutrophils to emigration sites: a molecularly distinct process from adhesion in the recruitment cascade. *The Journal of Experimental Medicine, 203*(12), 2569-2575. doi:10.1084/jem.20060925

Bixel, M.G., Li, H., Petri, B., Khandoga, A.G., Khandoga, A., Zarbock, A., et al. (2010). CD99 and CD99L2 act at the same site as, but independently of, PECAM-1 during leukocyte diapedesis. *Blood, 116*(7), 1172-1184. doi:10.1182/blood-2009-12-256388

Sullivan, D.P., & Muller, W.A. (2014). Neutrophil and monocyte recruitment by PECAM, CD99, and other molecules via the LBRC. *Seminars in Immunopathology, 36*(2), 193-209. doi:10.1007/s00281-013-0412-6

Mamdouh, Z., Chen, X., Pierini, L.M., Maxfield, F.R., & Muller, W.A. (2003). Targeted recycling of PECAM from endothelial surface-connected compartments during diapedesis. *Nature, 421*(6924), 748-753. doi:http://www.nature.com/nature/journal/v421/n6924/suppinfo/nature01300_S1.html

Mamdouh, Z., Kreitzer, G.E., & Muller, W.A. (2008). Leukocyte transmigration requires kinesin-mediated microtubule-dependent membrane trafficking from the lateral border recycling compartment. *The Journal of Experimental Medicine, 205*(4), 951-966. doi:10.1084/jem.20072328

Boekhorst, V., Luigi Preziosi, and Peter Friedl. (2016). Plasticity of Cell Migration In Vivo and In Silico. *Annual Review of Cell and Developmental Biology, Vol.32:491-526*.

Gardel, M., Ian C. Schneider, Yvonne Aratyn-Schaus, and Clare M. Waterman. (2010). Mechanical Integration of Actin and Adhesion Dynamics in Cell Migration. *Annual Review of Cell and Developmental Biology, 26*, 315-333.

Insall, R.H. (2010). Understanding eukaryotic chemotaxis: a pseudopod-centred view. *Nat Rev Mol Cell Biol, 11*(6), 453-458.

Insall, R. (2013). The interaction between pseudopods and extracellular signalling during chemotaxis and directed migration. *Current Opinion in Cell Biology, 25*(5), 526-531. doi:http://dx.doi.org/10.1016/j.ceb.2013.04.009

Khan, A.I., Heit, B., Andonegui, G., Colarusso, P., & Kubes, P. (2005). Lipopolysaccharide: A p38 MAPK-Dependent Disrupter of Neutrophil Chemotaxis. *Microcirculation, 12*(5), 421-432. doi:10.1080/10739680590960368

Hino, M., Kurogi, K., Okubo, M.-A., Murata-Hori, M., & Hosoya, H. (2000). Small Heat Shock Protein 27 (HSP27) Associates with Tubulin/Microtubules in HeLa Cells. *Biochemical and Biophysical Research Communications, 271*(1), 164-169. doi:http://dx.doi.org/10.1006/bbrc.2000.2553

Hino, M., & Hosoya, H. (2003). Small Heat Shock Protein Hsp27 Directly Binds to Alpha/Beta Tnbulin Heterodimer and Inhibits DMSO-Induced Tubulin Polymerization. *Biomedical Research, 24*(1), 27-30. doi:10.2220/biomedres.24.27

Jog, N.R., Jala, V.R., Ward, R.A., Rane, M.J., Haribabu, B., & McLeish, K.R. (2007). Heat Shock Protein 27 Regulates Neutrophil Chemotaxis and Exocytosis through Two Independent Mechanisms. *The Journal of Immunology, 178*(4), 2421-2428. doi:10.4049/jimmunol.178.4.2421

Barreiro, O., De La Fuente, H., Mittelbrunn, M., & Sánchez-Madrid, F. (2007). Functional insights on the polarized redistribution of leukocyte integrins and their ligands during leukocyte migration and immune interactions. *Immunological Reviews, 218*(1), 147-164. doi:10.1111/j.1600-065X.2007.00529.x

Barreiro, O., Martín, P., González-Amaro, R., & Sánchez-Madrid, F. (2010). Molecular cues guiding inflammatory responses. *Cardiovascular Research, 86*(2), 174-182. doi:10.1093/cvr/cvq001

Doerschuk, C., robert k. Winn, harvey 0. Coxson, and john m. Harlan. (1990). Cd18-dependent and -independent mechanisms of neutrophil emigration in the pulmonary and systemic microcirculation of rabbits. *Journal of Immunology, 144*, 2327-2333.

Hellewell, P.G., Scott K. Young, Peter M. Henson, and G. Scott Worthen. (1994). Disparate role of the beta2-Integrln CD18 in the Local Accumulation of neutrophils in pulmonary and cutaneous Inflammation in the Rabbit. *American Journal of Respiratory cell and molecular biology*.

Windsor AC, W.C., Mullen PG, Cook DJ, Fisher BJ, Blocher CR, Leeper-Woodford SK, Sugerman HJ, Fowler AA III. (1993). Tumor necrosis factor-alpha blockade prevents neutrophil CD18 receptor upregulation and attenuates acute lung injury in porcine sepsis without inhibition of neutrophil oxygen radical generation. *J Clin Invest, 91*, 1459-1468.

Sassetti, C., Van Zante, A., & Rosen, S.D. (2000). Identification of Endoglycan, a Member of the CD34/Podocalyxin Family of Sialomucins. *Journal of Biological Chemistry, 275*(12), 9001-9010. doi:10.1074/jbc.275.12.9001

Rosen, S.D. (2004). Ligands for L-selectin: homing, inflammation, and beyond. *Annual Review of Immunology, 22*, 129-156.

Fina, L., Molgaard, H.V., Robertson, D., Bradley, N.J., Monaghan, P., Delia, D., et al. (1990). Expression of the CD34 gene in vascular endothelial cells. *Blood, 75*(12), 2417-2426.

Pusztaszeri, M.P., Seelentag, W., & Bosman, F.T. (2006). Immunohistochemical expression of endothelial markers CD31, CD34, von Willebrand factor, and Fli-1 in normal human tissues. *J Histochem Cytochem, 54*(4), 385-395. doi:10.1369/jhc.4A6514.2005

Drew, E., Merkens H, Chelliah S, Doyonnas R, McNagny KM. (2002). CD34 is a specific marker of mature murine mast cells. *Exp. Hematol., 30*(1211-1218).

Radinger, M., Johansson, A.K., Sitkauskiene, B., Sjostrand, M., & Lotvall, J. (2004). Eotaxin-2 regulates newly produced and CD34 airway eosinophils after allergen exposure. *J Allergy Clin Immunol, 113*(6), 1109-1116. doi:10.1016/j.jaci.2004.03.022

Ladeby, R., Wirenfeldt, M., Dalmau, I., Gregersen, R., Garcia-Ovejero, D., Babcock, A., et al. (2005). Proliferating resident microglia express the stem cell antigen CD34 in response to acute neural injury. *Glia, 50*(2), 121-131. doi:10.1002/glia.20159

Schmidt, M., Sun G, Stacey MA, Mori L, Mattoli S (2003). Identification of circulating fibrocytes as precursors of bronchial myofibroblasts in asthma. *J. Immunol., 171:380–389.*

Beauchamp, J.R., Heslop, L., Yu, D.S., Tajbakhsh, S., Kelly, R.G., Wernig, A., et al. (2000). Expression of CD34 and Myf5 defines the majority of quiescent adult skeletal muscle satellite cells. *J Cell Biol, 151*(6), 1221-1234.

Suter, S.E., Gouthro, T.A., McSweeney, P.A., Nash, R.A., Haskins, M.E., Felsburg, P.J., et al. (2004). Isolation and characterization of pediatric canine bone marrow CD34+ cells. *Vet Immunol Immunopathol, 101*(1-2), 31-47. doi:10.1016/j.vetimm.2004.03.009

Tsumagari, S., Otani, I., Tanemura, K., Namba, S., Ohtaki, T., Kamata, H., et al. (2007). Characterization of CD34+ cells from canine umbilical cord blood, bone marrow leukocytes, and peripheral blood by flow cytometric analysis. *J Vet Med Sci, 69*(11), 1207-1209.

Kobayashi, T., Shimizu, A., Nishifuji, K., Amagai, M., Iwasaki, T., & Ohyama, M. (2009). Canine hair-follicle keratinocytes enriched with bulge cells have the highly proliferative characteristic of stem cells. *Veterinary Dermatology, 20*(5-6), 338-346. doi:doi:10.1111/j.1365-3164.2009.00815.x

Felschow, D.M., McVeigh, M.L., Hoehn, G.T., Civin, C.I., & Fackler, M.J. (2001). The adapter protein CrkL associates with CD34. *Blood, 97*(12), 3768-3775.

Alfaro, L.A.S., Dick, S.A., Siegel, A.L., Anonuevo, A.S., McNagny, K.M., Megeney, L.A., et al. (2011). CD34 Promotes Satellite Cell Motility and Entry into Proliferation to Facilitate Efficient Skeletal Muscle Regeneration. *Stem cells (Dayton, Ohio), 29*(12), 2030-2041. doi:10.1002/stem.759

AbuSamra, D.B., Aleisa, F.A., Al-Amoodi, A.S., Jalal Ahmed, H.M., Chin, C.J., Abuelela, A.F., et al. (2017). Not just a marker: CD34 on human hematopoietic stem/progenitor cells dominates vascular selectin binding along with CD44. *Blood advances, 1*(27), 2799-2816. doi:10.1182/bloodadvances.2017004317

Mrówczyński, W., Rungatscher, A., Buchegger, F., Tille, J.-C., Namy, S., Ratib, O., et al. (2014). Biological effects of anti-CD34-coated ePTFE vascular grafts. Early in vivo experimental results. *Kardiochirurgia i torakochirurgia polska = Polish journal of cardio-thoracic surgery, 11*(2), 182-190. doi:10.5114/kitp.2014.43848

Puri, K.D., Finger, E.B., Gaudernack, G., & Springer, T.A. (1995). Sialomucin CD34 is the major L-selectin ligand in human tonsil high endothelial venules. *The Journal of Cell Biology, 131*(1), 261-270. doi:10.1083/jcb.131.1.261

Mori, T., Ken Kitano, Shin-ichi Terawaki, Ryoko Maesaki, Yayoi Fukami and Toshio Hakoshima. (2008). Structural Basis for CD44 Recognition by ERM Proteins. *THE JOURNAL OF BIOLOGICAL CHEMISTRY, 283*, 29602–29612.

Maltby, S., Freeman, S., Gold, M.J., Baker, J.H.E., Minchinton, A.I., Gold, M.R., et al. (2011). Opposing Roles for CD34 in B16 Melanoma Tumor Growth Alter Early Stage Vasculature and Late Stage Immune Cell Infiltration. *PLoS One, 6*(4), e18160. doi:10.1371/journal.pone.0018160

Strilić, B., Kučera, T., Eglinger, J., Hughes, M.R., McNagny, K.M., Tsukita, S., et al. (2009). The Molecular Basis of Vascular Lumen Formation in the Developing Mouse Aorta. *Developmental Cell, 17*(4), 505-515. doi:https://doi.org/10.1016/j.devcel.2009.08.011

Blanchet, M.-R., Gold, M., Maltby, S., Bennett, J., Petri, B., Kubes, P., et al. (2010). Loss of CD34 Leads To Exacerbated Autoimmune Arthritis through Increased Vascular Permeability. *The Journal of Immunology, 184*(3), 1292.

Simson, L., Ellyard, J.I., Dent, L.A., Matthaei, K.I., Rothenberg, M.E., Foster, P.S., et al. (2007). Regulation of Carcinogenesis by IL-5 and CCL11: A Potential Role for Eosinophils in Tumor Immune Surveillance. *The Journal of Immunology, 178*(7), 4222-4229.

Tasev, D., Konijnenberg, L.S.F., Amado-Azevedo, J., van Wijhe, M.H., Koolwijk, P., & van Hinsbergh, V.W.M. (2016). CD34 expression modulates tube-forming capacity and barrier properties of peripheral blood-derived endothelial colony-forming cells (ECFCs). *Angiogenesis, 19*, 325-338. doi:10.1007/s10456-016-9506-9

Fackler, M.J., Krause, D.S., Smith, O.M., Civin, C.I., & May, W.S. (1995). Full-length but not truncated CD34 inhibits hematopoietic cell differentiation of M1 cells. *Blood, 85*(11), 3040-3047.

Marone, M., Scambia, G., Bonanno, G., Rutella, S., de Ritis, D., Guidi, F., et al. (2002). Transforming growth factor-β1 transcriptionally activates CD34 and prevents induced differentiation of TF-1 cells in the absence of any cell-cycle effects. *Leukemia, 16*, 94-105. doi:10.1038/sj.leu.2402334

Ieronimakis, N., Balasundaram, G., Rainey, S., Srirangam, K., Yablonka-Reuveni, Z., & Reyes, M. (2010). Absence of CD34 on Murine Skeletal Muscle Satellite Cells Marks a Reversible State of Activation during Acute Injury. *PLoS One, 5*(6), e10920. doi:10.1371/journal.pone.0010920

Grassl, G.A., Faustmann, M., Gill, N., Zbytnuik, L., Merkens, H., So, L., et al. (2010). CD34 mediates intestinal inflammation in Salmonella-infected mice. *Cellular Microbiology, 12*(11), 1562-1575. doi:10.1111/j.1462-5822.2010.01488.x

Maltby, S., Wohlfarth, C., Gold, M., Zbytnuik, L., Hughes, M.R., & McNagny, K.M. (2010). CD34 Is Required for Infiltration of Eosinophils into the Colon and Pathology Associated with DSS-Induced Ulcerative Colitis. *The American Journal of Pathology, 177*(3), 1244-1254. doi:https://doi.org/10.2353/ajpath.2010.100191

Tschernig, T., Pabst, R., Kasper, M., El-Hadi, M., & Singh, B. (2014). Expression of caveolin-1 and podocalyxin in rat lungs challenged with 2-kDa macrophage-activating lipopeptide and Flt3L. *Cell and Tissue Research, 356*(1), 207-216. doi:10.1007/s00441-013-1771-y

Miettinen, A., Solin, M.L., Reivinen, J., Juvonen, E., Väisänen, R., & Holthöfer, H. (1999). Podocalyxin in rat platelets and megakaryocytes. *The American Journal of Pathology, 154*(3), 813-822. doi:10.1016/S0002-9440(10)65328-X

Ma, A.C., & Kubes, P. (2008). Platelets, neutrophils, and neutrophil extracellular traps (NETs) in sepsis. *Journal of Thrombosis and Haemostasis, 6*(3), 415-420. doi:10.1111/j.1538-7836.2007.02865.x

Doyonnas, R., Kershaw, D.B., Duhme, C., Merkens, H., Chelliah, S., Graf, T., et al. (2001). Anuria, Omphalocele, and Perinatal Lethality in Mice Lacking the Cd34-Related Protein Podocalyxin. *The Journal of Experimental Medicine, 194*(1), 13-28. doi:10.1084/jem.194.1.13

Takeda, T., Go, W.Y., Orlando, R.A., & Farquhar, M.G. (2000). Expression of Podocalyxin Inhibits Cell–Cell Adhesion and Modifies Junctional Properties in Madin-Darby Canine Kidney Cells. *Molecular Biology of the Cell, 11*(9), 3219-3232.

Debruin, E.J., Hughes, M.R., Sina, C., Liu, A., Cait, J., Jian, Z., et al. (2014). Podocalyxin Regulates Murine Lung Vascular Permeability by Altering Endothelial Cell Adhesion. *PLoS One, 9*(10), e108881. doi:10.1371/journal.pone.0108881

Cait, J., Hughes, M.R., Zeglinski, M.R., Chan, A.W., Osterhof, S., Scott, R.W., et al. (2019). Podocalyxin is required for maintaining blood-brain barrier function during acute inflammation. *Proceedings of the National Academy of Sciences of the United States of America, 116*(10), 4518-4527. doi:10.1073/pnas.1814766116

Zarbock, A., Singbartl, K., & Ley, K. (2006). Complete reversal of acid-induced acute lung injury by blocking of platelet-neutrophil aggregation. *The Journal of Clinical Investigation, 116*(12), 3211-3219. doi:10.1172/JCI29499

Card, J.W., Carey, M.A., Bradbury, J.A., DeGraff, L.M., Morgan, D.L., Moorman, M.P., et al. (2006). Gender Differences in Murine Airway Responsiveness and Lipopolysaccharide-Induced Inflammation. *The Journal of Immunology, 177*(1), 621-630. doi:10.4049/jimmunol.177.1.621

Reutershan, J., Abdul Basit, Elena V. Galkina, & Klaus Ley. (2005). Sequential recruitment of neutrophils into lung and bronchoalveolar lavage fluid in LPS-induced acute lung injury. *American*

Journal of Physiology-Lung Cellular and Molecular Physiology, *289*(5), L807-L815. doi:10.1152/ajplung.00477.2004

Xing, Z., Jordana, M., Kirpalani, H., Driscoll, K.E., Schall, T.J., & Gauldie, J. (1994). Cytokine expression by neutrophils and macrophages in vivo: endotoxin induces tumor necrosis factor-alpha, macrophage inflammatory protein-2, interleukin-1 beta, and interleukin-6 but not RANTES or transforming growth factor-beta 1 mRNA expression in acute lung inflammation. *American Journal of Respiratory cell and molecular biology*, *10*(2), 148-153. doi:10.1165/ajrcmb.10.2.8110470

Li, X., Donaldson, K., & Macnee, W. (1998). Lipopolysaccharide-induced Alveolar Epithelial Permeability. *American Journal of Respiratory and Critical Care Medicine*, *157*(4), 1027-1033. doi:10.1164/ajrccm.157.4.9605080

Stapleton, R.D., Suratt, B.T., Neff, M.J., Wurfel, M.M., Ware, L.B., Ruzinski, J.T., et al. (2019). Bronchoalveolar fluid and plasma inflammatory biomarkers in contemporary ARDS patients. *Biomarkers*, *24*(4), 352-359. doi:10.1080/1354750X.2019.1581840

Gao, J.L., Wynn, T.A., Chang, Y., Lee, E.J., Broxmeyer, H.E., Cooper, S., et al. (1997). Impaired host defense, hematopoiesis, granulomatous inflammation and type 1-type 2 cytokine balance in mice lacking CC chemokine receptor 1. *The Journal of Experimental Medicine*, *185*(11), 1959-1968. doi:10.1084/jem.185.11.1959

Abdi, K. (2002). IL-12: The Role of p40 Versus p75. *Scandinavian Journal of Immunology*, *56*(1), 1-11. doi:10.1046/j.1365-3083.2002.01101.x

Panopoulos, A.D., & Watowich, S.S. (2008). Granulocyte colony-stimulating factor: molecular mechanisms of action during steady state and 'emergency' hematopoiesis. *Cytokine*, *42*(3), 277-288. doi:10.1016/j.cyto.2008.03.002

Aldinucci, D., & Colombatti, A. (2014). The inflammatory chemokine CCL5 and cancer progression. *Mediators of inflammation*, *2014*, 292376-292376. doi:10.1155/2014/292376

Takeda, K., & Akira, S. (2004). Microbial recognition by Toll-like receptors. *Journal of Dermatological Science*, *34*(2), 73-82. doi:https://doi.org/10.1016/j.jdermsci.2003.10.002

Bosmann, M., Russkamp, N.F., & Ward, P.A. (2012). Fingerprinting of the TLR4-induced acute inflammatory response. *Experimental and molecular pathology*, *93*(3), 319-323. doi:https://doi.org/10.1016/j.yexmp.2012.08.006

Zhao, X. (2009). *Development and characterization of humanized and human forms of ELR-CXC chemokine antagonist, bovine CXCL8(3-74)K11R/G31P* (Doctor of Philosophy (Ph.D.)), University of Saskatchewan. Retrieved from http://hdl.handle.net/10388/etd-03122009-113704